THÈSE

En vue de l'obtention du

DOCTORAT DE L'UNIVERSITÉ DE TOULOUSE

Délivré par :

Institut National Polytechnique de Toulouse (Toulouse INP)

Discipline ou spécialité :

Genie industriel

Présentée et soutenue par :

M. MONCEF SOUALHI

le jeudi 14 janvier 2021

Titre :

Contribution to intelligent monitoring and failure prognostics of industrial systems.

Ecole doctorale :

Systèmes (EDSYS)

Unité de recherche :

Laboratoire de Génie de Productions de l'ENIT (E.N.I.T-L.G.P.)

Directeur(s) de Thèse :

M. KAMAL MEDJAHER

MME THI PHUONG KHANH NGUYEN

Rapporteurs :

M. ANTOINE GRALL, UNIVERSITE DE TECHNOLOGIE DE TROYES

M. MOAMAR SAYED MOUCHAWEH, IMT LILLE DOUAI

Membre(s) du jury :

M. NOUREDDINE ZERHOUNI, UNIVERSITE DE FRANCHE COMTE, Président

M. DO PHUC, UNIVERSITÉ LORRAINE, Membre

M. JOSEBA QUEVEDO, UNIV POLITECNICA DE CATALUNYA BARCELONA, Invité

M. KAMAL MEDJAHER, ECOLE NATIONALE D'INGENIEUR DE TARBES, Membre

Mme THI PHUONG KHANH NGUYEN, ECOLE NATIONALE D'INGENIEUR DE TARBES, Membre

Contents

List of Figures

List of Tables

Nomenclature

Abbreviations

Acc	Accuracy
$ADAM$	Adaptive Moment Estimation
AE	Auto-Encoder
$ARIMA$	Autoregressive Integrated Moving Average
GRU	Gated Recurrent Unit
HI	Health Indicator
$LSTM$	Long-Short Term memory
MAE	Mean Absolute Error
$MAPER$	Mean Absolute Percentage Error
ML	Machine Learning
$NARX$	Nonlinear Auto-Regressive Exogenous Model
PH	Prognostic Horizon
PHM	Prognostics and Health Management
$Prec$	Precision
$RMSE$	Root Mean Square Error
$RMSprop$	Root Mean Square Propagation
RUL	Remaining Useful Life
$SGDM$	Stochastic Gradient Descent Momentum

Symbols

ΔT_m	Logarithmic mean temperature difference
GP	Global prediction sequences
l	Length of sequence S_i

l_tgt	Long-term target data sequences
l_trn	Long-term training data sequences
ML_1	Long-term predictor
$ML_{2.i}$	i-th Short-term predictor
Q	Heat transfer
s_trn	Short-term training data sequences
s_tgt	Short-term target data sequences
$starget$	Sequence time to start the predictions
$strain$	Sequence time of training observations
t_c	Current time
t_i	Prediction time of the i^{ith} short-term predictor
Thr	Threshold of fouling
TTC	Time-to-Clean
U	Heat transfer coefficient

General introduction

In the last decade, small and medium-sized companies are evolving towards Industry 4.0, which is an evolution from automatic to cyber-physical systems (CPS), fully integrated, automated, and optimized. This evolution offers promising perspectives to enhance the reliability, availability, maintainability, and safety systems but also poses many challenges in system health management. Indeed, due to ultra-connection properties, when a simple anomaly occurs in a component of the system, it will impact the quality product line and leads to serious faults in subsystem operation, and therefore causes a series of repercussions such as system failure, downtime, high maintenance costs, and even casualties. For instance, one can cite the refinery explosion disaster that occurred in Philadelphia on June 21st, 2019 (Coglianese, 2019). During the production activity, a failing pipe (faulty elbow joint) due to the corrosion from the hydrofluoric acid, which was in the process fluid, caused disastrous refinery fire and explosions. The incident led the release of thousands of pounds of potentially deadly chemicals into the air, including hydrofluoric acid as shown in Figure 1.

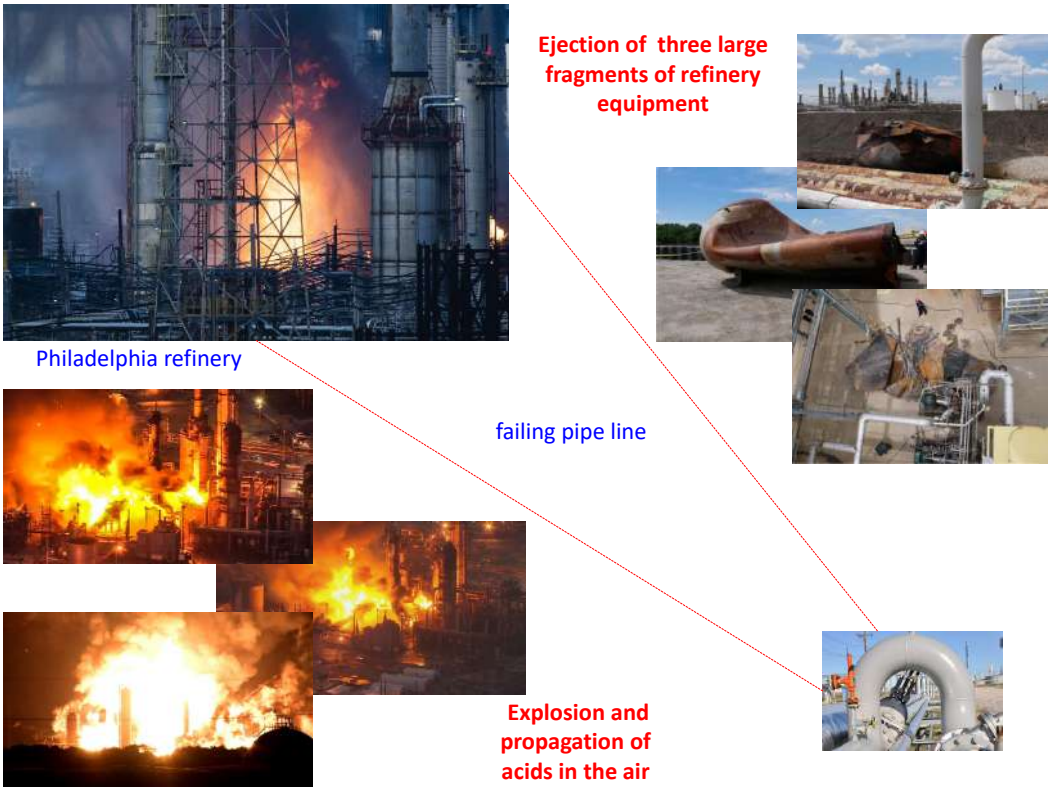

Figure 1: Refinery explosion disaster.

In this regard, it is crucial to continuously monitor and evaluate the equipment's health state to detect anomalies at the earliest possible stage, to diagnose their origin and predict the failure time and thus act in advance to avoid disaster events in human, environmental and economic terms.

For these reasons, predictive maintenance policy has been developed and has shown its superiority over other traditional ones. It aims to project the system's health state into the future to predict the failure event and therefore to schedule, in advance, a maintenance activity. This latter action allows avoiding downtime and significantly reducing the maintenance cost, especially for big-size companies that should have a large quantity and more important industrial systems. For illustration, according to the synthesis of some literature works (Zhang, 2018, Deloux, 2008), Figure 2 shows an overview of the maintenance costs comparison between the corrective, preventive, and predictive maintenance strategies.

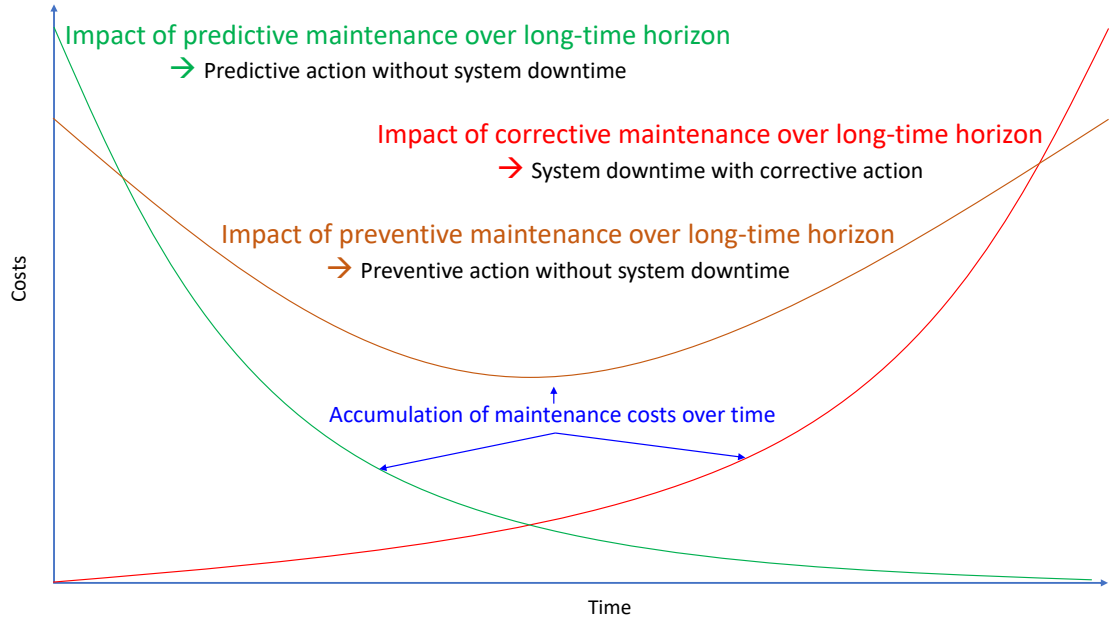

Figure 2: Corrective *vs.* preventive *vs.* predictive maintenance costs.

To improve the performance of a predictive maintenance strategy, it is necessary to obtain the actual and future information about the system, which is done through Prognostics and Health Management (PHM) algorithms. On one hand, PHM allows effectively monitoring the system behavior and facilitate the detection and diagnostics of its faults as well as the prognostics of failures. On the other hand, it allows system health management to minimize the overall maintenance cost and to enhance the availability, reliability and security of the system.

In literature, the PHM techniques are classified into three groups, model-based, data-

driven, and hybrid. Model-based approaches use mathematical equations to represent system behavior. As this latter behavior can be represented by a set of physical laws, this approach gains in terms of precision and allows to interpret well the different phenomena that occur in the system. The second group is based on the analysis of data collected from different types of sensors. It uses sensors placed on the system parts needed to be monitored and then exploits the recorded data from these sensors and transforms them into another form of information that allows the assessment of the system. The hybrid approach aims to use both of the system model and its sensor measurements to interpret global behavior.

In the context of industry 4.0, the systems are more complex and therefore the construction of their physical model becomes infeasible. Besides, with the development of sensing technologies, the data-driven approaches and their hybrid models are gaining more and more attention making them the most appropriate for monitoring. Within this framework, our research work is oriented towards the development of data-driven PHM approaches. This work is part of a European project, namely "SMART", whose main objective is to enhance the manufacturing toward industry 4.0. In this project, we focus on developing intelligent and innovative monitoring algorithms for fault detection, diagnostics, prognostics, and dynamic production and maintenance planning. Figure 3 gives an overview on the SMART project and its main objectives.

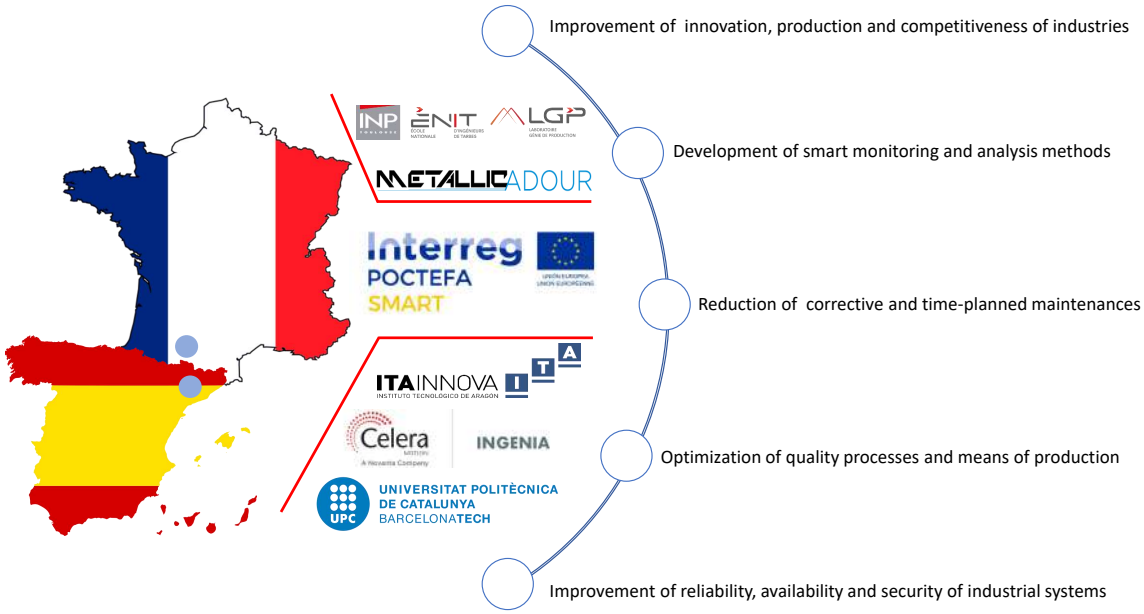

Figure 3: SMART project presentation.

The value of our work is further enhanced by a real demonstrator (industry) during an international mobility support (IMS) in Canada. This collaboration context is summarized and presented in Figure 4.

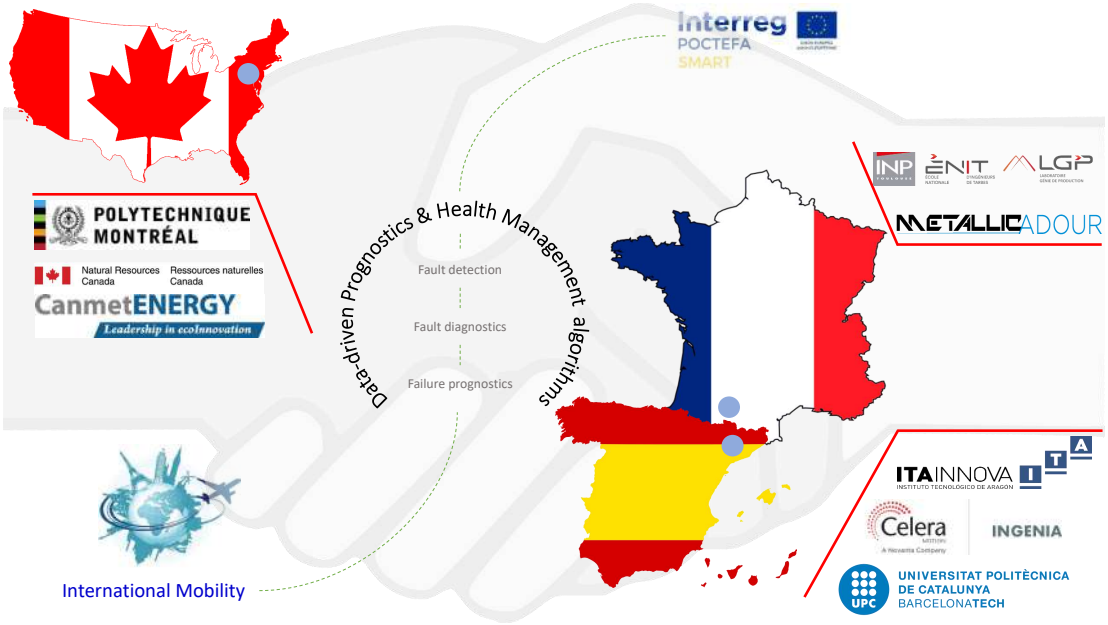

Figure 4: Collaboration context of the thesis.

Research questions and main contributions

One of the challenges for PHM posed by the revolution of Industry 4.0 is the increase of interconnections at multiple levels: components, sub-systems, and systems. Hence, the systems become more complex, more dynamic, and more autonomous. Thus, it requires a more intelligent system health management methodology that allows handling different anomalies of numerous connected equipment. It also enables us to deal with dynamic system behaviors in various operation conditions and even more adaptive with the effects of automatic control processes. In that perspective, it is necessary to address the following research questions.

1. Construction of a robust health indicator for fault detection

To meet the above-mentioned challenges, it is essential in the first step to build a robust health indicator (HI) that allows effectively characterizing the different system states. This HI should handle uncertain, heterogeneous, and incomplete data. Furthermore, it should be reliable for a wide range of fault types, different measurements, and operating condition variations.

2. Development of an online diagnostic method for dynamic systems with unknown fault types

Once the HI is built, it allows separating different health states of the system and can

be used as the pattern information for an automatic diagnostic procedure. Technically, the diagnostic methods based on pattern recognition techniques aim to learn, in an offline phase, the system health states represented by the constructed health indicators (HIs) and then use the model to identify the membership class of new observations. However, these methods have a critical drawback, that is their performance strictly depends on the prior knowledge of fault types labels.

In the context of Industry 4.0, as systems become more complex and more dynamic, it becomes difficult to recognize all eventual faults that will occur during the process. One can cite a multi-axis robot, it is composed of multiple arms that collaborate in series and can perform complicated motions during the machining process. Considering a six-axes robot, there exist a large number of cases, in which the movement drifts can come from the deviation of any axis or any combination of axes. Therefore, it is necessary to develop a new diagnostics method that allows effectively diagnosing online the origin of unknown drifts whose patterns have not been recognized before in the offline phase.

3. Development of an effective hybrid adaptive approach for failure prognostics of controlled processes in long-term horizon

After detecting and diagnosing an anomaly, the current system state can be projected in future operation conditions to estimate its remaining useful life. However, under controller activities, the future operation parameters will be not fixed but depend on the system state at that moment. For instance, when detecting the anomaly, the controller can attempt to fix it by updating the operation setting points. Consequently, this poses multiple challenges on the prediction of the system residual lifetime (SRUL) in long-term horizon. Hence, it is essential to develop an adaptive prognostics method that allows precisely predicting the SRUL in long-term horizon by taking into account the instantaneous changes in the system caused by the controllers' activities.

Thesis outlines

The previously mentioned contributions will be positioned with regard to the state of the art in Chapter 1. Then, Chapters 2, 3, and 4 present in details each contribution starting with an introduction and concluding by an application(s) and discussions on the obtained results.

- **Chapter -1- Literature review and problem statement:** The first chapter of this manuscript covers a global overview on data-driven approaches for condition monitoring in PHM framework. In details, this chapter reports three main parts: fault detection, fault diagnostics, and failure prognostics. The first part aims to

discuss the literature works on data processing algorithms used to build HIs to detect faults. Here we introduce different techniques and strategies used to transform raw data into another form of information (HIs) that represent the system health state and then discuss the advantage(s) and the limitation(s) of each technique. The second part relies on addressing fault diagnostics methods. In this case, we report the literature works on pattern recognition methods due to their large application for isolating, localizing, and identifying the origin of faults. Also, we discuss the benefits and what should be taken into account to further improve these methods. Next, we move to the prognostics concept, which has only emerged since the 2000s, through a synthesis of the developed works in this research field. Finally, the analysis of major limitations in the literature allows us to position our research work and highlight the methodology undertaken to contribute and overcome them.

- **Chapter -2- New health indicator construction for fault detection:** This chapter presents the first contribution of our work that presents a generic methodology of data processing to build an effective and robust HI. This new HI is easy for implementation and can be applied to detect various faults of most of rotating and electrical machines. Its robustness relies on the capacity on detecting major of the fault types that exist in a rotating machine such as bearing, gear, rotor bar, and also tool wears in machining systems. Moreover, this indicator is also able to proceed with heterogeneous measurements used for monitoring, such as current, voltage, vibration, force, and torque signals. Finally, another benefit of this indicator is its capability of detecting faults in different systems operating conditions. To highlight the performance of the proposed HI, we investigate different case studies and evaluate the relevant robustness metrics.

- **Chapter -3- Information fusion for online diagnostics of unknown fault types:** Chapter 3 aims to address the online diagnostics of unknown fault types in dynamic systems, particularly machining robots. In detail, we develop a new method based on information fusion of two monitoring techniques. The first one aims to build the diagnostics model for the identification of the robot axes drifts origin in the offline phase using the previously proposed HI. The second one relies on a new processing technique that allows locating the origin of unknown drifts and therefore update online the diagnostics model. The effectiveness of the proposed method is highlighted by investigating a real manufacturing system and a part of industry 4.0 framework, i.e. machining multi-axis robot.

- **Chapter -4- Adaptive prognostics approach in a controlled process:** The last contribution of our work focuses on handling the challenges posed by fault prognostics of controlled processes. Particularly, we develop an adaptive method based

on information fusion of multiple machine learning predictions in different horizon times. The proposed method allows capturing the degradation trend in long-term while taking into account the state changes in short-term caused by controller activities, to improve the accuracy of prognostics results. We apply this method to a real case study where we attempt to predict the time-to-clean of the heat exchanger tubes in the pulp and mill industry.

Finally, a general conclusions, as well as perspectives considered for future work is given in the last part of the thesis.

Figure 5 presents a synoptic scheme of the thesis, illustrating the overall work presented in each chapter.

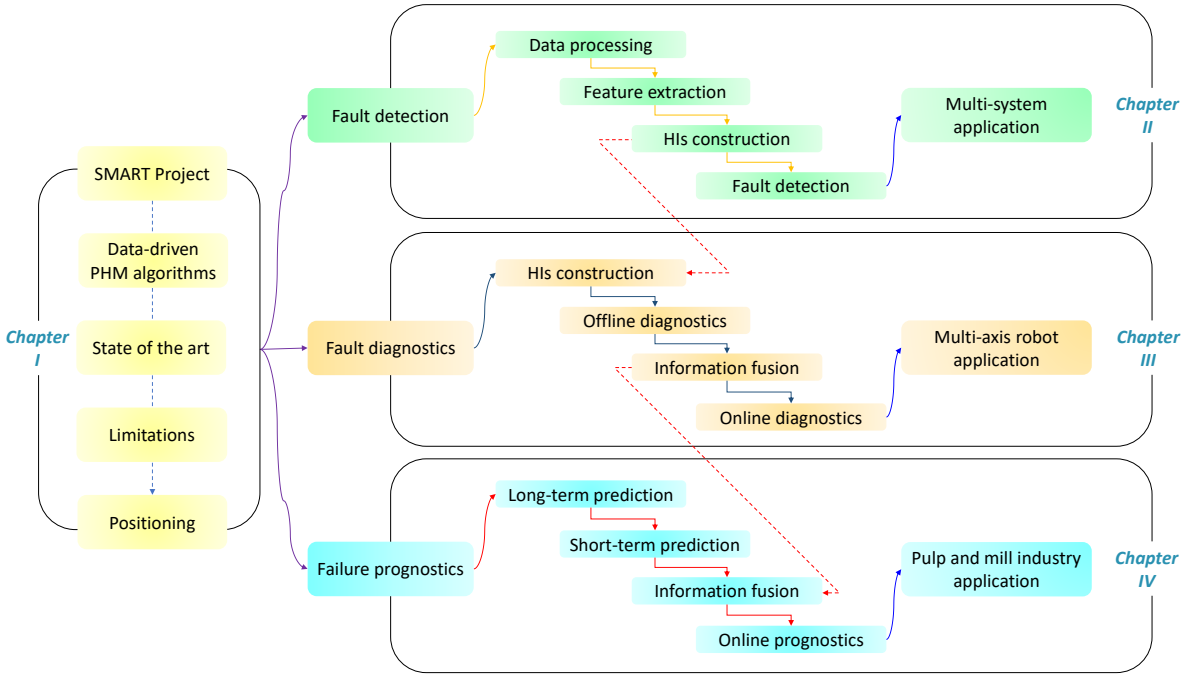

Figure 5: Overall synoptic scheme of the thesis.

Chapter 1

Literature review and problem statements

Contents

1.1 Introduction

As mentioned in the general introduction, this thesis aims to deploy intelligent monitoring algorithms for fault detection, diagnostics, and failure prognostics of complex and dynamic systems in the context of Industry 4.0. Regarding the difficulties when constructing exploitable physical models, and the availability of multiple data sources (e.g. sensor measurements, and expert knowledge), data-driven PHM approaches are the most appropriate to address the complexity of this kind of modern industry. Hence, this chapter of the manuscript presents a comprehensive overview of data-driven PHM approaches. It offers a systematic review of existing works in the literature in order to position our contributions. To do this, in Section 1.1, a brief overview of PHM and its constituent elements are presented. Next, the three principal modules (fault detection, fault diagnostics, and failure prognostics) are deeply discussed. Specifically, Section 1.3 provides an overall view on data processing techniques to construct health indicators for fault detection. Section 1.4 is dedicated to present fault diagnostics methods using pattern recognition techniques while in Section 1.5 a general summary of the latest developments in prognostics methods is presented. Finally, based on these syntheses, a scientific positioning with regard to each of the above sections within the SMART project demands is discussed in Section 1.6.

1.2 Data-driven system health management in PHM framework

The British standards (BS), updated in 2017, defines predictive maintenance (PdM) as *"condition-based maintenance carried out following a forecast derived from repeated analysis or known characteristics and evaluation of the significant parameters of the degradation of the item"* (EN, 2017). In other words, it can be simply defined as *"The set of actions that maintain systems in good operational conditions based their current health states to anticipate failures and enhance the reliability, availability, maintainability and safety systems"*. To reach all of these requirements, the PHM provides the necessary tools, methods and algorithms that allow to reach these requirements.

PHM was developed in the early 2000s and constitutes a full monitoring process with a compilation of eight modules: system analysis, data acquisition, data processing, fault detection, fault diagnostics, failure prognostics, decision making, and maintenance scheduling (Jouin et al., 2013). On one hand, it allows fault detection diagnostics and failure prognostics. On the other hand, based on the results of the latter activities, PHM facilitates system health management to anticipate failures and downtimes. The general structure of PHM is shown in Figure 1.1. From this figure, one can group the overall process into four main

activities consisting of two interdependent parts. These activities are system characteristic study, condition monitoring, degradation modeling, and system health management. The following subsections give an overview of each part.

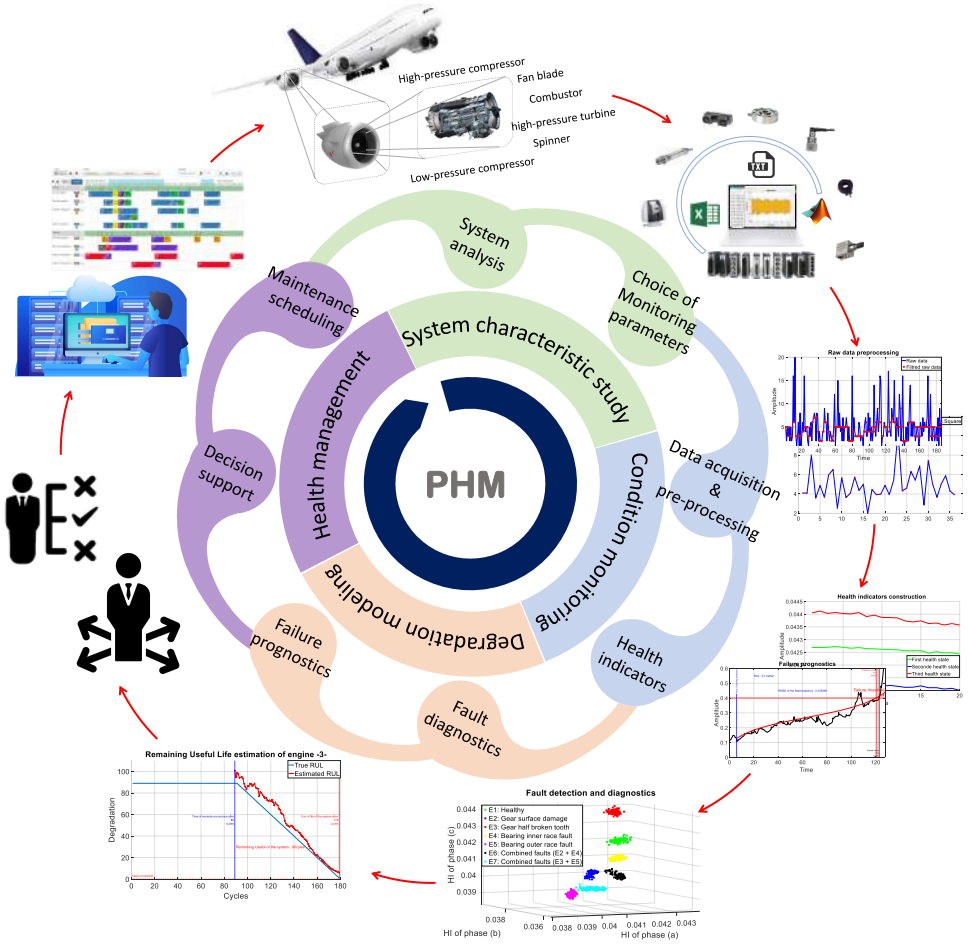

Figure 1.1: Overview of the PHM system.

1.2.1 System characteristic study

The first task in system health management is to analyze the studied system to identify the appropriate physical parameters leading to sensors placement and data acquisition to monitor the system degradation process. Figure 1.2 presents a simplified overview of a system analysis procedure for condition monitoring.

In the beginning, this step aims to explore the architecture, structure, and functionality of the system in order to isolate its failure mechanisms. This latter action, also known as critical component identification, can be performed using many approaches such as

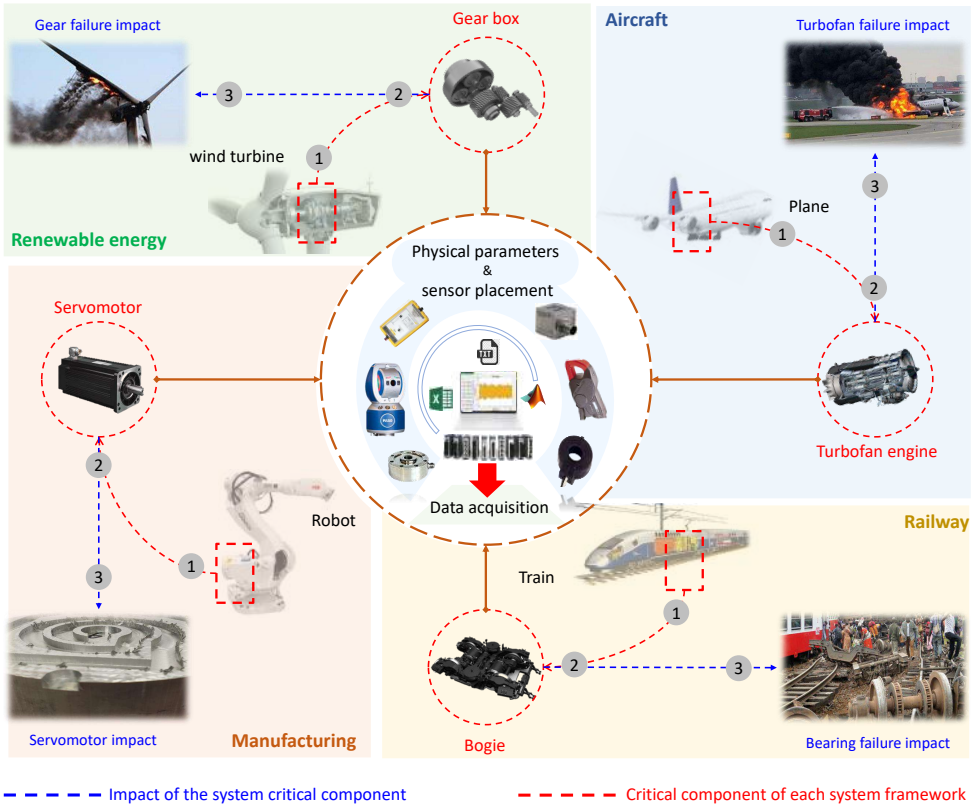

Figure 1.2: Illustration of system analysis for identification of critical components.

experience feedback, failure tree, event tree, cause, and effect tree, or through operator knowledge in case of insufficient information about the system (Gouriveau et al., 2016). Next, once the critical components are localized, the appropriate physical parameters are chosen to be the parameters that reveal the failure modes. Technically, these parameters allow reflecting the degradation phenomena of the components to identify their health states and track the degradation evolution. Finally, the last task of this step consists of collecting, and this, by exploiting the already installed sensors in the system or by choosing new proper sensors and installing them in the appropriate places.

1.2.2 Condition monitoring

In this second step, it is recommended for industrial companies to install a reliable acquisition system for an optimal data quality and consequently a more accurate and efficient monitoring.

After collecting and storing the raw data, these measurements are injected into processing algorithms, one of the most important steps in PHM (see Figure 1.3).

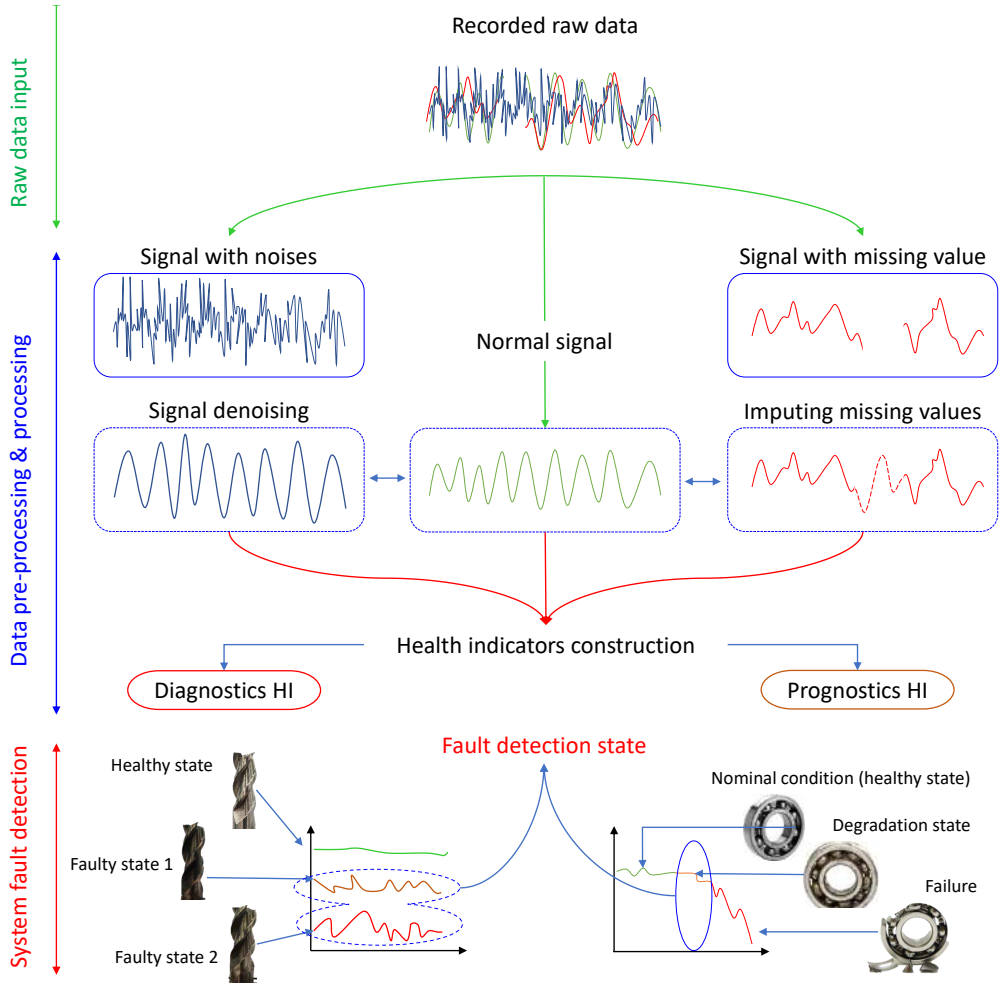

Figure 1.3: Data processing and HI construction for system monitoring.

The data processing starts by checking the observations (pre-processing) to verify if there are missing values, noises, or outliers. If true, it is necessary to apply filtering techniques to remove outliers and reduce noises, and also imputation techniques to handle missing values. Then, if the quality of the data is good, they are processed to extract useful features and build health indicators that detect the different health states of the system. For fault detection and diagnostics (FDD) purposes, these health indicators aim at identifying, localizing, and interpreting the system states (i.e. healthy state, faulty state 1, faulty state 2, etc.) (Lee et al., 2014). In general, the FDD health indicators take a form of separated patterns making it easy to assign each pattern to the corresponding health state of the system. Besides, for prognostics, the constructed health indicators represent the system's degradation trend over time. These indicators are an ensemble of observations that represent the system behavior from its nominal condition (healthy state) to its critical state (failure) (Goebel et al., 2008). The effectiveness of the constructed health indicators

in both diagnostics and prognostics depends on the processing algorithms, that at least, provide efficient results for the modeling step.

1.2.3 Degradation modeling

After the data are successfully processed, an analytical model is constructed based on the health indicators to automatically provide information about the system's health state and generate alarms or alerts when this system has a fault or reaches a critical issue. This model is a tool of diagnostics or of prognostics that represents the system's behavior by using only the already processed data. Because, in data-driven approaches, the obtained results from the processing step need to be approximated in an automatic model that will be used, on one hand, as a predictor of the system health state, on the other hand, as a model that reflects the system behavior (Medjaher et al., 2012). Hence, in diagnostics, this model can be a classifier algorithm that indicates the actual system health state, while it can be a regression predictor that estimates the RUL for prognostics purposes as shown in Figure 1.4.

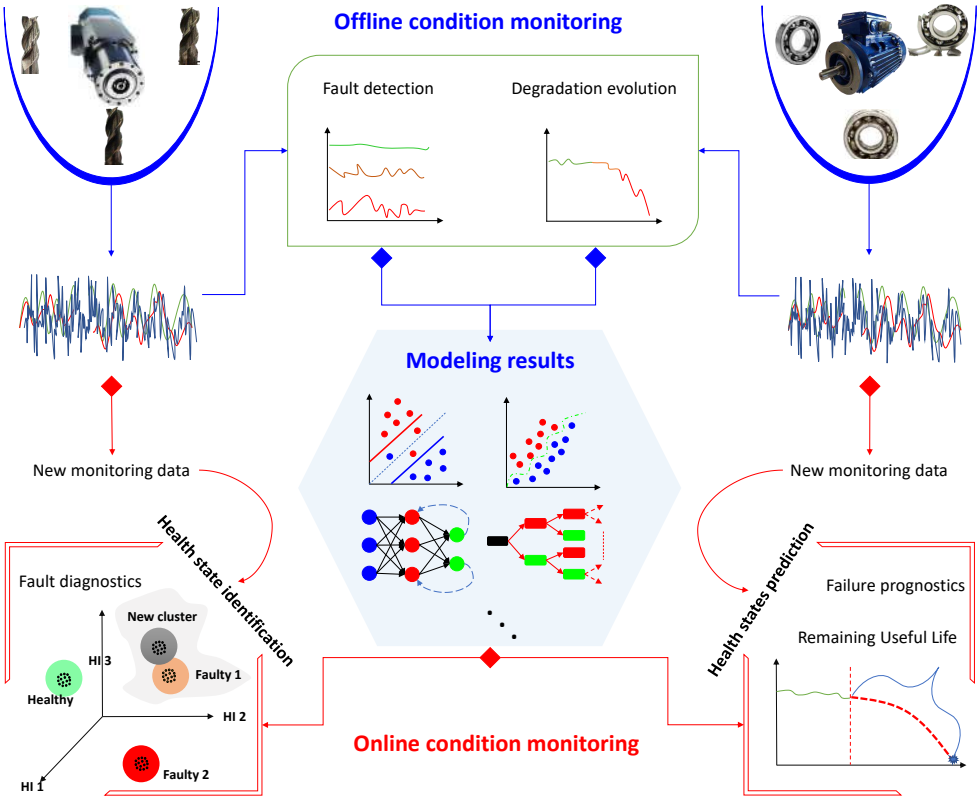

Figure 1.4: System health states modeling.

1.2.4 Health management

In general, obtaining the output information of constructed diagnostics and prognostics models is not sufficient to maintain the system in good operational condition. Indeed, besides generating alarms when detecting anomalies, it is necessary to decide on system health management, such as scheduling maintenance actions or production planning. Hence, in addition to the current system states, one needs to acquire complementary information, e.g. production plan and inventory management, for making proper decisions in unexpected new situations (Mobley, 2002).

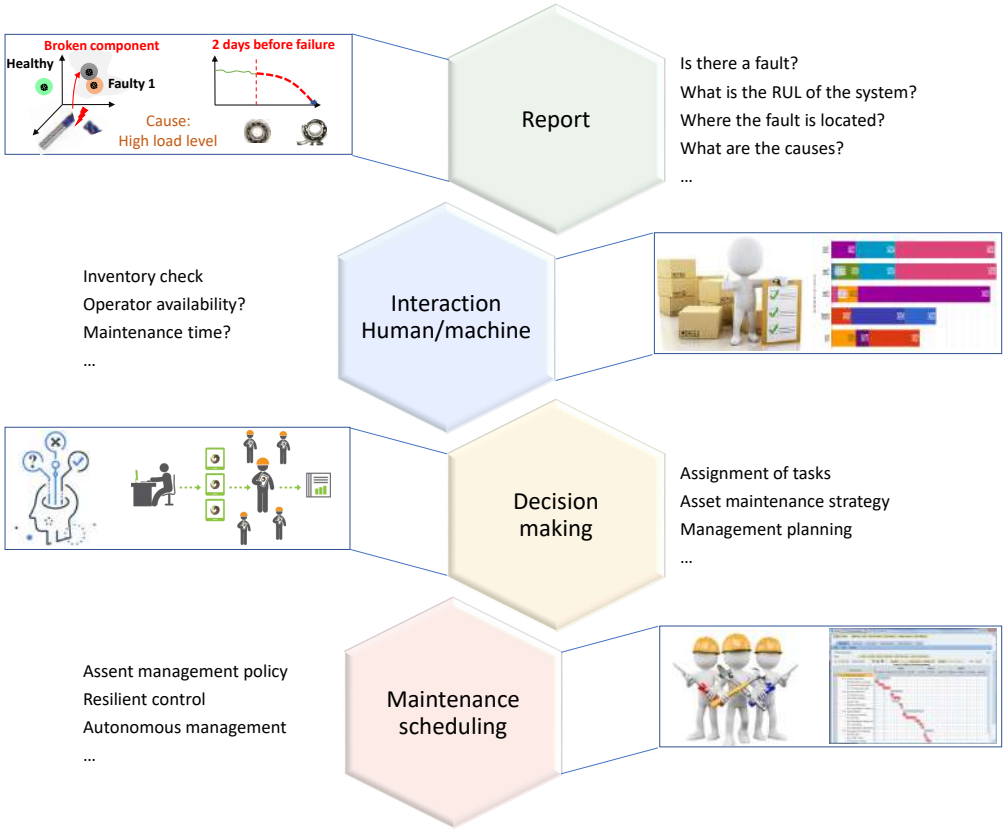

Figure 1.5: System health management overview.

Figure 1.5 shows an overview of a system health management steps based on the system modeling report. Mainly, these steps are in form of questions, e.g. Where is the location of the fault? What to do in this case? Whose engineers are available for the maintenance task? etc. For example, let assume that the constructed model indicates that the system has a defect in a specified component or this component will fail after a specified time. This information is automatically associated, on one hand, with the time of the availability of the component, on the other hand, with operators' agenda for fast maintenance action

scheduling. Thanks to this complete information, the time that company managers spend on these tasks can be reduced, and therefore the emergency management costs will be saved.

Within the data-driven PHM framework presented above, and according to the SMART project's objectives, this thesis focuses on three principal tasks: fault detection, diagnostics, and failure prognostics. The following sections aim to report the literature works related to these contributions.

1.3 Health indicators construction

As previously mentioned, the data processing step is one of the most important pillars in the PHM process. In general, the data processing techniques aim to extract meaningful features from the recorded raw data that, at least, provide enough information on the system's health state. Then, these features are directly used as health indicators or combined to be then projected on a graphical space to reveal the system health states (Nguyen and Medjaher, 2020). This health state projection step relies on what is called *system signature analysis* which allows us to isolate the healthy state of the system from its faulty states (Benbouzid, 2000).

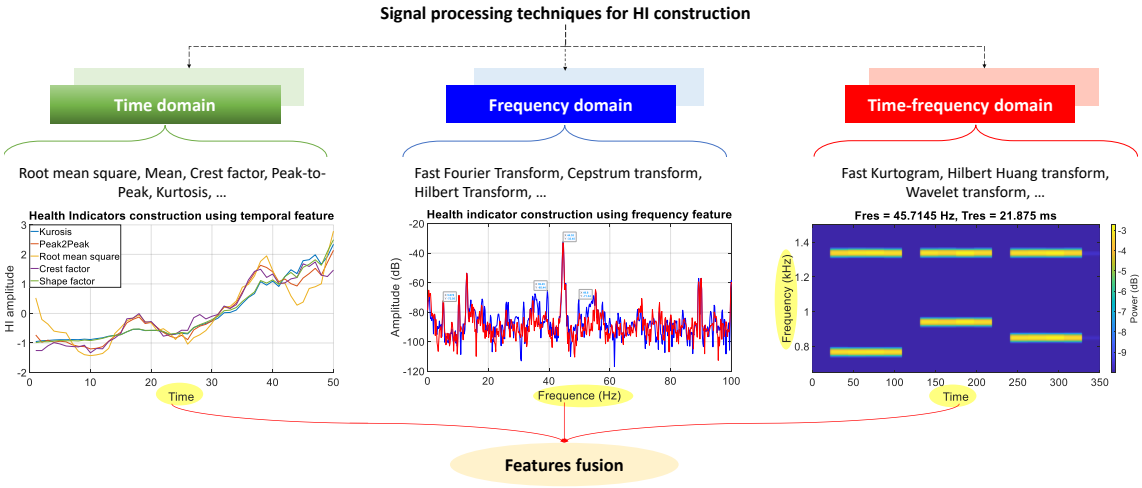

Figure 1.6: Signal processing techniques.

From the literature reviews (Benbouzid, 2000, Gouriveau et al., 2016, Atamuradov et al., 2017, Aggarwal and Chugh, 2019), the already existing methods of data processing can be classified into three groups: time domain, frequency domain and time frequency domain (Figure 1.6).

1.3.1 Time domain

The time-domain techniques aim to extract statistical features from raw data. These features are developed on the basis of mathematical laws aiming to provide accurate results (Sait and Sharaf-Eldeen, 2011, Medjaher et al., 2013, Soualhi et al., 2016, Chen and Li, 2017, Khlaief et al., 2019). Table 1.1 shows mathematical expressions of the most common features that are used as health indicators for fault detection of industrial systems.

Peak =	$MAX \mid x_i \mid$	AVG =	$\frac{1}{ne}\sum_{i=1}^{ne} x_i$
RMS =	$\sqrt{\frac{1}{ne}\sum_{i=1}^{ne} {x_i}^2}$	StD =	$\sqrt{\frac{1}{ne}\sum_{i=1}^{ne} (x_i - \overline{x})^2}$
CF =	$\frac{Peak(x)}{RMS(x_i)}$	ER =	$\frac{\sqrt{\frac{1}{ne}\sum_{i=1}^{ne} {x_i}^2}}{\sqrt{\frac{1}{ne}\sum_{i=1}^{ne} {d_i}^2}}$
FM_0 =	$\frac{\mathrm{PPA}(x)}{\sum_{i=1}^{n} \mathrm{FFT}(x_i)}$	KUR =	$\frac{\frac{1}{ne}\sum_{i=1}^{ne} (x_i - \overline{x})^4}{\left(\frac{1}{ne}\sum_{i=1}^{ne} (x_i - \overline{x})^2\right)^2}$
SKW =	$\frac{\frac{1}{ne}\sum_{i=1}^{ne} (x_i - \overline{x})^3}{\left(\frac{1}{ne}\sum_{i=1}^{ne} (x_i - \overline{x})^2\right)^{\frac{3}{2}}}$	FM_4 =	$\frac{\frac{1}{ne}\sum_{i=1}^{ne} \left(d_i - \overline{d}\right)^4}{\left(\frac{1}{ne}\sum_{i=1}^{ne} \left(d_i - \overline{d}\right)^2\right)^2}$

Table 1.1: Proposed temporal features for HI construction in literature.

Among them, the peak value is the simplest feature developed in statistics. It calculates the absolute of the max value of an ensemble of observations to evaluate their high tendency. This latter tendency varies from a state to another (i.e. normal, abnormal) according to observation values (low, high).

The mean (AVG) value aims to evaluate the average of the signal's tendency and generally is used to smooth data that present noises or for normalizing all observations as presented in StD, SKW, KUR, etc.

The root mean square (RMS), also known as *quadratic mean*, mathematically, it calculates the square of all observations (positive and negative) of a signal and then estimates the average of these values under the square root to finally obtain the RMS. In practice, this calculation defines the energy of a signal, it allows evaluating variations in a system by observing the changes in the signal amplitudes. In the case of a healthy state of the system, the averaged amplitudes of the recorded signal are supposed to be constant. Otherwise, in case of anomaly appearance, the instantaneous amplitudes will vary and consequently indicates a disturbance in the system.

The crest factor (CF) is a combined characteristic between the RMS and MAX features. It is used to identify the impulse amplitudes of a signal by comparing these impulses to a defined threshold. If the majority of the calculated impulses are greater than the defined threshold, it is therefore related to a system anomaly.

The standard deviation (StD) is used to evaluate the dispersion of a signal using the RMS equation and by normalizing each observation to the mean value of the signal. It can be used as an indicator to evaluate the system health state by calculating the dispersion of the observations in a specified given time and, based on it, interpret the system functionality i.e. if it could be considered as a healthy state or not.

The skewness (SKW) is the cubed ratio between the distance of each observation and the standard deviation of the overall signal, its principal function is to evaluate the symmetry and asymmetry of signal distribution. This distribution will be symmetric in the case where the skewness is equal to 0, otherwise, the distribution will be asymmetric with a positive or negative rate and can be interpreted as a faulty state in monitoring systems.

The feature Zero-order figure of merit (FM_0) is a temporal feature extracted in the frequency domain. It calculates the ratio of the peak-to-peak amplitude of a signal and the sum of its spectrum values.

The kurtosis (KUR) represents the fourth moment normalized by the square of the variance, it allows calculating the peakedness of signals. It is a good feature to be used for detecting faults and also evaluating their severity.

The energy ratio (ER) is the ratio between the RMS of the raw signal and the RMS of the difference signal which is the difference between the raw signal and its AVG value. Its interpretation is that when the difference is regular, that means the system operates under good conditions, otherwise it means that an anomaly occurs. Also, this feature is good for the detection of heavy faults.

The fourth-order figure of merit (FM_4) indicator is constructed by calculating the difference signal and then apply the KUR feature on the obtained new signal. Its functionality is to evaluate the severity degree of the detected heavy fault.

Table 1.2 presents the relevant literature works that use temporal health indicators and techniques to detect faults in different industrial systems using different measurement types and system operating conditions. From this table, it can be seen that the temporal features are widely used to detect faults in different components (gears, bearings, machining tools, etc.). Their advantages and disadvantages are summarized in Table 1.3.

1.3.2 Frequency domain

The frequency-domain allows analyzing the raw data through frequency transform methods, such as fast Fourier transform (FFT), Hilbert transform (HT), cepstrum transform (CP), spectral kurtosis (SK), etc. These techniques aim to convert each time-series obser-

Paper reference	Case study	Measurement type	Health indicator	System condition
(Lamraoui et al., 2015)	Tool chatter defect	Current signals	Variance	Unique
(Sevilla et al., 2011)	Roughness quality	Current signals	Mean	Unique
(Ammouri, 2011)	Tool wear damage	Current signals	Root mean square	Unique
(Zhou et al., 2007)	Incipient bearing fault	Current signals	Root mean square	Unique
(Lu et al., 2017)	Multi gear faults	Current signals	variance	Speed variation
(Lo et al., 2018)	bearing & gear faults	Current signals	Standard deviation	Unique
(Atamuradov et al., 2020)	Point railways machine	Current signals	Standard deviation	Speed variation
(Lezama et al., 2014)	Machine arc fault	Current signals	Separate features	Load variation
(Zarei, 2012)	Bearing faults	Vibration signals	Features fusion	Speed variation
(Zarei et al., 2014)	Bearing faults	Vibration signals	Features fusion	Unique
(Elangovan et al., 2011)	Machining defects	Vibration signals	Separate features	Speed variation
(Yuqing et al., 2015)	Tool breakage	Vibration signals	Features fusion	Unique
(Khlaief et al., 2019)	Bearing fault	Vibration signals	Separate features	Unique
(Lei et al., 2012)	Gear faults	Vibration signals	Root mean square	Speed variation
(Han and Pan, 2015)	Rolling element fault	Vibration signals	Energy ratio	Speed variation
(Sharma and Parey, 2016)	Gear broken teeth	Vibration signals	Fourth order FM_4	Speed variation
(Bensaad et al., 2017)	Bearing and gear faults	Vibration signals	Kurtosis	Unique
(Atamuradov et al., 2020)	Gearbox	Vibration signals	Features fusion	Speed variation
(Ahamed et al., 2014)	Gear faults	Vibration signals	Separate features	Speed variation
(Zhou et al., 2010)	Tool Wear	Acoustic emissions	Features fusion	Unique
(Skrickij et al., 2016)	Gear faults	Acoustic emissions	Separate features	Load variation
(Ozevin et al., 2014)	Misalignment shaft	Acoustic emissions	Multi features	Load variation
(Toutountzakis et al., 2005)	Gear fault	Acoustic emissions	Root mean square	Load variation
(Guo and Ammula, 2005)	Quality damage	Acoustic emissions	Root mean square	Unique
(Harvey et al., 2007)	Rolling element fault	Oil temperature	Root mean square	Unique
(Tonks and Wang, 2017)	Rotor shaft misalignment	Torque temperature	Peak	Speed variation
(Zaher et al., 2009)	Gearbox faults	Lubricant temperature	Mean	Unique
(Yang et al., 2019)	Turbine faults	Bearing temperature	Mean & variance	Speed variation
(Harrou et al., 2018)	Partial shading fault	Solar temperature	Standard deviation	Sunshine variation

Table 1.2: Synthesis on time features application for fault detection.

Advantages	Disadvantages
Easy implementation	Difficult to detect faults in different conditions
Fast computation time	Cannot identify the origin of the faults
Can reflect physical characteristics	Sensitive to data types

Table 1.3: Advantages and disadvantages of existing temporal features.

vation into a frequency value that is sensitive to the anomaly appearance. This frequency is called characteristic frequency and can be considered as health indicators of the system.

Technically, the frequency values obtained by these methods are compared to the ones calculated theoretically to verify whether or not there is an anomaly in the system. If the spectrum extracted by the frequency transform techniques does not correspond to the theoretically calculated one, that means that the system presents an anomaly, otherwise, the system is in a good health. In fact, some defects can be represented by their characteristic frequencies. For example, in electrical machines, bearing, gear, rotor bar, rotor shaft and other components in these engines has their own frequency of defect and which are evaluated mathematically by their equations. These defects are successfully detected with spectral analyzes. Multiple studies have shown their effectiveness in detecting and

localizing these defects.

One can cite the authors in (Cheng et al., 2010), they extracted fault characteristic frequency to detect the broken teeth of a gearbox using envelope analysis, while in (Mehala and Dahiya, 2008), the authors used the FFT transform to detect and localize multiple gear fault types such as a worn tooth, broken tooth and gear unbalance (Wu et al., 2012). The presented work in (Rai and Mohanty, 2007) used the HT to detect the different bearing element faults (inner race, outer race, and rolling ball). Another work was proposed in (Saidi et al., 2017) which used the peaks of SK as a health indicator for detecting the evolution of the fault severity of wind-turbine bearing.

Table 1.4 summarizes the main advantages and disadvantages of frequency analysis works. They do not require a lot of time to perform and nor much data to extract the characteristic frequency of faults. Also, the major benefit of this type of analysis is its ability to locate the origin of the fault as well as to locate several faults in the same signal, simultaneously.

Advantages	**Disadvantages**
Can localize the origin of faults	Cannot detect faults in non-stationary conditions
Do not require a lot of time	Loss information in high harmonic levels
Do not require amount of data	Require signal spectrum knowledge

Table 1.4: Advantages and disadvantages of frequency analyzes.

However, regardless of the capacity of frequency-domain analysis, these techniques have some disadvantages such as the loss of information when transforming the time-series signal into frequencies due to the non-uniformity of the signals known as non-stationary conditions. Moreover, note that such techniques require signal spectrum knowledge and are limited to the equipment having fault characteristic frequencies. For example, considering the machining tool of computer numerical control machine (CNC) and/or multi-axis machining robots, no existing studies identified their fault characteristic frequencies.

1.3.3 Time-frequency domain

To cope with time and frequency domain limitations, time-frequency methods are developed. They analyze the raw data in both of the time and frequency domains. Especially, this combination represents the energy of the signal waves (see Figure 1.6 by using the temporal and spectral features. It allows building effective health indicators to well reveal system health states (Jardine et al., 2006). There exists numerous techniques applied for fault detection such as wavelet transform (WT), Hilbert-Huang transform (HHT), short-time Fourier transform (STFT), Wigner-Ville distribution (WVD), Choi-Williams distribu-

tion (CWD), etc. According to the literature works, one can remark that the applications of these techniques can be classified into two groups.

The first one consists of signal processing in the time domain and then injecting this output in frequency analysis. For instance, the authors in (Yeap et al., 2018) extracted, first, the signal envelope and then used the STFT to separate the healthy state from the faulty state of capacitors. In (Rahman and Uddin, 2017), the authors proposed to extract KUR feature from the raw data and then used an ensemble of frequency and time-frequency techniques to evaluate the severity of a motor rotor eccentricity fault. Besides, the authors in (Li et al., 2018b) selected the most appropriate ones among multiple temporal features and then used the several time-frequency transforms to identify and specify the different faults of bearing elements.

The second group is to inject the raw data observations into a time-frequency analyzer and then use temporal features to extract and to build the health indicators. For instance, the presented work in (Soualhi et al., 2016) used the HHT to decompose the raw data and then extracted the RMS to estimate the instantaneous frequencies of bearing defect. In (Sait and Sharaf-Eldeen, 2011), after performing the STFT of the signal, the authors calculated the ratio between the maximum peak-to-peak of the signal and the sum of the frequency amplitudes to detect a gear fault. Besides, the work presented in (Taghizadeh-Alisaraei and Mahdavian, 2019) used multiple time-frequency methods, STFT, WVD and CWD to have various resolutions of the signal and then used the KUR function to build the health indicator. The study in (Wodecki et al., 2016) proposed, instead of using multiple time-frequency transform methods, to apply principal component analysis (PCA) technique for the dimensional reduction of multiple data recorded from different places on the system.

Although the effectiveness of the time-frequency analyzes has been shown through numerous studies, there also exists several limitations. One of the main drawbacks of these techniques is high resolution and computational time. Furthermore, it is difficult to implement such techniques for real-time applications and interpret the obtained health indicators. These weak-points alongside the main advantages are summarized in Table 1.5.

Advantages	**Disadvantages**
Be appropriate for non-stationary data	Require high computational resolution
Be effective for numerous applications	Take a lot of computation times
Track fault frequency signatures over time	Difficult for interpreting results

Table 1.5: Advantages and disadvantages of time-frequency analyzes.

1.3.4 Multiple feature fusion for health indicator construction

All of the features extracted from the signal processing techniques mentioned in the previous sections can be used as health indicators. Their effectiveness has been proven in multiple research areas thanks to their explicit mathematical expressions. However, in reality, there exists some systems that present complicated degradation phenomena, and consequently, it is difficult to extract the information using these health indicators separately. For this purpose, another solution is proposed by the researches. This solution consists of extracting multiple features from heterogeneous or from the same measurement types and then inject them into a fusion technique to build a representative health indicator.

For instance, the presented work in (Chen and Li, 2017) proposed to use the measurements of vibration sensors placed at different parts of the system, and then extract multiple time and frequency health indicators to inject them into a sparse auto-encoder (SEA) network for the fusion to detect bearing faults. Besides, the authors in (Sun et al., 2016) used a neuro-fuzzy system for fusing the sensor measurements acquired from two different types of sensors (velocity, GPS) to build the health indicator that detects faults in bridges. Another way of fusion approach used to construct the health indicator is pointed out in (Ng and Srinivasan, 2010). In this latter work, the authors injected heterogeneous data obtained from the Tennessee Eastman platform into different fusion techniques such as the PCA, self-organizing maps, and NN. Then, the obtained health indicators from each fusion model are injected into a Bayesian probability model to build the final health indicator.

As a synthesis, each of these approaches inherits a part of strengths and shortcomings. Tables 1.6 gives ideas of the main benefits and drawbacks of the fused health indicators.

Advantages	**Disadvantages**
	Loss of physical meaning
Do not require priori system knowledge	Black-box architecture
Reinforce the understanding system	Difficult for interpreting results
Provide more efficient results	Risk of loss main information data
	Sensitive to model parameters variations

Table 1.6: Advantages and disadvantages of fusion approach for HI construction.

1.4 Fault diagnostics

According to the definition provided by the French national organization for standardization (AFNOR) (AFNOR, 2001) NF EN 13306 8.10, fault diagnostics is the *"Actions taken*

for fault recognition, fault localization and cause identification". In the context of industry 4.0 where systems become more complex and ultra-connected, it is difficult to use traditional diagnostics techniques such as the graph-theoretic approach, expert system, and qualitative simulation (Wang, 2017). Thus, it is not practical to make proper decisions on the system of health states.

Besides, modern technologies of sensors and acquisition devices prompt the use of advanced techniques for fault diagnostics. Among these techniques, pattern recognition (fault recognition) becomes one of the promising methods used for diagnostics purposes. In fact, with constructed health indicators that indicate the system health state combined with sophisticated techniques, the pattern recognition methods can perform all actions of the definition NF EN 13306 8.10. It uses, in an off-line phase, the health indicators of the system to learn models and then uses these latter ones, in an online phase, to evaluate new health states of the system and provide a diagnostics report. The reliability of this report depends on the quality of the health indicators and on the exploitation of appropriate patter recognition techniques. In industrial systems engineering, there exists two main categories of pattern recognition widely used for fault diagnostics: supervised and semi-supervised, as shown in Figure 1.7.

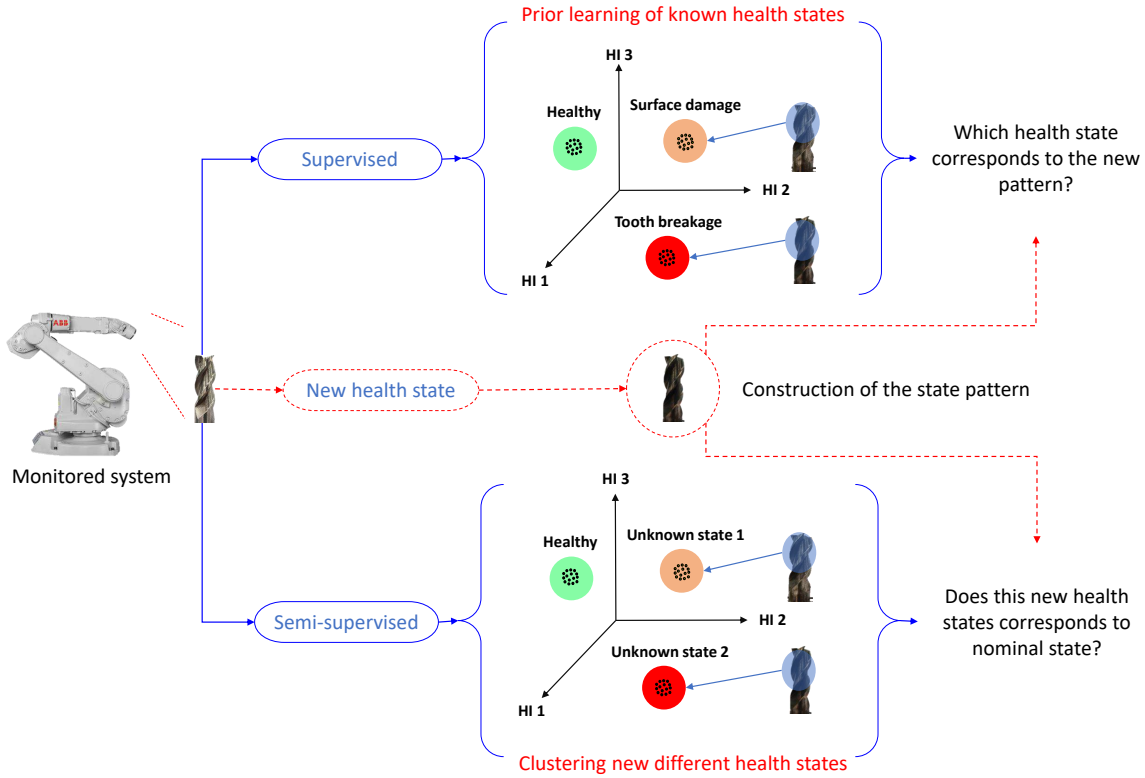

Figure 1.7: Illustration of supervised and semi-supervised pattern recognition diagnostics.

1.4.1 Supervised diagnostics

Supervised diagnostics is the most used technique to address a diagnostics problem. This technique learns the different health states of the monitored system with a priori knowledge on these states, called *labels* (healthy =1, faulty1 =2, faulty2 = 3, etc.) to build a model (Berrueta et al., 2007). This model is used to classify the new observations carried out from the system and determine their pattern by mapping them to the corresponding membership class defined and learned previously.

Actually, due to the widespread use of pattern recognition concept in various research fields (i.e. medical, food science, industry, security defense, etc.) (Berrueta et al., 2007, Gouriveau et al., 2016, Martinez-Luengo et al., 2016, Fusco et al., 2016), there exists a high number of developed techniques such as artificial neural network (ANN), adaptive neuro-fuzzy Inference System (ANFIS), Fuzzy system (FS), Convolution Neural Network (CNN), long-short term memory (LSTM), support vector machine (SVM), K-nearest neighbor (K-NN), logistic regression (LR), logistic discriminant analysis (LDA), fault tree (FT), etc. All of these techniques can be used as a classification task for supervised pattern recognition diagnostics. Table 1.7 summarizes the main advantages and cites the drawbacks of this approach when it is used in electrical and/or mechanical systems. One can cite the published works (Ondel et al., 2006, Sun et al., 2017, Ziani et al., 2017) where, in (Ondel et al., 2006), the authors used K-NN to identify the fault type of motor broken bars and assigned a label to each state while the authors in (Sun et al., 2017) exploited a deep ANN to classify different bearing rolling element faults and the authors in (Ziani et al., 2017) used SVM to diagnose the cause of an outer race bearing fault. Another kind of diagnostics is performed in machining manufacturing where the work presented in (Kannatey-Asibu et al., 2017) used multiple classifiers information fusion to diagnose the origin of the tool wear component. In (Ragab et al., 2018), the authors proposed a new classifier model, logical analysis of data (LAD), to learn and then diagnose a recovery boiler fault of a pulp mill manufacturing. Besides, in (El Koujok et al., 2020), the authors performed a new causality analysis tool to reinforce the learning phase with additional information about pulp mill boiler conditions to deal with stochastic and dynamic behaviors. All of these techniques perform well the diagnostics by learning the healthy and the faulty states of the system.

However, regardless of the performance of the above mentioned techniques, the supervised diagnostics presents two main drawbacks. The first one is that this method requires prior knowledge on system fault states while, in reality, it is not possible to reproduce and learn all fault scenarios of the system. The second one relies on the fact that all supervised models of diagnostics classify the new observations into one of the previously learned classes, even if they do not belong to any of them and consequently produce false alarms.

Advantages	Disadvantages
Do not require expert knowledge	Requires prior knowledge on system fault states
Identify easily the learned patterns	Require large of data for learning
No human intervention needed	False alarms in case of new faults
Wide application domains	

Table 1.7: Advantages and disadvantages of supervised pattern recognition.

1.4.2 Semi-supervised diagnostics

The semi-supervised diagnostics is a concept that allows identifying the different health states of the system without prior knowledge on the system faults. Specifically, its main concept is based on clustering the data representing the faults with prior learning of the healthy state. Then it assigns labels to each corresponding class. Also, this kind of method is suitable for diagnosing the system states not studied before. This is because one of the characteristics of clustering algorithms is the ability to create new classes if these latter classes do not belong to the previously identified ones.

There exists various clustering algorithms, one can cite the most effective ones such as agglomerative hierarchical clustering (AGHC), k-means clustering, artificial ant clustering (AAC), hidden Markov model (HHM), etc. The basis of these algorithms is to find the clusters that present a high density of volume points around one observation which probably, this observation, is the centroïd of the clusters.

The use of clustering algorithms can be exploited in two manners. First, they are used for the recognition of the nominal health state of the system from the faulty states (faulty 1, faulty 2, faulty 3, etc.) without any information on the fault types. Many case studies were based on the idea to use the clustering algorithms to identify the healthy state patterns of the system, and then, in case of anomaly appearance, the clustering algorithm isolates the different faults by generating new labels of the new patterns corresponding to these faults (Farrar and Worden, 2012). In (Zhang et al., 2019), the authors used a deep neural network (DNN) to build an offline supervised diagnostics model (by learning the healthy state first) and then, in parallel, used data processing techniques to cluster the new health state of the system and assign them new labels to build a semi-supervised diagnostic tool of gear faults. Besides, the presented work in (Madani et al., 2018) used the only DNN to learn both the labeled and non-labeled data for diagnostics of cardiac disease in the medical field. Other work presented in (Lei et al., 2007) used an ANFIS to learn the healthy state of the system and combined it with a genetic algorithm (GA) to assign labels of the new faults. This kind of diagnostics approach allows an early assessment of the system by the recognition of the healthy state and anticipates its total failure but with much time of maintenance to localize the faults.

The second manner to exploit the clustering techniques is to be associated with expert knowledge to become a semi-supervised technique. This procedure is the commonly used one in case where no sufficient data on the system are available or when the system is not yet studied. In fact, it attempts to learn the data distribution and isolates the classes, and then, the industrial engineer assigns labels to each class. The presented works in (Kumar et al., 2008, Chinnam and Baruah, 2003) proposed to use HMM as a tool for classifying the different states of CNC machining system and then, with the operator interpretation and remarks on the machining quality, the authors assign labels to the obtained patterns by the HHM and build a semi-supervised diagnostics tool. This tool will facilitate the recognition of the faults with their types and origins and therefore reduce the maintenance downtime and costs. Also, in (Wang et al., 2015), the authors used a data quantity with labeled-health states and another amount of unlabeled data with expert knowledge to identify their membership class (labels) and build a neighborhood weighted graph for the diagnostics of complex processes.

However, without expert knowledge, the second group of semi-supervised diagnostics can only diagnose the healthy state of the system without identifying the origin of isolated faults as the first one do.

Hence, for more synthesis, Table 1.8 gives an overview of the advantages and the disadvantages of semi-supervised pattern recognition techniques.

Advantages	**Disadvantages**
Appropriate for incomplete and unlabeled data	Require human expertise
Allows wide range of applicability domains	Cannot localize the origin of faults
Can identify patterns of new faults	Uninterpretable new patterns
Identify easily the healthy patterns	Difficult to identify the health states of new labels

Table 1.8: Advantages and disadvantages of semi-supervised pattern recognition.

1.5 Failure prognostics

The first stage of research works for system health management focused on detection and diagnostics of faults (Goebel et al., 2008). Nowadays, during the last two decades, a new concept which is the system prognostics has emerged. This concept aims at estimating the Remaining Useful Life (RUL) of a given system. It calculates the residual lifetime of the system starting from the time of anomaly appearance to its total failure, offering promising perspectives to enhance the reliability, availability, and safety while reducing maintenance costs. Indeed, estimating the lifetime of a system during its operation helps the industrial operator to act on the system to correct the errors without stopping the production line, and therefore with no maintenance cost loses. Otherwise, in case of a real need to stop

the production line, it allows anticipating the failure by planning as fast as possible the maintenance action and prepare the component to be changed in the system before its total failure.

In literature, data-driven prognostics methods can be classified into three main groups (see Figure 1.8), namely statistical, neural network-based and hybrid methods (Liao and Köttig, 2014, Gouriveau et al., 2016, Atamuradov et al., 2017, Javed et al., 2017). These three groups are respectively presented in Subsection 1.5.1, Subsection 1.5.2 and Subsection 1.5.3. Then, Subsection 1.5.4 is dedicated to address, in details, different techniques for RUL estimation.

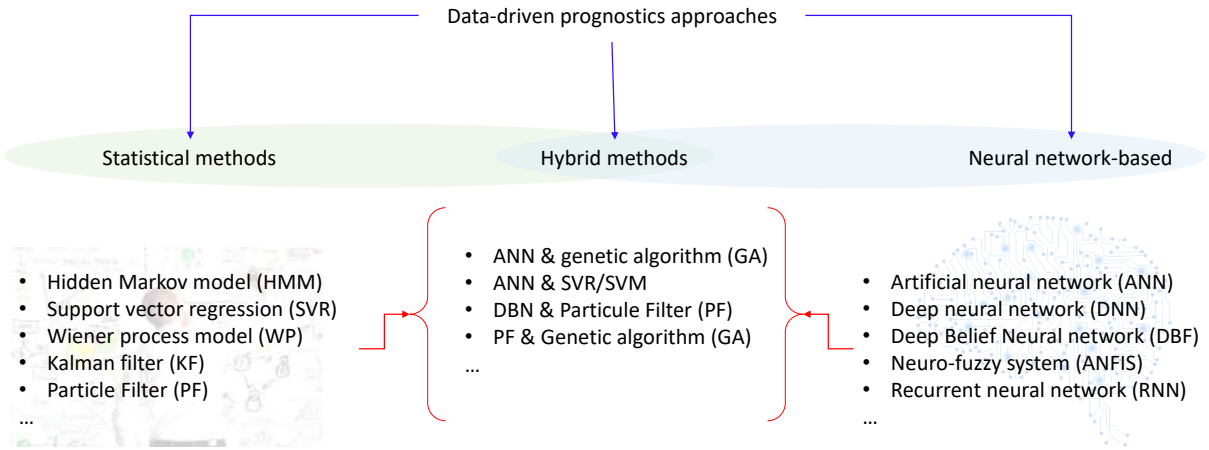

Figure 1.8: Categories of prognostics approaches.

1.5.1 Statistical methods

The statistical prognostics methods attempt to understand data based on statistics using mathematical equations for inference about the relationships between monitoring variables and system health states (Javed et al., 2017). This category of methods is suitable and more favorable in the case where the used model for prognostics can reflect the dynamic behavior of the system. In fact, the statistical techniques can reflect the system's behavior and introduce uncertainties on the degradation and is therefore more efficient in terms of predicting future health states for prognostics (Lei et al., 2018). Among the developed techniques in the literature, one can cite the most commonly used models (Gebraeel et al., 2005, Eker et al., 2011, Sbarufatti et al., 2016, Rabiei et al., 2016): support vector regression (SVR), support vector machine (SVM), hidden Markov model (HMM), auto-regressive integrated moving average (ARIMA), and particular filter (PF).

For instance, the presented work in (Soualhi et al., 2014) used SVR for modeling and

for the prognostics of bearing failure, while in (Khelif et al., 2016), the authors used the SVR for estimating the end-of-life of turbofan engines. In (Widodo and Yang, 2011), SVM was used, first, as a processing tool to build the degradation health indicator, and then, it was used to predict the RUL of the bearing. There exists other improved models based on SVM such as the work presented in (Cao and Gu, 2002), the authors proposed a modified version of the SVM model, named dynamic SVM, which dealt with non-stationary and variable system conditions. In parallel, the work in (Lu et al., 2016) also proposed a modified version of SVM, called least square SVM for prognostics of dynamic behaviors. Concerning the prognostics using the ARIMA model, it was used in several application domains and it is considered as a reference tool for comparison. It was used in (Liu et al., 2019) to estimate the RUL of machining cutting tools and combined with empirical mode decomposition technique (EMD) for the prognostics of battery systems in (Zhou and Huang, 2016). Another application was presented in (dos Santos et al., 2019) where the authors used an ensemble of ARIMA models with different parameters to estimate the RUL of turbo-fan engines. Moreover, in this new epidemiological situation of COVID-19, it is one of the first tools used for the prediction of the spread of the epidemic situation as presented in (Sahai et al., 2020). Finally, particle filtering becomes now one of the state-of-the-art techniques in statistical prognostics (Jouin et al., 2016). It was used for estimating the end-of-life of several systems. One can cite the wind turbine planetary gearbox in (Orchard and Vachtsevanos, 2009) and the turbine blade (creep growth) in (Baraldi et al., 2013a,c). It was used mostly for estimating the RUL of Li-ion batteries due to the availability of the mathematical degradation models of these systems (Tian et al., 2014, Hu et al., 2015, Xing et al., 2013). Besides, this tool was used in machining manufacturing systems for the prognostics of tool wear propagation (Yan et al., 2013), LED light sources attenuation (Fan et al., 2015), etc.

Advantages	**Disadvantages**
Do not require large amount of data	Not suitable for non-stationary conditions
Provide accurate degradation model	Require human expertise
Interpretable results	Limited applications
Less computing time	Require knowledge on the degradation process
Allow repeatably of results	Use various simplifying assumptions

Table 1.9: Advantages and disadvantages of statistical prognostics models.

An overview on the main advantages and disadvantages of the above mentioned techniques are summarized in Table 1.9. The choice of the appropriate models strictly depends on particular system characteristics such as linear, non-linear, or stochastic. However, it is difficult to generalize these methods for complex systems because, as several subsystems are connected to each others, the dynamic behavior of one subsystem impacts the others leading to random variance in the overall system's behavior and therefore raises various challenges in finding the mathematical laws that characterize all degradation phenomena.

1.5.2 Neural network-based methods

The second category of data-driven prognostics relies on NN techniques. These kinds of techniques attempt to predict the future health states of the system using only the sensor measurements without including the physics of the system. Also, they do not require a lot of knowledge about the distribution of the data and the variables dependencies (Lei et al., 2018), and usually, there are no hypotheses and assumptions before running the prediction algorithms. Their effectiveness strictly depends on a large amount of data to learn the degradation and to predict the system's future states (Lei et al., 2007).

For instance, the authors in (Gebraeel et al., 2004) proposed to use an ANN for failure prognostics of bearings in a test bench while in (Saon et al., 2010), the ANN model was applied for the prognostics of real industrial bearings. The published work in (Gope et al., 2015) attempted to regularize the tuning parameters (epochs, activation functions, etc.) of the ANN architecture to obtain the best results. Besides, in (Deutsch and He, 2017) the authors dealt with varying a DNN structure (hidden unit, hidden layers) for prognostics of bearing and gear failures. The presented work in (Soualhi et al., 2013) proposed fuzzy NN to deal with the prognostics of non-stationary bearing failure. Another version of a NN, which is the recurrent neural network (RNN), was proven as an effective prognostics tool for bearing failures (Malhi et al., 2011). Also, this RNN model was successfully applied to estimate the RUL of aero-propulsion engines in (Hsu and Jiang, 2018). Based on the same model, authors in (Rigamonti et al., 2016) presented a new variant of RNN, named echo state network (ESN), which allowed performing good learning than the basic RNN architecture and proved its effectiveness in estimating the RUL of the same data of aero-engines. In (Li et al., 2018a), the authors preferred to use a convolution neural network (CNN) instead of the RNN due to its capacity of feature extraction and representing well the degradation evolution of the engines. To further improve the accuracy of the estimated RUL, the authors in (Li et al., 2019, Ren et al., 2020) combined the CNN model, by exploiting their capacity of modeling the degradation trend, and the RNN model, due to its high prediction accuracy of time series data, to build a hybrid tool for the prognostics of the engines in (Li et al., 2019), and the battery degradation in (Ren et al., 2020).

Advantages	**Disadvantages**
Do not require expert knowledge	Non transparency of the prediction models
Appropriate for complex systems	Require large amount of data for learning
Adaptable to different applications	High computational time
Deals with high dimensional data	Dependent of performance on model architecture
Easy optimization of tuning parameters	High risk of over and under fitting

Table 1.10: Advantages and disadvantages of neural network prognostics models.

These above mentioned models showed their performance in different applications.

They are gaining more and more attention in many research areas thanks to the ability to address the prognostics issues posed by complex and dynamic systems. Indeed, they can capture the non-linear, uncertain, and sequential characteristics of the degradation processes and then predict the RUL of the monitored systems. However, it is difficult to interpret their obtained results because of the non-transparency of the complex combination functions. Their advantages and disadvantages are summarized in Table 1.10.

1.5.3 Hybrid methods

The third category, which consists of hybrid data-driven approaches, combines different techniques to leverage the advantages of these approaches while minimizing their limitations for better prognostics results (Lei et al., 2018). This combination depends on the system requirement in terms of prognostics accuracy, degradation modeling, and decision.

For example, the presented work in (Deutsch et al., 2017) used a deep belief network (DBN) to estimate the system model parameters that are taken into account in a PF model for RUL prediction of hybrid ceramic bearings. In (Baraldi et al., 2013b), the authors used a PF tool which parameters are optimized by an ensemble of NNs for prediction of the crack propagation trend in bearings. Besides, the hybrid approach developed in (Byington et al., 2004) is based on the combination of Kalman filter (KF) and fuzzy logic to enhance the prognostic accuracy. Another work presented in (Liao and Köttig, 2016) proposed to combine a PF prognostics tool with two other techniques. The first technique was the construction of the degradation model by analytical system equations of a lithium battery system. The second technique aimed at using real sensor measurements for estimating the model parameters constructed previously and to interpolate these parameters to update the PF predictions for RUL estimation of the battery lifetime. In (Skima et al., 2016), the authors used the sensor measurements to estimate the parameters of the degradation model of a micro electro mechanical system (MEMS) and then exploit the PF for the propagation of its health state and RUL estimation. For different techniques that deal with other applications, the interested readers can consult the works presented in (Chen et al., 2010, 2012, Saha et al., 2008, Xu et al., 2013).

The above mentioned hybrid approaches are dedicated to specific case studies. For synthesis, Table 1.11 gives some benefits and limitations of the prognostics hybrid models.

Advantages	**Disadvantages**
Applicable for system level prognostics	Difficult for implementation
Appropriate for dynamic, complex systems	Require more computational times
More reliable prognostics	Require identification of many parameters

Table 1.11: Advantages and disadvantages of hybrid prognostics models.

1.5.4 Remaining useful life estimation for prognostics

Subsections 1.5.1, 1.5.2 and 1.5.3 presented an overview on data-driven prognostics approaches. However, no discussion has yet been initiated on how to calculate the system RUL that is a crucial issue. To this end, the following points aim to discuss in detail RUL estimation techniques that can be classified into three groups: similarity-based, recursive, and direct RUL estimation, as shown in Figure 1.9.

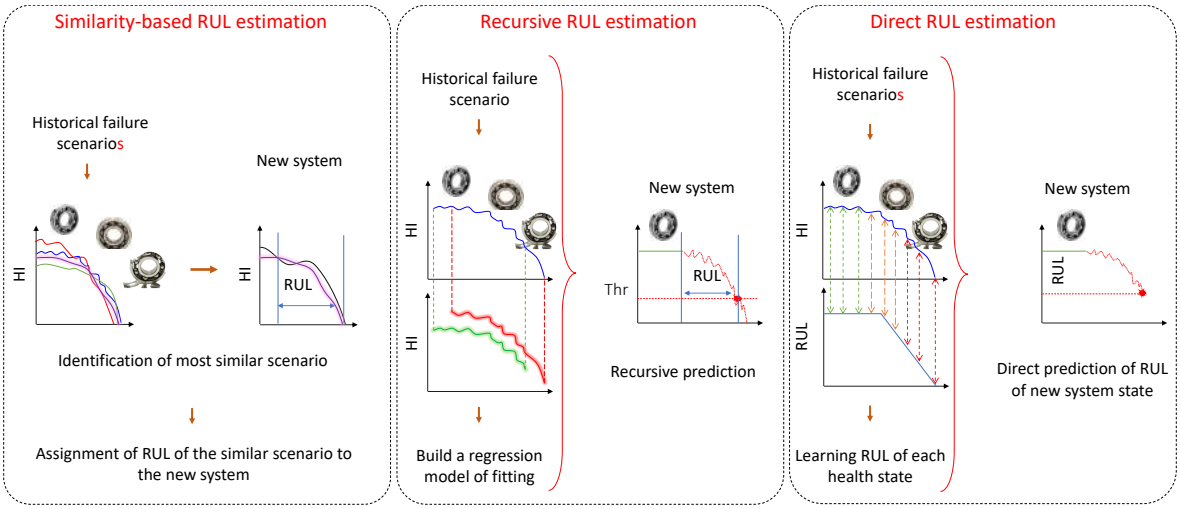

Figure 1.9: Overview of remaining useful life techniques.

The main advantages and disadvantages of three above mentioned techniques are summarized in Table 1.12.

	Advantages	Disadvantages
Similarity	Perform good predictions	Sensitive to condition variations
	Easy for implementation	Require large amount of similar data
	Fast computation time	Difficult to fix a failure threshold
Recursive	Easy for threshold identification	False alarms in non-stationary conditions
	Appropriate for incomplete data	Require expert knowledge for modeling
	Perform high accuracy predictions	Reduced modeling quality due to low data
Direct	Perform good predictions	Difficult to fix a failure threshold
	Perform high accuracy prediction	Require large amount of similar data
	Adaptive to the system variation	High computation time

Table 1.12: Advantages and disadvantages of RUL estimation techniques.

Similarity-based RUL estimation

RUL estimation using similarity was the first technique applied in the prognostics framework (Wang et al., 2008). It is developed with the idea to be easier to implement without any knowledge of the degradation physics of the system (Cai et al., 2020). Technically, this method is based on collecting historical degradation health indicators constructed from run-to-failure raw data. These indicators consist of the patterns that represent the degradation evolution trend of the system state from its nominal condition (healthy state) to its critical condition (total failure). Then, based on these indicators, the new patterns representing new system health states are compared to the historical indicators of the run-to-failure data collected previously. The best matching pattern from the latter comparison will be the database for the failure estimation (Wang et al., 2008). On a more technical level, the similarity-based RUL can be interpreted as a comparison between the system that has similar physics and behavior during a time range than reference behaviors and therefore assumes that they have a similar lifetime (Wang, 2010, Ramasso, 2014). In general, the comparison is based on distances to assess the degree of similarity between the two or more than two patterns. However, the key to achieving this aim lies in data processing techniques and the construction of health indicators to facilitate the comparison test.

Hence, in literature, many research ideas have been conducted, one can cite the works presented in (Wang, 2010, Bektas et al., 2019, Yu et al., 2020a). Here, the authors used training data of run-to-failure scenarios to construct health indicators to obtain a good separation between the different scenarios patterns. In (Wang, 2010), the health indicators were constructed through a feature selection algorithm to define the most representative one for the degradation evolution, while in (Bektas et al., 2019, Yu et al., 2020a), the authors used a simple ANN and a deep RNN, respectively, to fuse the raw data. In the end, with the constructed indicators, the proposed works use the distance to find the nearest patterns to the new set of observations and take the mean of their RULs. The authors in (Chen et al., 2018) proposed a new similarity technique based on the optimization of parameters of a distance estimator using GA. Another work in (Liu et al., 2015) combined a probabilistic approach with a constructed health indicator to increase the accuracy of the identification of the most similar pattern for RUL estimation. In the same way, the author in (Ramasso, 2014) used another approach based on computational geometry that takes into account the noise proprieties and transforms them into a range of multiple health indicators to obtain a polygon-shaped representation of the health indicators and to have the best matching for RUL estimation. The presented work in (Ragab et al., 2019) proposed a pattern recognition technique based on multiple prediction models that separate the health indicators into many categories (i.e. short, long, medium) to facilitate the recognition of the best matching pattern and estimate the RUL.

The main drawback of this RUL estimation approach is, on one hand, it requires a

huge amount of historical degradation scenarios. On the other hand, it can generate false alarms in case of operating condition variations that create different mission profiles.

Recursive remaining useful life

This kind of RUL estimation techniques is based on the regression concept that uses predictors for estimating the future health states of the system using its actual condition observation to predict the next value, then uses this latter value as an input to predict the following one, and therefore may capture useful information on the degradation trend. To obtain a good fitting of the degradation trend, it is necessary to use reliable prediction models able to capture the behavior of the system, especially the dynamic behaviors.

The application of the recursive methods is generally good in cases when the system operating conditions are, at least, constant and also in a case where there is not high difference between the failure times of the historical scenarios (minimum time to failure, maximum time to failure). In this case, with these two mentioned conditions, the regression predictors can predict well the system behavior and also define more accurately the system RUL due to the possibility to define a threshold. For instance, several works were based on this concept. One can cite the presented works in (Soualhi et al., 2014, Chang et al., 2017), where the authors used SVR as a model to predict the end of life of bearings in (Soualhi et al., 2014) and the end of lighting time of LEDs in (Chang et al., 2017). The presented work in (Wu et al., 2016a) used random forest (RF) for predicting the tool wear critical stages while in (Wu et al., 2016b) the authors used an ANN as a regression tool to estimate the attenuation life of charging and discharging of the lithium battery. Besides, in the same case study, the authors in (Liu et al., 2014) used a combination of the ARIMA method with PF as RUL estimators to well represent the degradation trend of the battery capacitors. Another combination is developed in (Baraldi et al., 2013b), where the authors preferred to combine the ANN regression with the PF to estimate the end of life in turbo-fan engines. Moreover, as the nature of prognostics requires to accurately predict the lifetime of the system, the authors in (Javed et al., 2018) proposed to use the distribution of multiple prediction models to well estimate the level of a tool wear in a machining system.

The overall developed models for RUL estimation with recursive predictions have successfully proven their effectiveness. However, their application remains limited to cases that do not present any perturbations such as dynamic behavior and non-stationary conditions.

Direct remaining useful life

The last group of RUL estimation techniques is the one that directly calculates the end-of-life of a system from its actual health state and estimate, at any time of the degradation

process, the RUL of the system (Khelif et al., 2016). Its application is feasible when failure time data of similar systems are available. The estimations of these failure times are usually performed using machine learning (ML) models that are trained to learn the model how to map each of the observations of the system health state to its corresponding lifetime, and this, from the starting life cycle to its end-of-life. In detail, when the system is in a healthy state, its supposed RUL is very high (maximum lifetime) and almost constant over time. Then, when a fault occurs, the RUL of the system starts decreasing according to the degree of severity, speed, and conditions of the system. In this case, the learning model is then carried out to learn two phases: the nominal phase where the system is in good health, and the decreasing phase where the system is in a faulty condition.

In literature, many types of research have emerged using ML for this kind of RUL estimation. In fact, the ML methods are widely used for failure prognostics of various and multiple industrial systems thanks to their high capacity of dealing with system complexity. They have successfully proven their effectiveness in prediction tasks. However, their performance depends on the chosen model for prediction. For this purpose, the following works are reported based on a unique data repository which is the NASA turbofan engines CMPASS (Saxena et al., 2008). This data repository has been used by many researches due to the amount of historical run-to-failure of aircraft engines (Ramasso and Saxena, 2014). The direct RUL techniques deal with this published data, making them a reference to compare proposed techniques for prognostics. The work in (Zheng et al., 2018) used the filtering temporal method to denoise different sensor measurements and inject the overall variables into an extreme learning machine (ELM) model to learn the degradation and predict the RUL. Besides, the authors in (Zheng et al., 2018) developed a comparative study between the traditional machine learning models to predict the RUL using Linear regression (LR), decision tree (DT), SVM, RF, K-NN, Gradient Boost (GB) and ANN. Among these models, it was found that the ANN is the suitable one in terms of accurate predictions and execution time. Because, as the turbofan data presents several operating conditions and fault types, the ML models constructed based on defined and fixed functions cannot perform good modeling of the dynamic behavior. For this purpose, the latest researches focused on the use of ANN network, more particularly DNNs such as long-short term memory (LSTM), bi-directional LSTM, deep RNN, CNN. In (Heimes, 2008, Wu et al., 2018a), the authors used a deep RNN architecture to train the overall data variables and predict the RUL. In (Wu et al., 2018a, 2020, Elsheikh et al., 2019, Yu et al., 2020b) the authors fused the data variables to obtain a unique representative pattern for each engine and used an LSTM and bi-LSTM networks, respectively, for RUL prediction. Another work in (Wen et al., 2019) proposed to use the CNN to fuse and predict the RUL. Finally, (Jin et al., 2020) proposed a combined model CNN-Bi-LSTM to exploit the capacity of feature extraction with CNN and the prediction capacity for time-series data using Bi-LSTM.

1.6 Literature discussion and positioning

In this section, we firstly discuss the limitations of existing approaches to data-driven system health assessment. Then, we highlight the motivations of this work which contributes to answering some of the issues already mentioned.

1.6.1 Limitations of the existing works

The review of existing works for data-driven system health management presented in the previous sections provides us an insight into the literature gaps of fault detection, diagnostic and failure prognostics.

First, in fault detection, considering all studies for the construction of health indicators in the three data processing domains, one can notice that the proposed works can be classified into two groups with their own gaps as follows:

- The first group uses only one unique meaningful feature or combined features extracted from sensor measurements to build health indicators that characterize the component defects. However, **none of the proposed health indicators are generalized to different systems.**
- The second group consists of the extraction of several features from sensor measurements to collect as many as possible information and represent the degradation process in high dimensional space. Then, the obtained vectors are reduced through dimensional reduction and fusion techniques to well represent the system health state. However, the main drawback of this approach is **the loss of the physical meaning** of the obtained health indicators leading to the difficulty of interpreting the results. Moreover, the performance of the published methods is **limited to specific applications and cannot be generalized.** In addition, few works in both groups deal with the **data heterogeneity issue** and also take into account the **operating condition variations**.

Secondly, in fault diagnostics of manufacturing processes, most of the existing works are concentrated on supervised and semi-supervised learning techniques with the following limitations:

- In the first group, the supervised pattern recognition can learn the causes and origins of the faults, but its **performance strictly depends on the priori knowledge** to label the faults and learn the classifier model.

- In the second group, the semi-supervised pattern recognition learns the healthy state of the system and then identifies the different faults using clustering algorithms but **cannot diagnose the causes of these latter faults.**
- To our humble knowledge, none of the existing studies effectively addresses the challenges posed by fault diagnostic of systems dynamic behaviors, e.g. localize the drifts origin in robots axes movements.

Finally, in prognostics, despite the rapid growth of its different approaches, **making an accurate estimation of the RUL** of a system remains always **a difficult challenge**, especially in the cases of complex and dynamic systems with effects of closed-loop controller activities. Moreover, in literature, the existing RUL estimation techniques, that can be classified into two groups according to prediction horizons, present the following limitations:

- In the long-term horizon group, the predictor is dedicated to predict multi-step ahead system health states. It uses the predicted value as input to estimate the next observation and so forth. This kind of prediction procedure provides information in long-term, from the nominal conditions of the system to its failure, and makes an overview of the degradation trend. However, the disadvantage of this approach is **the accumulation of the error predictions when using the predicted value as the next input.** Specifically, the predicted value can contain a certain error that accumulates and increases over time. Moreover, this approach only captures the trend of the degradation process and leads to a **loss of information on the degradation state.**
- In the short-term horizon group, the proposed approaches perform only one prediction of the system health state after a defined short-time period. The obtained results by these predictors are more accurate than the long-term prediction ones. However, these predictors **require new observations for the only one prediction value** and consequently **do not provide an overview of the degradation trend**.

1.6.2 Positioning and contributions of this work

Regarding the above mentioned limitations, this manuscript aims to contribute to the literature works and fill the cited gaps. The contributions can be divided into three principal parts: health indicators construction for fault detection, fault diagnostics, and failure prognostics.

The first contribution (corresponding to Chapter 2) aims to propose a data processing methodology for the **construction of an effective new health indicator for fault**

detection of various systems in the smart manufacturing field. First, the methodology uses frequency domain analysis to normalize data and reduce the signals dispersion and then combines three effective features to build a new health indicator. This health indicator can be applied to detect critical component defects such as bearings, rotor bar and unbalanced supply in railways motors, booth bearing and gear faults in wind turbine generators, and finally machining tool defects in manufacturing spindle motors. Moreover, the performance and robustness of the proposed health indicator are highlighted when detecting these faults by using different signal types (current, vibration, voltage, force, and torque) in different operating conditions of the systems i.e. different rotating speed and different load levels of the engines. The implementation of the proposed methodology is very appreciated in case of production line as there is no need for implementing and adding new sensors. Indeed, it allows detecting fault by using electrical signals that are already accessible from control systems.

The second contribution (in Chapter 3) concerns the **development of a new online diagnostics methodology that allows automatically labeling the unknown fault types by fusion information of two monitoring techniques, direct and indirect**. This methodology uses the previously proposed health indicator to construct a supervised pattern recognition model as an indirect monitoring way. Then, the results of this latter model will be combined with the information of another health indicator used for direct monitoring to build an effective new semi-supervised diagnostics model. More precisely, this model is dedicated to the diagnostics of multi-axis robot drifts (i.e. which axis deviates from its nominal trajectory). In an offline phase, the supervised method learns the historical robot health states (healthy and faulty) from measurements acquired by *indirect monitoring*. Then, as it is not possible to reproduce all the fault scenarios of the system, it happens that new drifts may occur during the operation of the robot. In this case, the previously learned classifier is updated online by exploiting the proposed new monitoring technique, *direct way*, to localize the origins of the robot drifts by using its already installed encoders at each axis actuator. The information fusion consists of labeling the newly detected drifts during the system operation and using them to re-train the classifier automatically. Therefore, the fusion of the two techniques can be a promising contribution. It allows practitioners to monitor their robot behavior from the beginning, detecting and localizing axes deviation origins and proposing appropriate decisions for more availability, security, and quality.

Considering the strengths and drawbacks of both long- and short-term prediction models, the last contribution of the manuscripts (presented in Chapter 4) aims to propose **an adaptive hybrid prognostics approach for more accurate predictions in long-term horizon.** It combines both of the long- and short-term prediction models to build a new adaptive approach. This approach inherits the advantages and overcomes the disadvantages of each predictor. In detail, it uses short-term predictions at specified instants

to update the long-term predictor. Indeed, as the short-term predictor is more accurate that the long-term, this latter model takes the obtained predictions of the short-term at a specified instant and replaces its value corresponding to these instants and predicts again the new evolution trend of the system degradation. The proposed approach is applied to a real controlled manufacturing (pulp and mill) system.

1.7 Conclusion

In this chapter, we presented a synthesis of the literature works concerning data-driven prognostics and health management. This overview highlighted the limitations in each step: fault detection, diagnostics, and failure prognostics when dealing with complex and dynamic systems. In fault detection, we noticed the necessity of building an effective and reliable health indicator that can be used to separate the different health states of various systems. This health indicator could be used to enhance the performance of automatic fault diagnostic procedures based on the pattern recognition concept. However, the brief review of pattern-recognition-based fault-diagnostic approaches indicated the limitations in both supervised and semi-supervised learning techniques. Particularly for fault diagnostic of dynamic systems, e.g. location of the drift origin in robot axes movements, it is necessary to develop a new on-line diagnostics methodology that allows automatically updating the unknown fault types by a combination of two proposed direct and indirect monitoring methods. Finally, as the prognostics have attracted more attention since the 2000s, we reported the different prognostics approaches and the different techniques used for the estimation of the RUL of a system. In this part, the main identified challenge is to provide accurate predictions in a long-term horizon, taking into account the system changes under the effect of control activities.

In the next chapter, we will present the first contribution of this thesis, which is the construction of a new effective and robust health indicator for fault detection.

Chapter 2

New health indicator construction for fault detection

Contents

2.1 Introduction

The state of the art discussion presented in the previous chapter pointed out the literature gaps compared to scientific and practical requirements. One of the critical gaps is that none of the proposed methods for health indicator construction can be generalized for different systems and handle at the same time multiple issues such as data heterogeneity, and operating conditions variation.

Therefore, in this chapter, the problem of building an effective and practical health indicator is addressed. Especially, this indicator aims to separate the information such as patterns that represent the different health states of the system, i.e. identification of

the healthy and the faulty states of a given system. Its strengths can be summarized as follows:

- This health indicator can be generalized for various applications. It is applied to most rotating/electrical machines of different manufacturing fields, such as railway, renewable energy, and machining platforms.
- It can deal with the data heterogeneity issue. That means the input data that the proposed health indicator takes into account can be from multiple sources such as voltage, current, vibration, force, and torque signals.
- It is robust under different operating conditions. Technically, the recorder data for HI construction can be from different operating conditions such as speed variation, load level variation, and machining parameter variation in the case of machining systems.

To do this, Section 2.2 presents an overall view of the processing steps to construct the health indicator. Section 2.3 introduces one of the demonstrators of the thesis partners, in addition to of other application systems as case studies, to verify the effectiveness and the robustness of the proposed HI. Each case study presents a specified range of defects to be considered.

In detail, the first case study relies on monitoring bearing and gear faults of a gearbox using current and voltage signals (Subsection 2.3.1). Besides, the second application presented in Subsection 2.3.2 investigates a broken rotor bar, unbalanced supply motor, and bearing faults using current, voltage, and vibration measurements. The last application, which is the thesis first demonstrator (Subsection 2.3.3), aims to monitor a machining tool states such as surface damage, flack damage, and broken tooth by using the current, vibration, force, and torque signals. All of these case studies investigate different operating conditions to further highlight the effectiveness of the methodology and the health indicator.

2.2 Proposed methodology for new health indicator construction

This section aims to present the main steps of the proposed methodology of data processing to built health indicators and propose a new robust one for fault detection. This methodology stars from data acquisition and passes through, data preparation, data processing and health indicators construction as shown in Figure 2.1

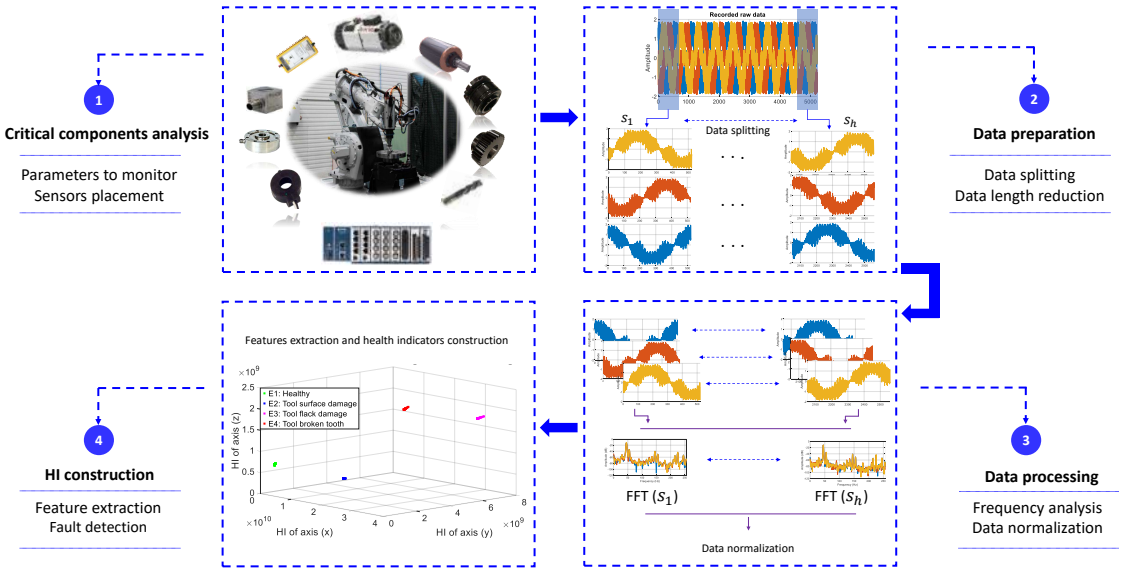

Figure 2.1: Overview of the proposed processing methodology for HIs construction.

As mentioned in Subsection 1.2.1 of the first chapter, system analysis is a preliminary step that must be studied first before proceeding the next steps. Thus, the methodology starts by analyzing the system structure to identify its failure mechanisms and define the right parameters to record the data. Then, the data provided by the sensors are processed to extract meaningful features. Finally, the extracted features are combined to build a new health indicator that reveals the system health state.

2.2.1 Critical components analysis and data acquisition

In the age of industry 4.0, the automated systems evolve to cyber-physical systems (CPS) that are fully integrated, automated and optimized (Lee et al., 2015a, Xu, 2017). This evolution makes the manufacturing to be equipped with more and more machinery systems to increase the production and competitiveness towards big size companies. Among these machinery, electrical motors are the most omnipresent in many activities such railway, renewable energy and machining manufacturing companies. They are widely used thanks to their optimal effectiveness and their low costs. However, regardless of their advantages, they are subject to faults that can occur at any time during their operating process. In general these faults are localized in the critical components of the engines. The studies (Gouriveau et al., 2016, Soualhi et al., 2016, Lu et al., 2017, Ondel et al., 2006, Quiroz et al., 2018, Pezzani et al., 2018) indicate that bearings, gears and rotors are the most susceptible parts to fail in electrical machines. In addition, the cutting tool of machining systems, such robots and computer numerical machines, is also considered as one of the main factors of

machining processes defects (Tobon-Mejia et al., 2012, Terrazas et al., 2018).

The monitoring of the critical components mentioned above is addressed by using various sensor types, such as acoustic, vibration, current, force and torque sensor. Figure 2.2 shows an illustration of the polarity of each sensor type within its application framework.

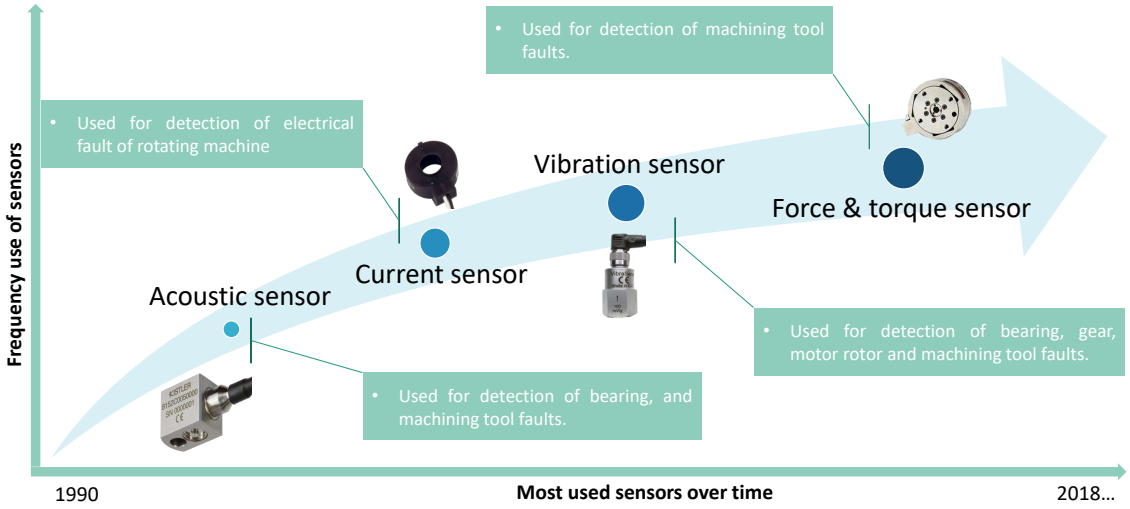

Figure 2.2: Polarity of acoustic, current and vibration sensors for monitoring.

In this figure, one can see that the vibration signal is the widely used one in literature for the monitoring of bearing, gear, rotor, machining tool and electrical faults of the machine while, in parallel, force and torque sensors are most used for monitoring machining systems. Besides, current sensor is used to remedy faults such as unbalanced supply motors, squirrel cage motor broken bars of the electrical motors. Hence, in this manuscript, the above mentioned measurements are chosen to verify the effectiveness and robustness of the proposed health indicator.

2.2.2 Data preparation

The obtained signals (such the current signal of phase a, the vibration signal of axis x, the force signal of axis z, etc.) denoted by S are split into several segments of length L, as shown in Figure 2.3. Each segmented signal is labeled by s_h, where h represents the segment index ($h \in [1, ..., \frac{N}{L}]$) and is calculated by Equation 2.1. This segmentation allows reducing the signal length to process at each instant while keeping the signal characteristics to take only the relevant features. It also allows reducing the computing time in case of big data size. Furthermore, the choice of the length L is twofold: if the data acquisition time is long, L takes a big value, otherwise, L takes a small value. In this manuscript, the

data are split into segments of 0.1 second when the recorded data are equal or less than 5 minutes.

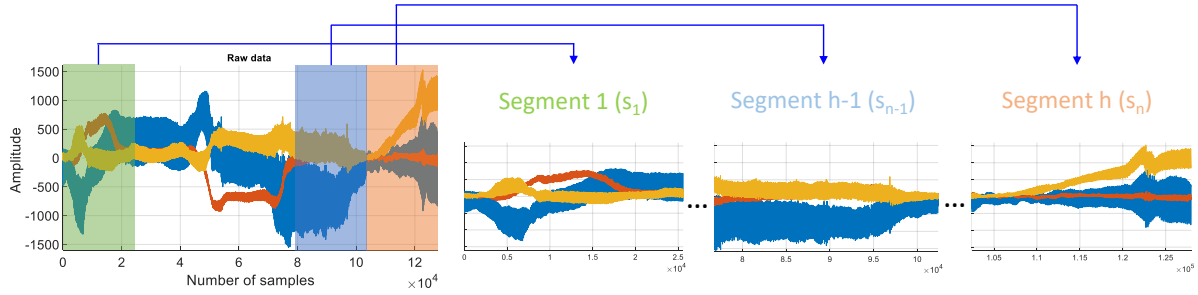

Figure 2.3: Raw data segmentation.

$$h = \frac{N}{L} \tag{2.1}$$

where L and $N$are the length of the segments s_h and the total signal S respectively and must be equal to an integer.

Figure 2.3 shows how to split the signals into several windows, marked by the different colors. Each segment is used to extract one feature value that represents the total observations within the same segment.

2.2.3 Data normalization

Before extracting features, each segment (s_h) of raw data is normalized to its non-stationary variations induced during the operating process of the engine. These variations are generally caused by speed variations during the data acquisition step. They impact the electromotive force of the motor and therefore generate outlier values on the measured signals. In reality, the motor speed is not constant all the time and oscillates around the target speed, this is due to the inaccuracy tolerance of the sensors. In order to prove this appointment, a Fast Fourier Transform (FFT) is applied to a signal segments taken from the same state of the system (e.g. healthy state) to observe the impulses of the signal's fundamental frequency, because the rotating speed is directly related to the frequency that corresponds to the motor speed as shown in Equation 2.2.

$$\omega = 2 \times \pi \times f \tag{2.2}$$

Where ω is the angular speed and f the motor frequency.

From Figure 2.4, one can see fluctuations in amplitude around the fundamental frequency of the different segments representing the same health state and which consequently lead to a dispersion of the observations in the feature extraction step. To remedy this situation, the ratio between each segment s_h of the raw data and the maximum value of the signal spectrum (FFT) is calculated (Equation 2.3). It normalizes the signal to its dispersion.

$$s_h^{'} = \frac{s_h}{\mathrm{MAX}\left(\mathrm{FFT}(s_h)\right)} \tag{2.3}$$

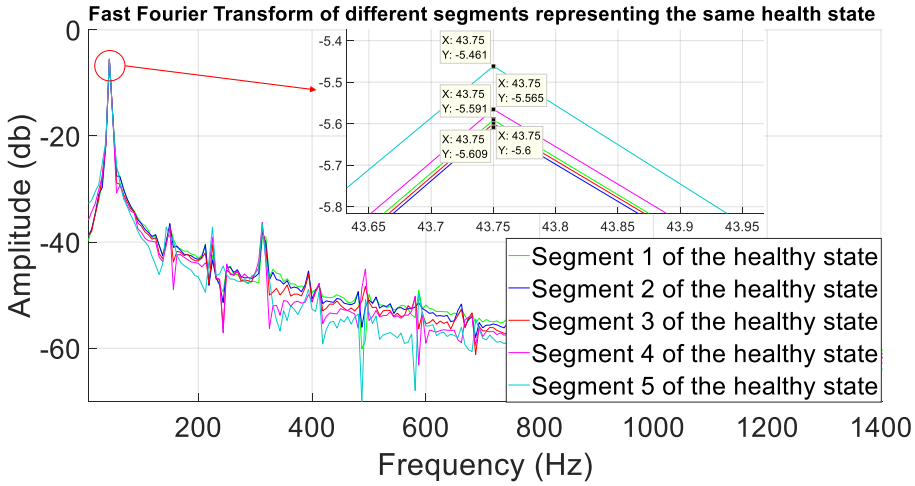

Figure 2.4: Illustration of speed oscillations impact using FFT.

2.2.4 Health indicators construction

After normalizing the segmented raw signals, the final step deals with the extraction of statistical features to build the health indicator for assessing the health state of the system. In this subsection, a new health indicator is proposed by a combination of the three features (KUR, VAR, MEAN). These features are chosen due to their dependencies to each other where the mean value is investigated in both VAR and KUR features and the VAR feature in used in the KUR feature (see Table 1.1). The proposed health indicator is expressed by Equation 2.4 and its physical meaning is discussed to explain how it works in the case of system condition monitoring.

$$HI = MEAN\left(F_1, F_2, F_3, ..., F_m\right) \tag{2.4}$$

where m represents the number of sub-segments needed to calculate the MEAN value. In this work, the value of m is chosen in such a way to finally obtain 100 observations of each health indicator.

$$F = KUR(s'_h) \times VAR(S)^2 \tag{2.5}$$

$$F = \frac{1}{L}\sum_{h=1}^{N/L}\left(s'_h - \overline{s'_h}\right)^4 \times \frac{\left(\frac{1}{N}\sum_{i=1}^{N}\left(S_i - \overline{S}\right)^2\right)^2}{\left(\frac{1}{L}\sum_{h=1}^{N/L}\left(s'_h - \overline{s'_h}\right)^2\right)^2} \tag{2.6}$$

where S is the total raw data with $i \in [1, N]$ points, s'_h is the normalized raw segment s_h of length L, expressed by equation 2.3.

From Equation 2.6, one can see two terms of the proposed health indicator. The first term represents the numerator of the KUR feature. It calculates the flattening of each signal segment s'_h around its MEAN value and the obtained results are illustrated in Figure 2.5.

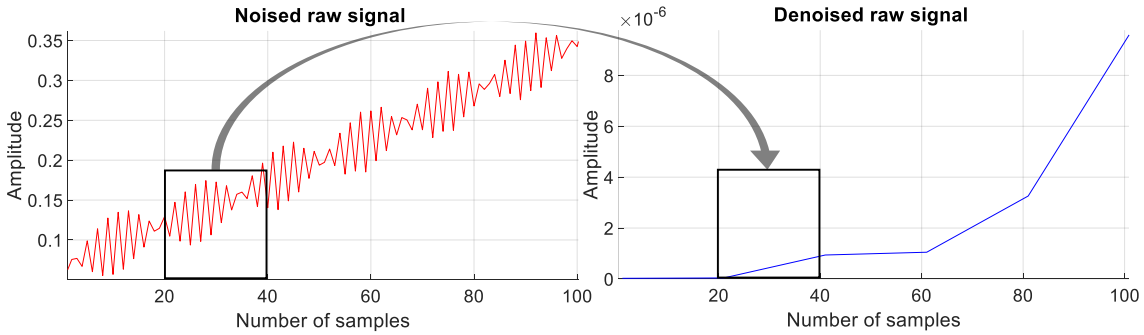

Figure 2.5: Result of the evaluation of the first term of the proposed HI.

$$feat_1 = \frac{1}{L}\sum_{h=1}^{N/L}\left(s'_h - \overline{s_h{}'}\right)^4 \tag{2.7}$$

This calculation allows reducing the signal noise while keeping the main information of the signal (Figure 2.5). Furthermore, Equation 2.7 allows the attenuation of the noise without losing the signal trend.

The second term of the proposed health indicator is the ratio between the squared variance of the total raw signal S and the squared variance of each segment s'_h. It consists

of a variance gain and is expressed by the following equation:

$$feat_2 = \frac{\left(\frac{1}{N}\sum_{i=1}^{N}\left(S_i - \overline{S}\right)^2\right)^2}{\left(\frac{1}{L}\sum_{h=1}^{N/L}\left(s_h^{'} - \overline{s_h^{'}}\right)^2\right)^2} \tag{2.8}$$

It evaluates the dispersion of each segment $s_h^{'}$ to the total dispersion of S. In fact, the increase in the VAR values indicates the appearance of a degradation. Moreover, to separate the health states of the system, the product of $feat_1$ by $feat_2$, that provides the F values presented by Equations 2.5 and 2.6, allows clearly separating different states of the system. Figure 2.6 shows a part of the result obtained after this multiplication.

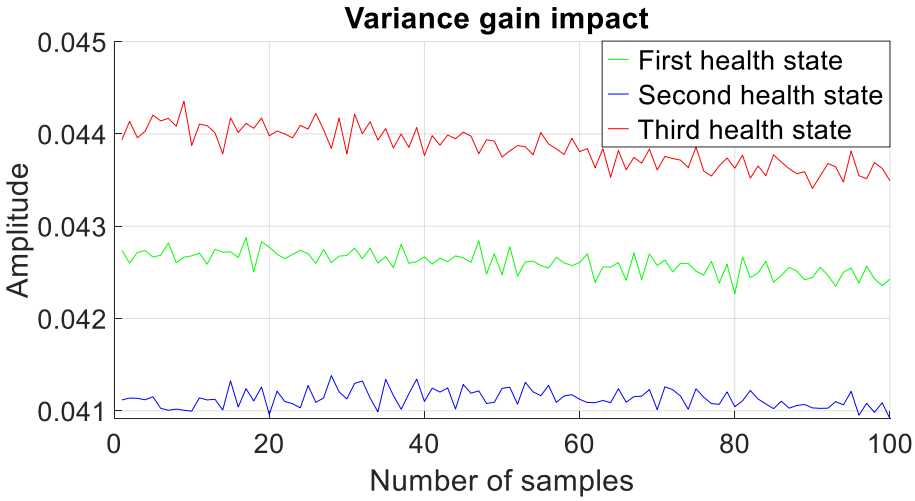

Figure 2.6: Result of the evaluation of the second term of the proposed HI.

Finally, the MEAN value calculated by Equation 2.4. It allow smoothing the extracted features F (Equation 2.6). The obtained result of this calculation is shown in Figure 2.7.

Comparing Figures 2.6 and 2.7, one can see that the MEAN operation allows reducing the outliers, which can be caused by the transient effect of the engine (engine starting). Figure 2.8 shows a multi-space representation (3D) of an extracted health indicators using three-phase current signals (i_a, i_b and i_c). One can see a clear separation between the classes of different states with negligible dispersion. Thus, the proposed health indicator can be easily applied to detect different health states of the system.

Note that the use of only one indicator representing a health state may not be sufficient to characterize different fault types as shown in Figure 2.9. In this situation, it is easy to get confusion between the constructed health indicators.

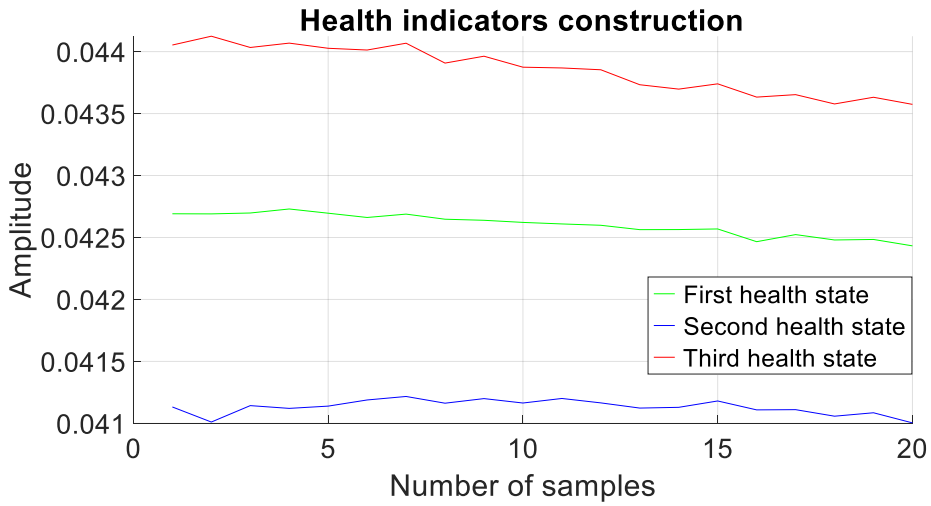

Figure 2.7: Health indicators construction.

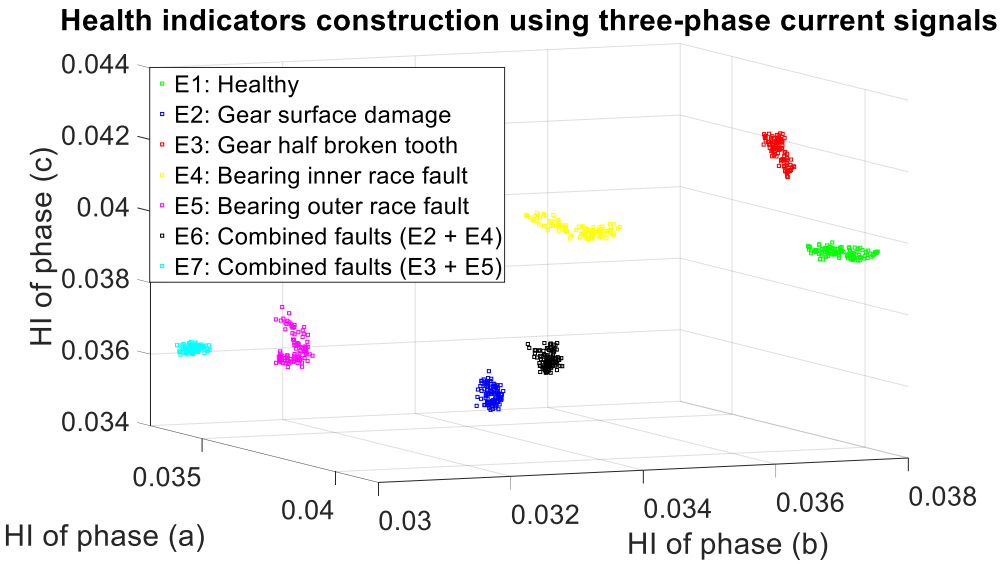

Figure 2.8: Illustration of the health indicators result in three-dimensional space.

Furthermore, data normalization to limit the dispersion plays an important role in the proposed method. Figure 2.10 illustrates the impact of feature extraction with and without data normalization.

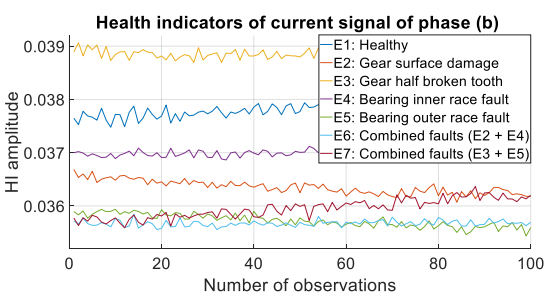

a) Health indicators of current Ib

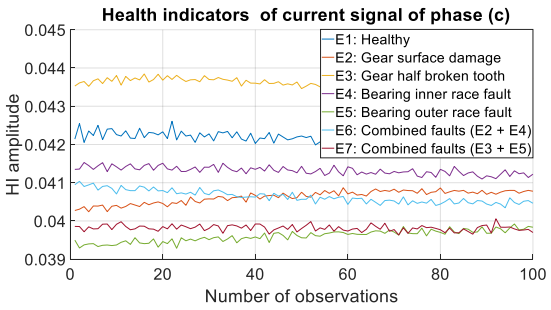

b) Health indicator of current Ic

Figure 2.9: Health indicators construction in one-dimensional space.

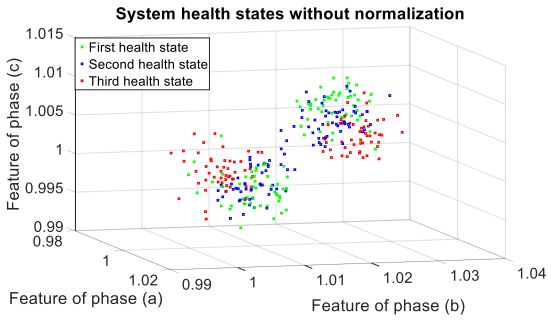

a) Feature extraction without normalization

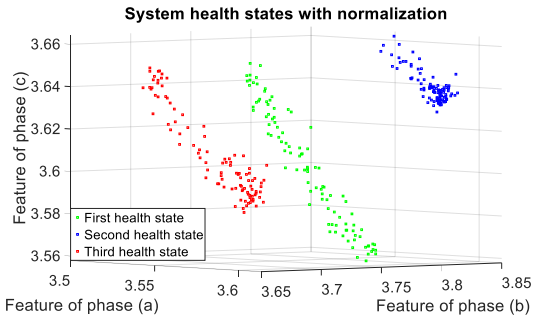

b) Feature extraction with normalization

Figure 2.10: Features representation considering the normalization step.

2.3 Fault detection case studies

This section aims to verify the effectiveness and the robustness of the proposed methodology based on a new health indicator to detect faults of different components in electrical motors. For this purpose, three different case studies are investigated taking into account numerous fault types of critical components such as bearing, gear, rotor-bar, unbalanced supply motor and cutting tool defects. This investigation can be, for example, helpful in a production line where several systems are connected to each other and therefore no need to develop several techniques to monitor each critical components defects. As mentioned in data acquisition (Section 2.2.1), we have considered, for monitoring the defects of the motor critical components, heterogeneous sensor measurements such as three-phase current and voltage signals, three-axis vibration, force and torque measurements. The raw data are recorded by National Instrument acquisition cards under various operating conditions. Then, the recorded data are injected into the signal processing algorithm to

extract the features and build the health indicator using Equation 2.4. The performance of the constructed health indicator is highlighted when comparing with the ones reported in the literature for detection of machinery faults. Note that the obtained health indicator observations are represented in three-dimensional space for more precise and clear results. The axes x, y and z represent respectively the health indicators of the phases a, b and c in the case of the current and the voltage signals, while they characterize the horizontal, the vertical and the axial directions in the case of the vibration, force and torque signals.

2.3.1 First application: Detection of bearing and gear faults

The first case study concerns FDD of bearing and gear components in a test bench named LASPI and installed at the LASPI laboratory (Figure 2.11).

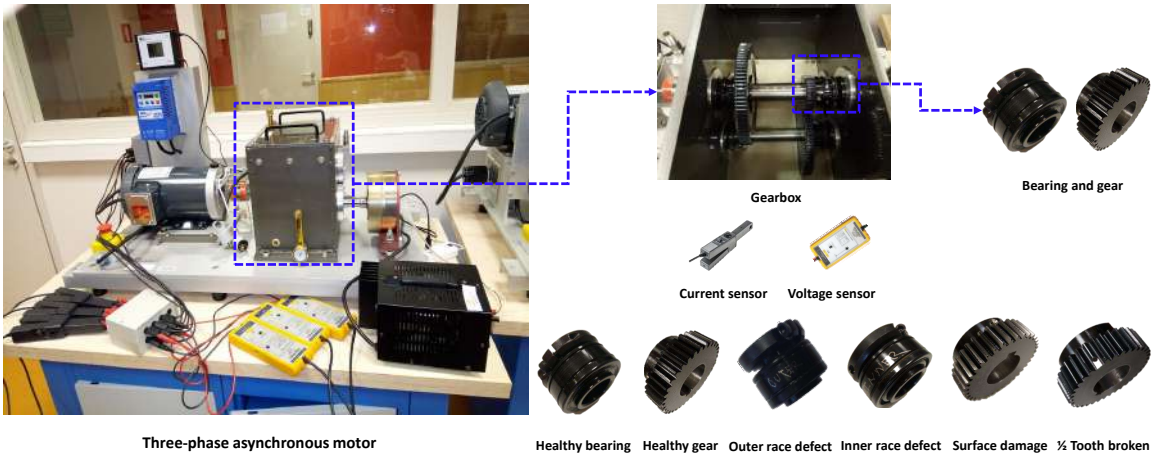

Figure 2.11: Test bench at LASPI laboratory.

In this case study, an asynchronous motor, powered by a pulse generator, drives a gearbox of three shafts, input shaft, intermediate shaft and output shaft. Each shaft contains bearing and gear components that are changed at the intermediate shaft level for the experiments. At the output shaft, an electromagnetic brake is placed in order to apply a load level to the motor. This test bench uses three-phase current and voltage signals (i_a, i_b, i_c and v_a, v_b, v_c) corresponding to the phase (a), phase (b) and phase (c) of the pulse generator for the assessment of the gearbox components. The data are recorded with a duration of 10 seconds at a sampling frequency equal to 25.6 kHz under different operating conditions, see a brief summary in Table 2.1.

System 1: LASPI test bench			
Speed (rpm)	Load level (%)	Health state	Acquisition parameters
		E1: Healthy motor	
1477	0%, 25%, 50%, 75%	E2: Gear surface damage	
		E3: Gear $\frac{1}{2}$ broken tooth	Hardware: NI
2077	0%, 25%, 50%, 75%	E4: Bearing inner race fault	Sampling rate: 25,6 kHz
		E5: Bearing outer race fault	File extension: .csv
2677	0%, 25%, 50%, 75%	E6: Combined faults (E2 + E4)	Duration file: 10s/.csv
		E7: Combined faults (E3 + E5)	

Table 2.1: Experiment tests performed on the LASPI test bench.

2.3.1.1 Investigation of literature HIs on LASPI platform

In this subsection, the performance of the literature health indicators (RMS, VAR, Kurtosis, FM_4, FM_0 and ER) are investigated to show their limits. To perform this task an example of using the three-phase current signals under speed corresponding to 45 Hz (2677 rpm) and a load level of 75% are considered for the highlights.

From Figure 2.12, one can see that each proposed health indicator in the literature has its own contribution to fault detection performance. However, these results cannot clearly separate the classes representing the different health states of the gearbox parts. In detail, the RMS and ER values cannot group the observations of the same state in the same class. Besides, the VAR, FM_0, FM_4 and KUR features allow grouping the observations in the corresponding class but with low distance between classes and large dispersion within a class.

2.3.1.2 Performance of the proposed HI on LASPI platform

Figure 2.13 presents the performance of the proposed health indicator for FDD of bearing and gear components when investigating the LASPI test bench under different operating conditions: speed corresponding to 25 Hz (2077 rpm) and 45 Hz (2677 rpm) with 0% and 75% load levels, respectively. The results corresponding to the speed of 35 Hz (2077 rpm) with 0% and 75% load levels are shown in Appendix A.

From Figure 2.13, one can see that using either the current or voltage signals, the proposed method allows clearly separating the healthy state from different fault types (single and combined defects) of the bearing and the gear parts in LASPI test bench. In addition, there exists a negligible dispersion of the observations within each class. The robustness of the proposed health indicator is also highlighted when considering different operating conditions and different types of measurements.

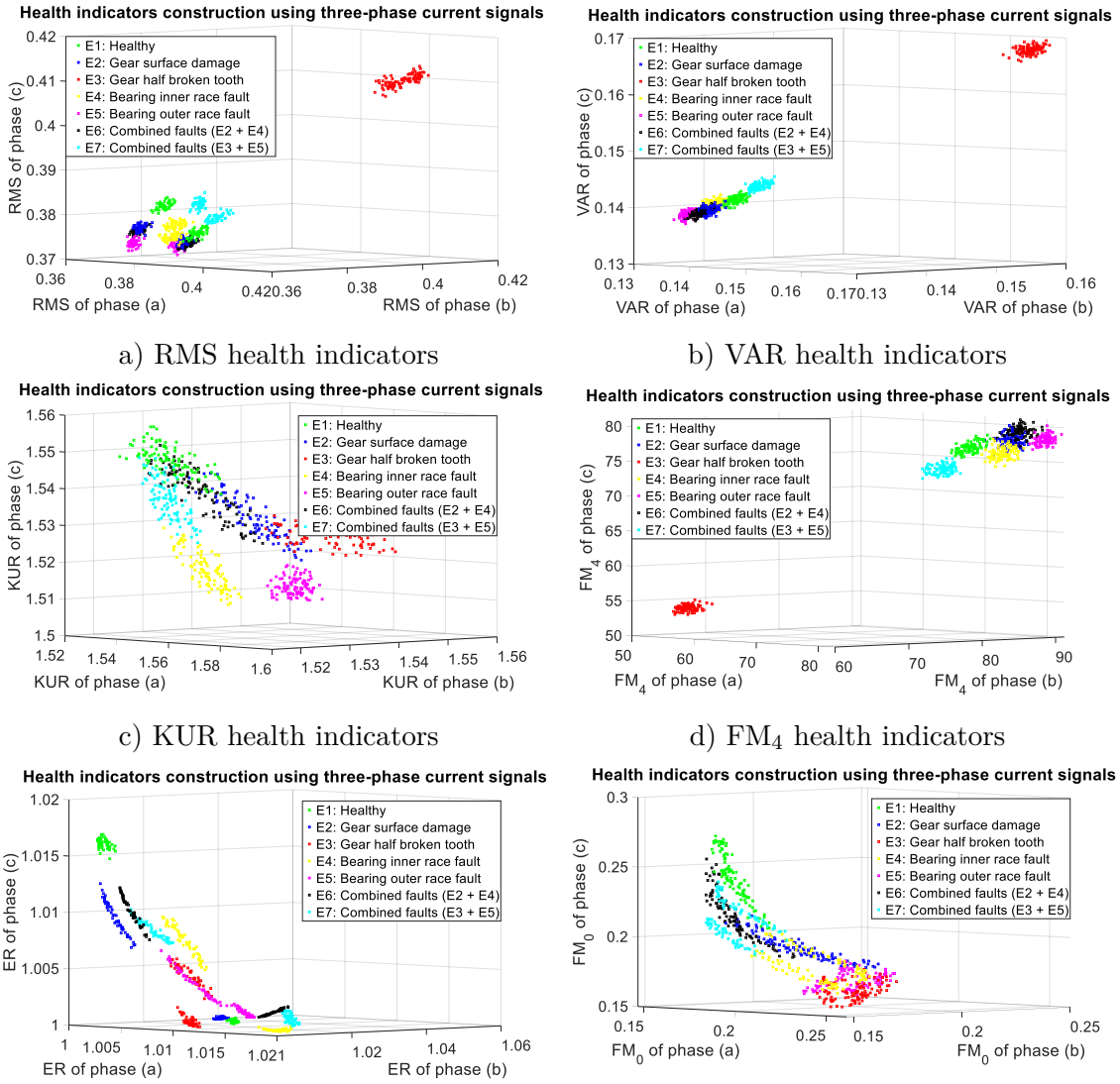

a) RMS health indicators

b) VAR health indicators

c) KUR health indicators

d) FM_4 health indicators

e) ER health indicators

f) FM_0 health indicators

Figure 2.12: Application of the literature HIs on LASPI platform.

2.3.2 Second application: Detection of bearing and rotor faults

The second case study concerns FDD of a motor on AMPERE laboratory test bench, see Figure 2.14. In this system, a three-phase induction motor drives a rotating shaft, which is the squirrel cage rotor. This motor part is made of 28 bars. For each experiment, the rotor is replaced by the one containing the defect (one, three, four bars broken etc.). Note that the rotor bars were broken by brooking the conductors of the squirrel cage. In addition, an unbalanced stator defect (10%) is also investigated.

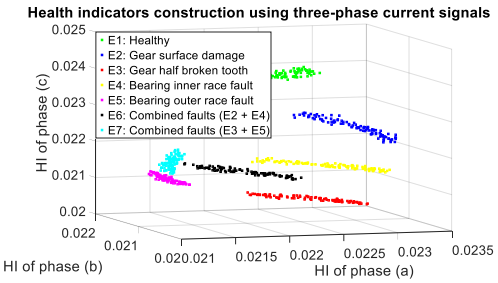

a) Current signals, 25 Hz, 0%

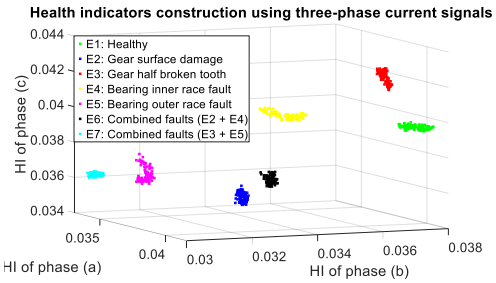

b) Current signals, 25 Hz, 75%

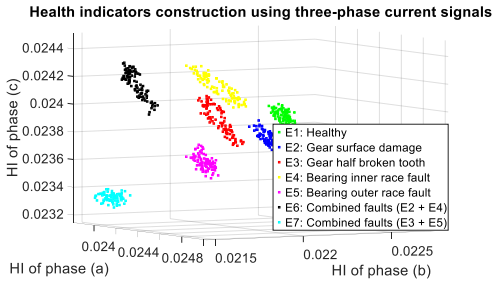

c) Current signals, 45 Hz, 0%

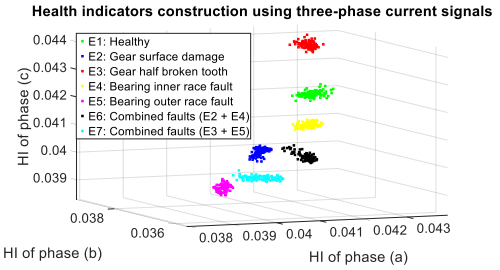

d) Current signals, 45 Hz, 0%

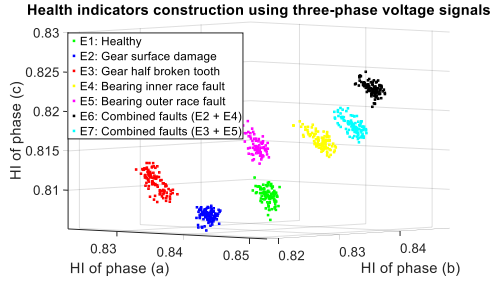

e) Voltage signals, 25 Hz, 0%

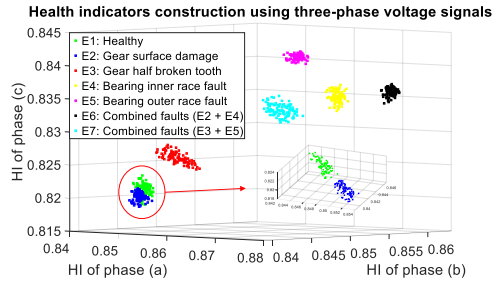

f) Voltage signals, 25 Hz, 75%

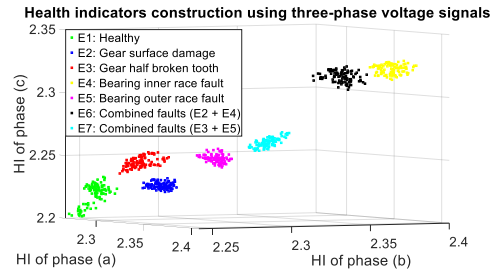

e) Voltage signals, 45 Hz, 0%

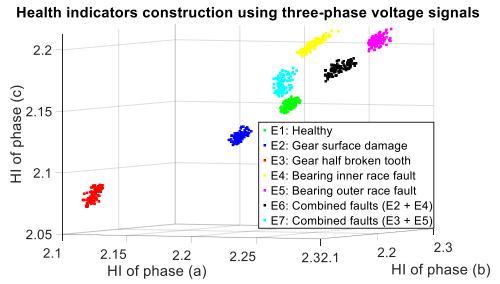

f) Voltage signals, 45 Hz, 75%

Figure 2.13: Proposed HI on LASPI platform using.

To monitor the motor health state, the three-phase current and voltage sensors, placed at the output of the inverter, and the three-axis vibration sensor are used, placed at the

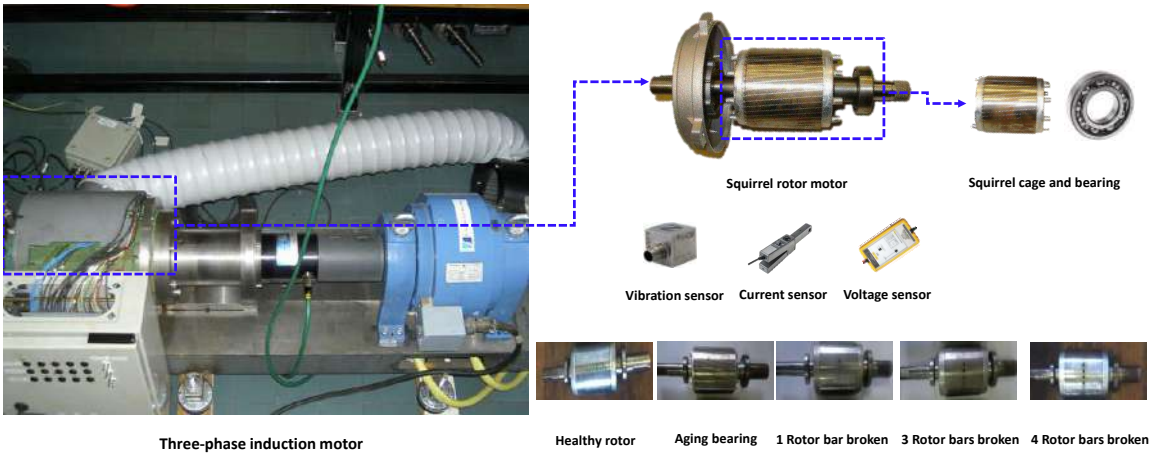

Figure 2.14: Test bench at AMPERE laboratory.

horizontal, the vertical and the axial flange of the motor. The sensor signals are recorded with a sampling frequency of 20 kHz with a duration of 5 seconds. The experimental tests are performed under five load levels (0%, 25%, 50%, 75% and 100%). These operating conditions are summarized in Table 2.2.

System 1: AMPERE test bench			
Speed (rpm)	Load level (%)	Health state	Acquisition parameters
1440	0%, 25%, 50%, 75%, 100%	E1: Healthy motor E2: One broken rotor bar Three broken rotor bars E4: Bearing inner race fault E5: Aging bearing E6: Unbalanced supply motor (10%)	Hardware: NI Sampling rate: 20 kHz File extension: .mat Time: 10 s/file

Table 2.2: Experiment tests performed on AMPERE test bench.

2.3.2.1 Investigation of literature HIs on AMPERE platform

In this subsection, the performance of the literature health indicators are investigated for FDD of the mentioned defects of the motor. Figure 2.15 presents the obtained results when using three-phase current signals under the operating condition defined by a motor speed corresponding of 25 Hz and a load level of 100%.

From Figure 2.15, one can see that the RMS and the VAR features allow separating different fault types of the motor, such as one, three, four broken rotor bars and bearing defects. However, the separability between the healthy state and unbalanced supply motor is not well performed. Besides, the KUR and FM_4 allow separating the bearing defect and unbalanced supply defect from the healthy class. Nevertheless, the difference between

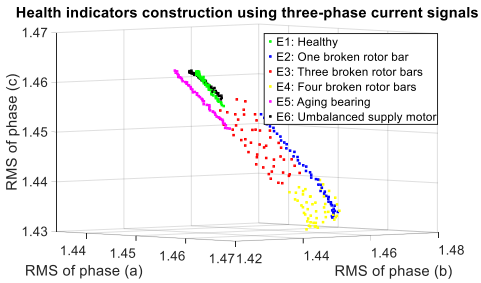

a) RMS health indicators

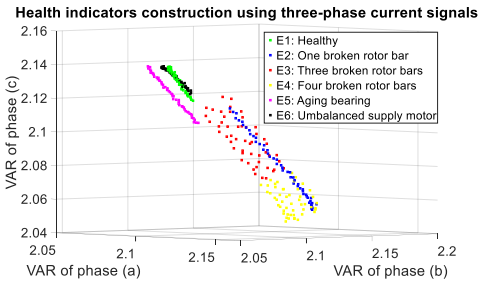

b) VAR health indicators

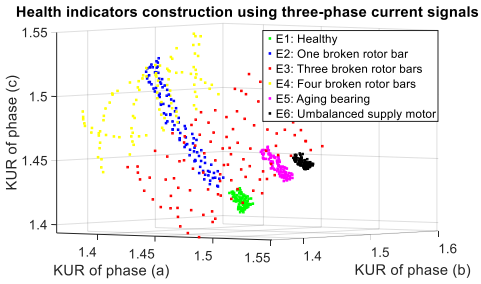

c) KUR health indicators

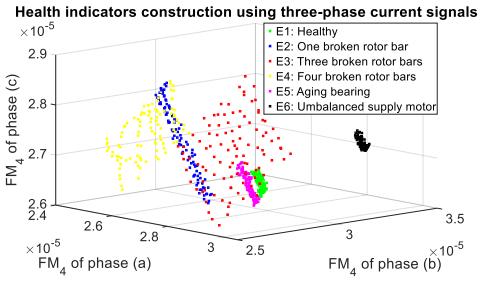

d) FM_4 health indicator

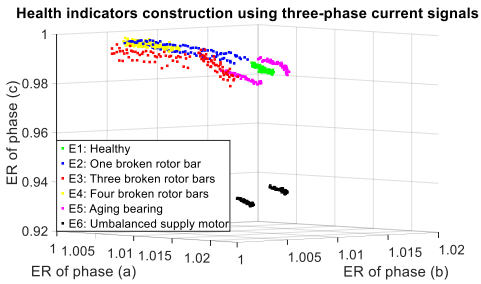

e) ER health indicators

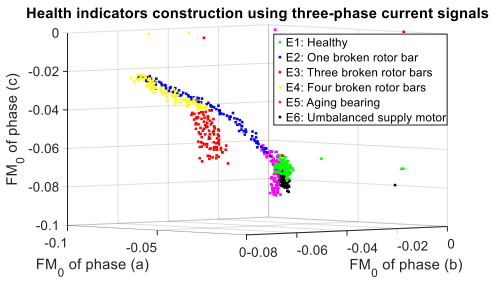

f) FM_0 health indicator

Figure 2.15: Application of the literature HIs on AMPERE platform.

one, two and four rotor broken bars cannot be detected. In addition, there exists a wide dispersion of the observations within a same class. Finally, the ER and FM_0 features do not allow separating the classes.

2.3.2.2 Performance of the proposed HI on AMPERE platform

Figure 2.16 shows the performance of the proposed health indicator for FDD of different motor defects on the AMPERE test bench.

One can notice that the proposed health indicator allows clearly separating the different health states of the motor with a low dispersion between the observations within a class.

The effectiveness of the health indicator is also highlighted when using different sensor measurements, such as three-phase current, voltage and three-axis vibration signals, to detect both electrical and mechanical defects. Moreover, the robustness of the proposed health indicator is investigated when considering different operating conditions (a motor speed corresponding to 25 Hz with a load level of 50% and 100%). The obtained results when investigating the operating condition of 0% and 75% load level are shown in Appendix A.

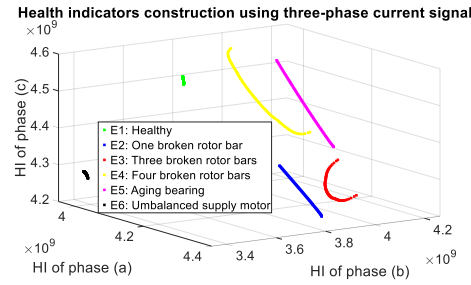

a) Current signals, 25 Hz, 50%

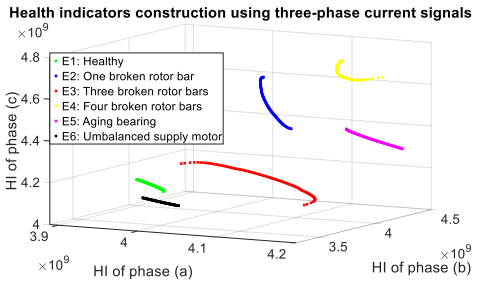

b) Current signals, 25 Hz, 100%

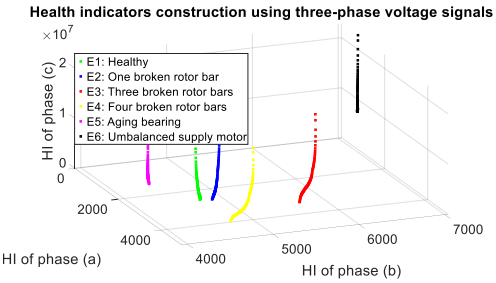

c) Voltage signals, 25 Hz, 50%

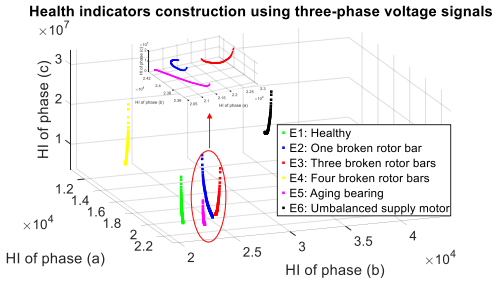

d) Voltage signals, 25 Hz, 100%

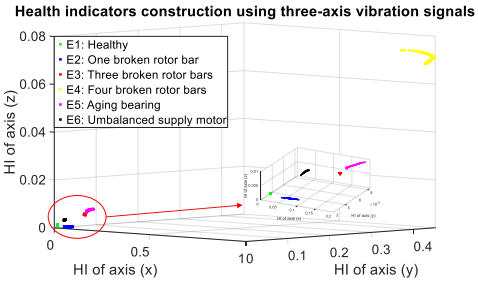

e) Vibration signals, 25 Hz, 50%

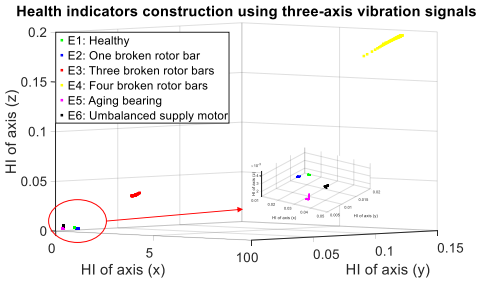

f) Vibration signals, 25 Hz, 100%

Figure 2.16: Proposed HI on AMPERE platform.

2.3.3 Third application: Detection of machining tool faults

The last case study investigates the thesis demonstrator and concerns fault detection of a cutting tool at the 6^{th} axis of the machining robot (ABB six-axis robot), see Figure 2.17.

The test bench is installed at METALLICADOUR, a resource and technology transfer center. In detail, a three-phase synchronous motor drives a cutting tool for machining aluminum pieces. Note that the cutting tool contains three cutting edges. In the case study, four components are used to achieve the experimental tests, as shown in Figure 2.17, healthy, surface damage, flack damage and broken tooth.

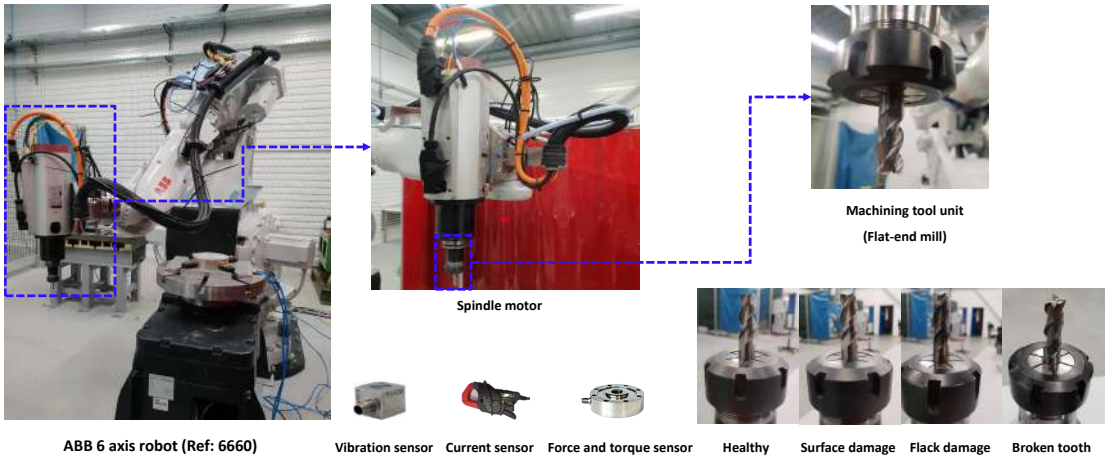

Figure 2.17: METALLICADOUR test bench.

Concerning the machining process, the manufacturing of an aluminum piece is investigated. This object is a small part used in aircraft industry. The machining parameters, which correspond to different operating conditions (i.e. two cutting depth levels, three different feed rates) of the machining process, are summarized in Table 2.3.

System 3: METALLICADOUR test bench				
Speed (rpm)	Feed rate (mm/min)	Cutting depth (mm)	Health state	Acquisition parameters
14000	1890	5	E1: Healthy tool	Hardware: NI
18000	1890	5	E2: Tool surface damage	Sampling rate: 25,6 kHz
14000	2730	5	E3: Tool flack damage	File extension: .csv
14000	1890	10	E4: Tool broken tooth	Time: 10 s/file

Table 2.3: Experiment tests performed on METALLICADOUR platform.

Regarding the data acquisition part, firstly, three-axis force and torque sensor are placed at the sixth axis of the robot. Secondly, the three-axis vibration sensors are placed as near as possible to the cutting tool. Finally, the three-phase current sensors are placed at the output of the inverter of the machining tool. The measurement data are then recorded with a sampling frequency of 25.6 kHz and a duration of 40 seconds for each file. Note that the data are collected in different range of time to observe the stationary of the results i.e. each experiments are performed three time a day, morning, noon and afternoon.

2.3.3.1 Investigation of literature HIs on METALLICADOUR platform

The traditional health indicators are extracted from the current signals recorded under the operating condition of 5 *mm* of cutting depth, 1890 *rpm* of feed rate and 14000 *rpm* of spindle speed and shown in Figure 2.18.

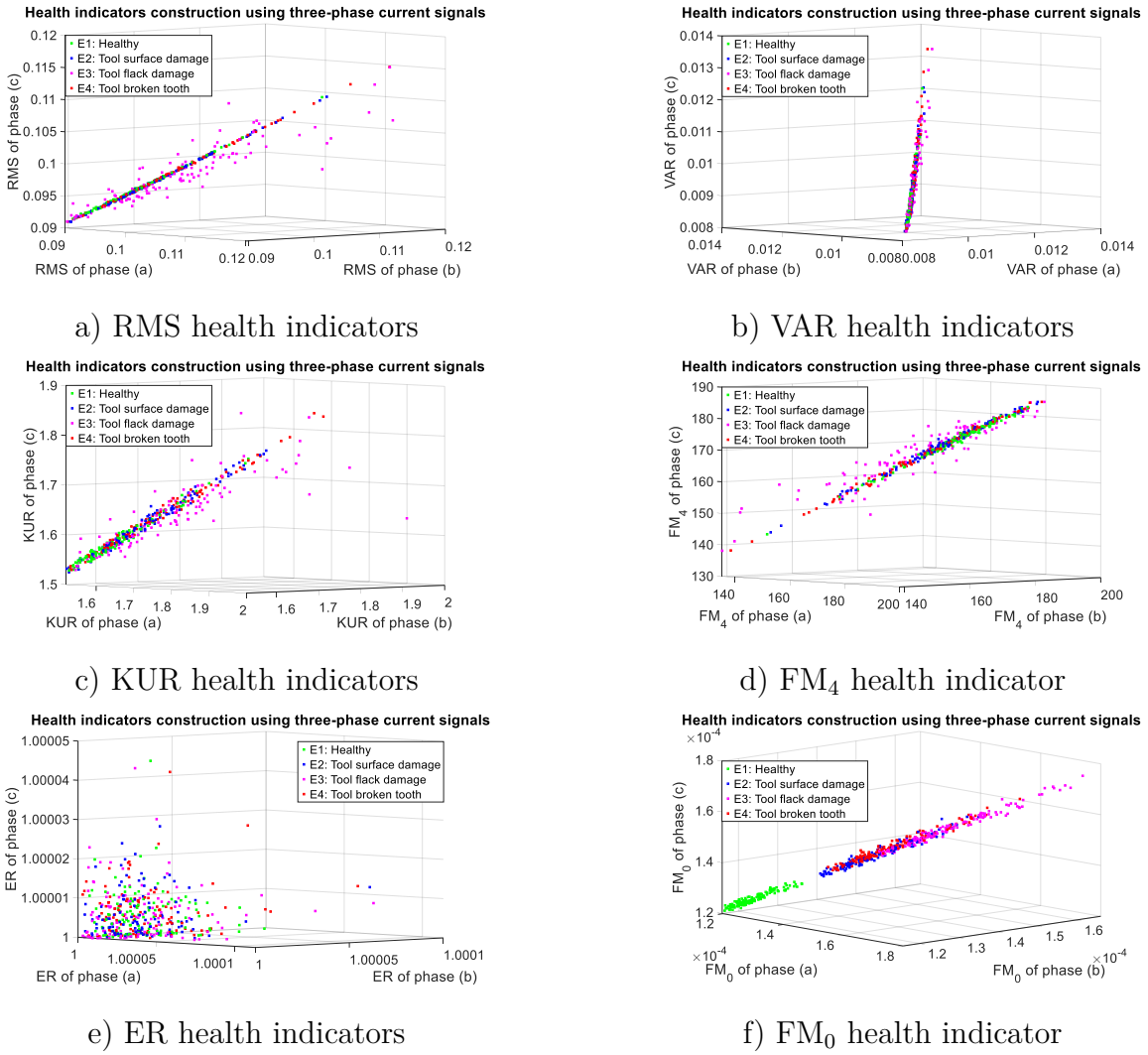

a) RMS health indicators

b) VAR health indicators

c) KUR health indicators

d) FM_4 health indicator

e) ER health indicators

f) FM_0 health indicator

Figure 2.18: Application of the literature HIs on METALLICADOUR platform.

From Figure 2.18, one can see that the health indicators taken from literature cannot separate the different classes of the cutting tools. In addition, there exists a wide dispersion of the observations within each class.

2.3.3.2 Performance of the proposed HI on METALLICADOUR platform

Figures 2.19, 2.20, 2.21 and 2.22, one more again, highlights the performance of the proposed HI for detecting different tool states in the METALLICADOUR test bench.

One can notice that the proposed health indicator allows clearly separating different health states of the cutting tool with a low dispersion between the observations within a class in most of the cases. The robustness of the health indicator is clearly proven when considering different measurements (three-phase current, three-axis vibration, force and torque signals) and when investigating different operating conditions.

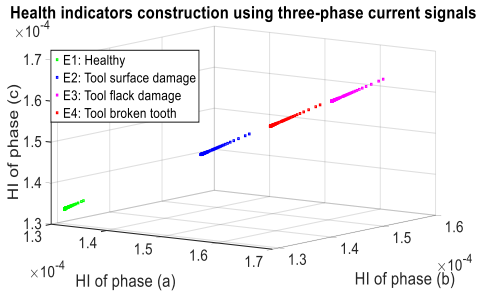

a) 233 Hz, 5 mm, 1890mm/mn

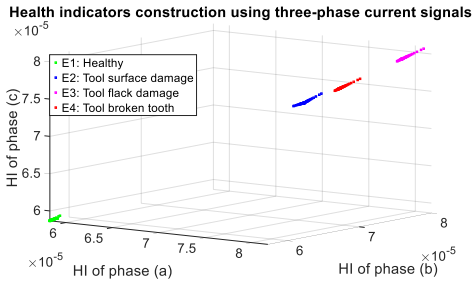

b) 300 Hz, 5 mm, 2730mm/mn

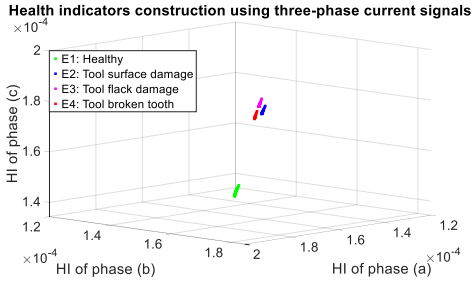

c) 300 Hz, 5 mm, 1890 mm/mn

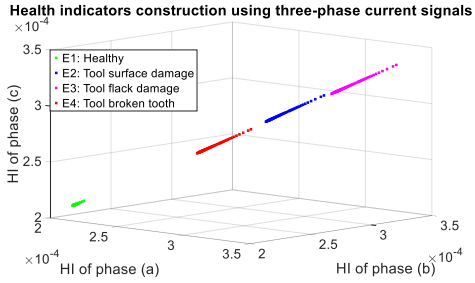

d) 233 Hz, 10 mm, 1890mm/mn

Figure 2.19: Proposed HI on METALLICADOUR platform using current signals.

2.3.3.3 Synthesis of the performance results of the proposed method

Table 2.4 summarizes the obtained results when using the proposed method, based on a new health indicator, and the ones reported in the literature. Considering the obtained results from three test benches, one can see that both electrical (i.e. unbalanced supply motor and broken rotor bars) and mechanical (i.e. bearing and cutting tool) faults can be clearly detected based on the proposed health indicator with high separability between the classes and low dispersion between each class observations. In addition, its robustness is proven through numerous systems under various operating conditions with different

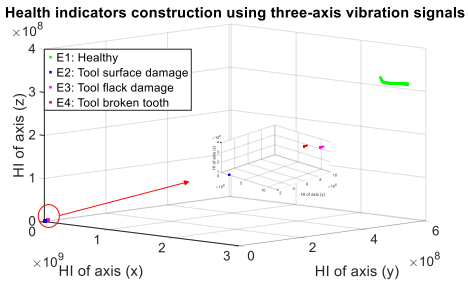

a) 233 Hz, 5 mm, 1890mm/mn

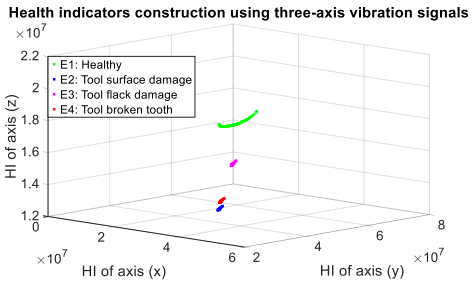

b) 300 Hz, 5 mm, 2730mm/mn

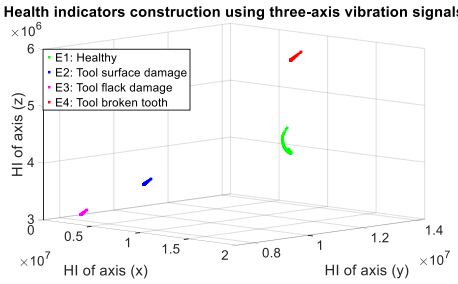

c) 300 Hz, 5 mm, 1890 mm/mn

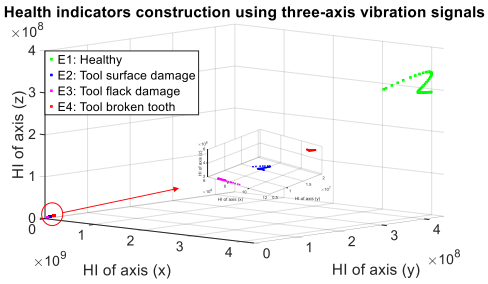

d) 233 Hz, 10 mm, 1890mm/mn

Figure 2.20: Proposed HI on METALLICADOUR platform using vibration signals.

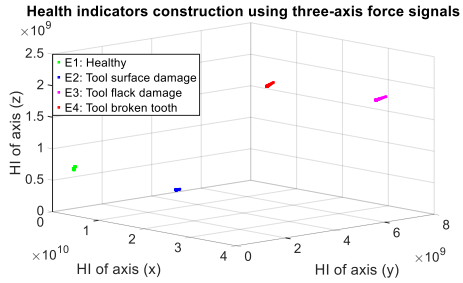

a) 233 Hz, 5 mm, 1890mm/mn

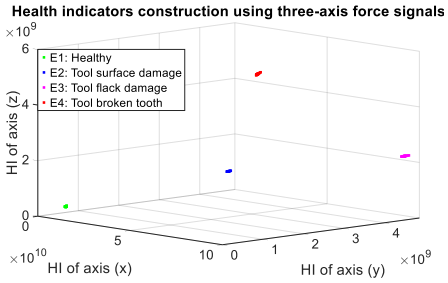

b) 300 Hz, 5 mm, 2730mm/mn

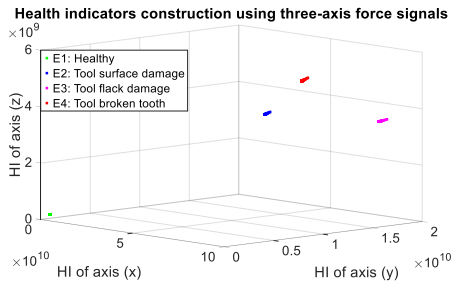

c) 300 Hz, 5 mm, 1890 mm/mn

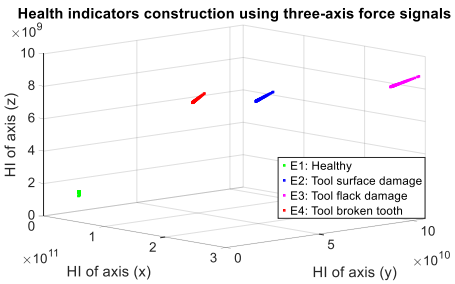

d) 233 Hz, 10 mm, 1890mm/mn

Figure 2.21: Proposed HI on METALLICADOUR platform using force signals.

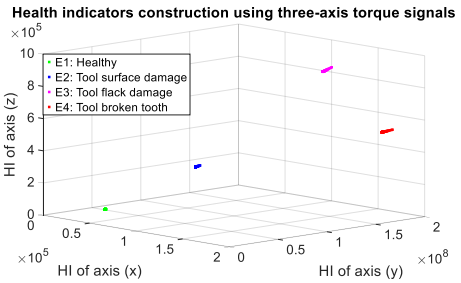

a) 233 Hz, 5 mm, 1890mm/mn

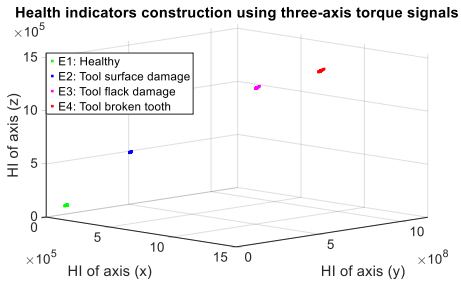

b) 300 Hz, 5 mm, 2730mm/mn

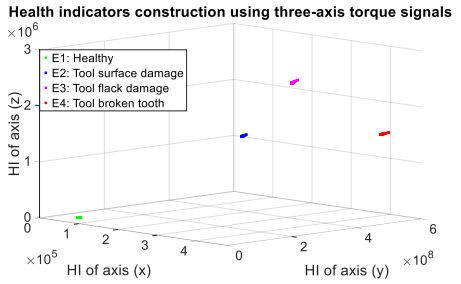

c) 300 Hz, 5 mm, 1890 mm/mn

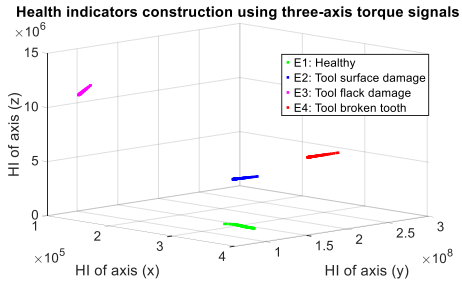

d) 233 Hz, 10 mm, 1890mm/mn

Figure 2.22: Proposed HI on METALLICADOUR platform using torque signals.

	First test bench		Second test bench		Second test bench	
	Literature HIs	Proposed HI	Literature HIs	Proposed HI	Literature HIs	Proposed HI
Separability	Low	High	Low	High	Low	High
Dispersion	High	Low	High	Low	High	Low

Table 2.4: Synthesis of the performance results of the health indicators.

sensor measurements. Hence, one can conclude that the proposed health indicator is a good candidate for non-invasive techniques to monitor the system health state based on electrical measurements, such as current and voltage signals.

2.4 Conclusion

A practical and generic methodology to construct HI for monitoring multi-components in industry have been presented in this chapter. In detail, the proposed health indicator was created based on a combination of meaningful features extracted from time and frequency domains. This explicit combination represents a particular physical meaning and allows clearly separating different system health states.

The performance and robustness of the proposed method were proven through numerous

case studies. The obtained results highlighted its health assessment ability for numerous critical components of different systems, such as bearing, gear, rotor bar in rotating machines and machining unit in cutting tools, placed at the sixth axis of machining robots. Considering various operating conditions with different sensor measurements, the proposed health indicator clearly separates the system health states with a low dispersion within the same class; whereas the health indicators reported in literature lead to less separability. In addition, the use of electrical signals, i. e. current signals instead of mechanical signals such as vibrations, brings significant practical benefits thanks to its non-invasive way of monitoring rotating machines. Indeed, generally, most of these machines originally include in their control systems current, voltage or power sensors, which can be used directly for fault detection purposes. Therefore, this is very appreciated by industrials as there is no need of new sensors to install and new certification to do, leading to money and time savings.

After fault detection, the next step deals with fault diagnostics. For this purpose, the constructed health indicators can provide useful pattern information for an automatic failure diagnostic procedure. However, in dynamic systems such as the multi-axis robots, it is difficult to recognize all eventual faults that will occur during the process. Hence, the next chapter aims to deal with online fault diagnostic for dynamic systems with unknown fault types.

Chapter 3

Information fusion for online diagnostics of unknown faults

Contents

3.1 Introduction

In the previous chapter, a new method for the construction of an effective, practical, and robust HI was presented. This HI is used to characterize the different health states of the system, e.g. healthy and faulty states, and can be used as the pattern information for an automatic diagnostic procedure. However, as mentioned in Chapter 1, there exists a critical drawback in such fault diagnostics approach, that is its performance strictly depends on the prior knowledge of fault types labels.

This chapter aims to address the gap mentioned above. It proposes a new and more efficient online fault diagnostics approach that allows automatically updating the unknown

fault types. Especially, the proposed method deals with the challenges posed for health monitoring of a system with dynamic behaviors, e.g. machining robots. More precisely, it is applied for monitoring the multi-axis robots to diagnose the origin of their drifts, i.e. which robot axis deviates from its nominal trajectories.

To do this, Section 3.2 gives a general overview of the challenges in fault diagnostic of multi-axis machining robots and highlights the need for a new and effective methodology of fault diagnostic for this type of system. In Section 3.3, the overall steps of the proposed methodology with a detailed flowchart is presented. Then, its performance is verified through an industrial six-axis machining robot, in Section 3.4. Finally, Section 3.5 gives a synthesis on the chapter.

3.2 Fault diagnostics of multi-axis robots

Nowadays, the rise of intelligent robots is one of the prominent enablers towards smart manufacturing facilities (Lee et al., 2015b, Diez-Olivan et al., 2019). Indeed, the implementation of Artificial Intelligence (AI) algorithms in robotic systems improves their efficiency as well as their interaction with other systems in the production lines. In this direction, one can cite the machining robots that facilitate complex manufacturing processes due to the flexibility of robot arms with high precision and high-performance (Gotlih et al., 2017). However, during the manufacturing process, the occurrence of machining tool defects or drifts in the robot arms impacts the accuracy of the robot Tool Center Position (TCP) and then leads to critical product quality damages. For example, the authors in (Qiao and Weiss, 2018, Kuric et al., 2018) show that the errors produced in the robot positioning significantly affect the repeatability of the robot motions and consequently lead to significant product quality damages. Therefore, it is necessary to deploy advanced monitoring techniques to maintain the system in good conditions and ensure adequate production quality.

The first issue concerning the monitoring of robot tool defect was addressed in Chapter 2 by proposing a new health indicator that separates the different health states of the tool wears using current, vibration, force and torque signals under different machining conditions. Besides, regarding the second issue related to robot behavior monitoring, it can be tackled in two ways, as shown in Figure 3.1: 1) by focusing on the product quality or 2) by analyzing the robot axes positioning.

The first possibility remains an efficient way to detect anomalies in the robot. However, it is not possible to track back the origin of the defect, i.e. to identify the axis that deviates from its nominal trajectory. A major part of researches on monitoring the product quality proposes alternative solutions such as using additional sensors on the robot and then,

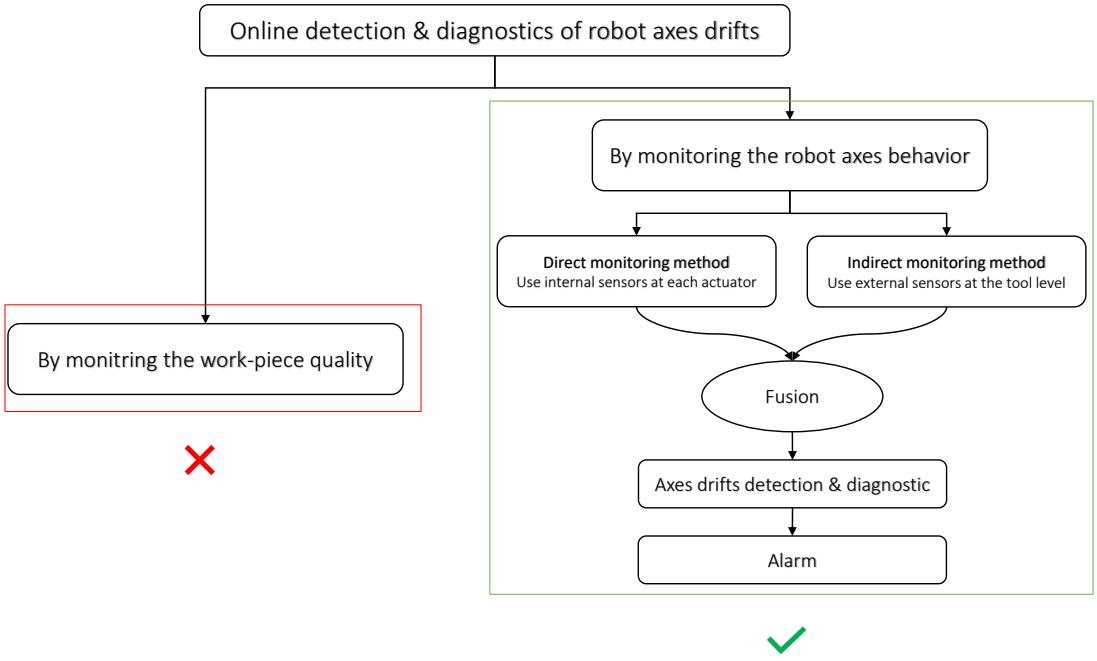

Figure 3.1: Overview of the positioning and contribution of the proposed method.

based on their processing results, act on the system to correct the errors. In (Segreto et al., 2015), the authors use an acoustic emission sensor placed at the robot tool level for pattern recognition of polished workpiece surface roughness. The presented work in (Chen and Nof, 2007) estimates that errors of the end-effector of a robot may highly impact the product quality. Regarding the second option, i.e. the monitoring of robot axes behavior, it remains unexplored. The first studies in this direction are conducted by the National Institute of Standards and Technology (NIST) center by implementing the PHM concept for condition monitoring of multi-axis robots. Their published works (Qiao and Weiss, 2018) propose the utilization of a multi-dimensional laser tracker sensor to monitor the robot tool center position in a multi-space dimension. However, this type of technology remains expensive for widespread use in real industrial processes. Therefore, the development of alternative techniques to monitor the behavior of the multi-axis robot is still an important challenge for researchers as well as for industrials.

Considering the above synthesis, one can notice that only a few works addressed the issue of condition monitoring of the robot axes behavior, despite its importance and the benefits it brings for the end-users. Therefore, we propose in the remaining of this chapter to deal with this issue.

Among different anomalies of a robot, the arms deviations from the nominal positions are one of the crucial degradations that must be cautiously tracked. Indeed, a small deviation in the robot positioning may significantly affect security and product quality. Hence,

it is necessary to develop an efficient monitoring methodology to detect and diagnose the origin of the drifts. The developed methodology should meet the following requirements:

- Capability for detecting and localizing the origin of the robot drifts from the starting point of the machining operation.
- Ability for automatic labeling of unknown drifts of the robot axes thanks to the direct monitoring mode.
- Capacity for providing more accurate and efficient fault diagnostic of the robot axes behavior.

This chapter aims to deal with the issue mentioned above. We developed a new efficient methodology for online diagnostics of robot drifts based on information fusion of indirect and direct monitoring. The direct monitoring exploits the already installed encoders on each servomotor of the robot while the indirect monitoring uses heterogeneous sensors (current, vibration, force and torque) placed at the robot tool level. The proposed methodology includes two phases: offline and online phase.

First, in an offline phase, the heterogeneous sensor measurements (current, vibration, force and torque signals) of the indirect monitoring mode are used to build health indicators which are then fused through an auto-encoder network. The output of this latter model consists of new relevant health indicators that are projected on a multidimensional space to reveal the health states of the robot. These states are then learned by a classifier for later detection and diagnostics. In practice, it happens that new drifts may occur during the operation of the robot. In this case, the previously learned classifier is updated online by exploiting the data provided by the direct monitoring and used to localize the origins of the drifts. The update consists of labeling the new detected drifts and using them to re-train the classifier. The advantage of using the indirect monitoring is that it can continuously assess the robot health state from the beginning to the end of the machining process. However, its performance strictly depends on the availability of the data related to all the possible drift scenarios that the robot may undergo to learn a representative classifier. Concerning the direct monitoring, it allows us to precisely localize the origin of any drift in the robot axes, even if it is not learned. Nevertheless, in this case, the drifts cannot be detected and localized online but with an elapsed time needed to collect sufficient data from the encoder sensors. Consequently, its practical implementation becomes questionable. Therefore, the fusion of the two techniques can be a promising contribution. It allows practitioners to monitor their machining processes from the beginning, quickly detecting and localizing axes deviation origins, and proposing appropriate decisions for more availability, security and quality.

3.3 Proposed methodology for new online fault diagnostics

This section presents the methodology based on the information fusion of direct and indirect monitoring approaches for multi-axis robot drifts diagnostics. It inherits the advantages of both monitoring and overcoming the drawbacks of each approach considered separately. The pros and cons are summarized in Table 3.1.

	Advantages	**Disadvantages**
Direct monitoring	No additional sensors No additional acquisition system Localize the origin of drifts	Require an elapsed time to start Discrete inspection Infeasible in case of encoder failure.
Indirect monitoring	Continuous health monitoring Early detection and diagnostics of known robot axis drifts.	Require additional sensor Require many historical scenarios to learn failure patterns.
Fusion of Direct & Indirect monitoring	Continuous monitoring Automatically update the failure patterns for early detection and diagnostics of robot axis drifts.	For unknown types of axis drifts, infeasible in case of encoder failure.

Table 3.1: Pros and cons of the proposed methodology.

In direct monitoring, the encoder sensors already placed on each robot actuator are used to track the errors between the nominal and the actual positions of the robot axes. Then, these errors are investigated to evaluate the health indicator of each robot axis, and thus localize the origin of the axes drifts. The direct use of the encoder measurements allows precisely and effectively identifying the drifts origin without need to have a priori knowledge on the faulty states and consequently become a good unsupervised diagnostics tool. However, this technique requires an elapsed time of few minutes to collect an essential amount of data for assessing the robot axis motions and therefore cannot be widely deployed in real-time applications for early anomaly detection.

In indirect monitoring, instead of directly tracking the robot motions, another part of the robot that is significantly affected by the robot axis deviations is investigated. In fact, the last robot arm (axis), which carries the end-effect tool, can represent the positioning of the previous articulations. When one of the arm motion deviates from its nominal position, it directly affects the accuracy of the tool center placement. Hence, monitoring the tool behavior can provide useful information about the deviation of the robot axes. Also, at the tool level, it is not difficult to install sensors for acquiring different signals such as vibration, force, and torque. Each of these signals brings a particular advantage to monitor the robot behavior, so the fusion of them can provide a promising alternative contribution to track

the robot motions in real-time for early anomaly diagnostics. However, as the sensors used in this monitoring approach do not directly reflect the robot motions, it is necessary to map the relation between the acquired measurements and the axis drift types in the offline phase before deploying continuous monitoring online. In other words, the indirect monitoring approach is a supervised learning technique that requires many historical data to learn the fault patterns before diagnosing them.

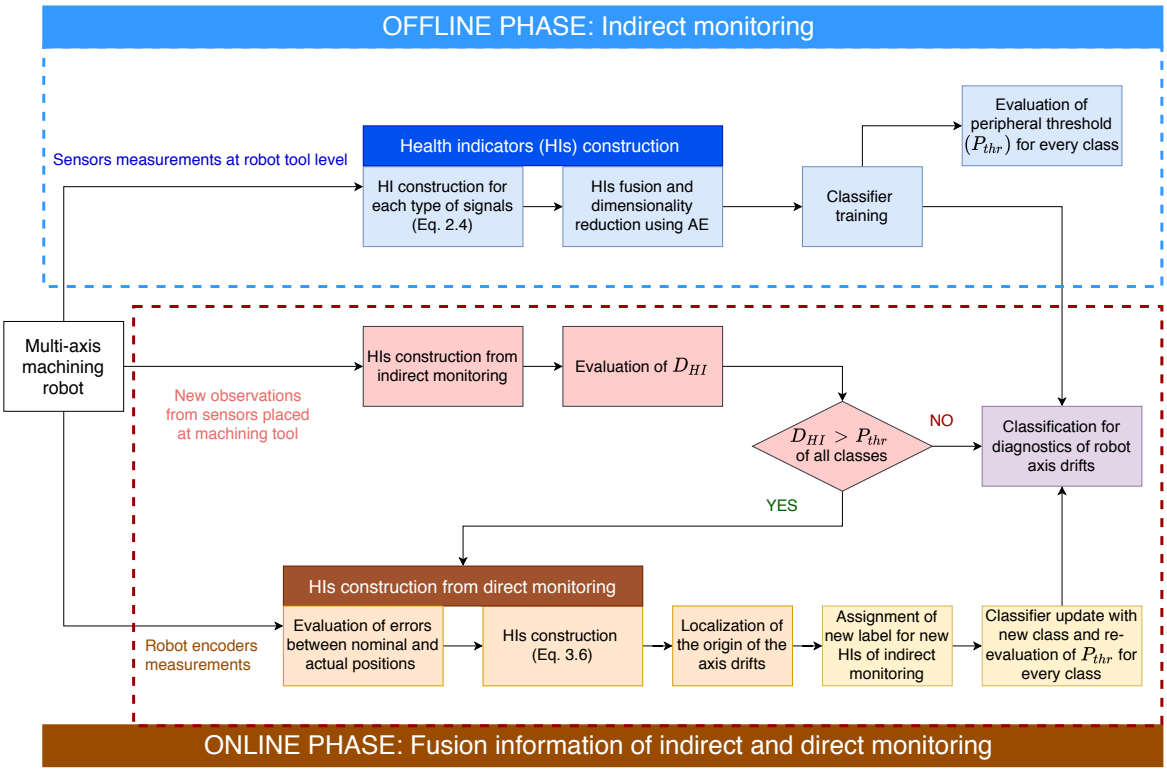

Figure 3.2: Flowchart of the proposed diagnostics methodology.

Inspiring from the advantages of direct and indirect monitoring approaches, the proposed methodology, presented in Figure 3.2, uses information of the former method to automatically label unknown anomalies and then update the classifier in the latter for early detection and diagnostics of these anomalies in future. This methodology is principally composed of two phases, offline and online. The details of the offline phase, that exploits measurements from the indirect monitoring method to build health indicators, train a classifier model, and evaluate the peripheral threshold of the existing classes, are described in Subsection 3.3.1. In the online phase (Subsection 3.3.2), the monitoring system uses measurements from the tool-level sensors to indirectly track the robot motions, and thus early detect and diagnose the axis drifts, whose fault patterns have already been learned in the offline phase. For unknown anomaly observations from the tool-level sensors,

the direct monitoring approach using the robot encoder measurements will be launched to localize the origin of the axis drifts. Using the information from the direct monitoring approach, the relevant observations from the indirect monitoring are labeled and thus, the classifier for online diagnostics of the robot axis drifts is updated. This update procedure will be presented in Subsection 3.3.2.1, while the principal steps of the direct monitoring mode will be detailed in Subsection 3.3.2.2.

3.3.1 Offline phase: Learning failure patterns from indirect monitoring

This phase aims to process the recorded raw data of the sensors placed at the robot tool level to learn failure patterns from the indirect monitoring. For this purpose, the collected observations, corresponding to the common types of the axis drifts, are injected into a treatment procedure consisting of the following steps:

- Construction of health indicator for each signal type (current, vibration, force and torque)
- Fusion of these health indicators based on an auto-encoder network
- Classification of the robot axis drifts and evaluation of the peripheral threshold for every existing class

3.3.1.1 Health indicators construction

In this step, the data recorded, e.g. the current, the vibration, the force and the torque signals will be injected into the proposed signal processing methodology in Section 1.2.2 to build health indicators. A brief illustration of this procedure is presented in Figure 3.3.

In summary, the constructed health indicators in this case are used to characterize different states of robot axis drifts. However, as the health indicators are extracted from the measurements of sensors placed at the tool level, it only indirectly reflects the deviation of the robot axes. Each health indicator extracted from each signal (current, vibration, force and torque) can bring a particular advantage to monitor the robot arms behavior. Hence, to reinforce the capacity to well detect and diagnose as many as possible multiple axis drifts, the fusion of these health indicators is investigated and presented in the following subsection.

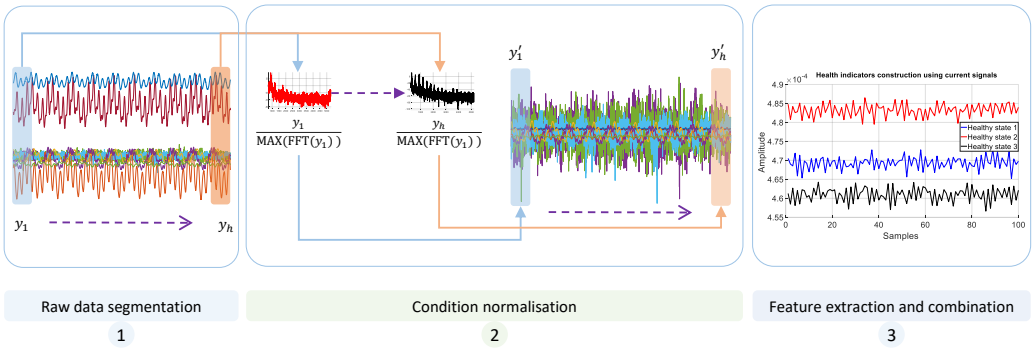

Figure 3.3: Reminder of health indicator construction methodology.

3.3.1.2 Health indicators fusion

This second step aims to combine the constructed health indicators from different signals to create a robust fused ones that detect well the origin of the robot deviations. In fact, as each measurement type has its own properties to reflect the system health states, considering simultaneously all the constructed health indicators from different measurements can be a promising solution to enhance the ability of system health assessment (Al Hage et al., 2017, Meng et al., 2020). However, processing these data separately may lead to confusion because, under the impact of the operating condition variations, some measurements do not properly reflect the actual status of the system. To remedy this situation, health indicators fusion is performed. This process aims to fuse all the processed raw data into one representative pattern.

For this purpose, different techniques were proposed in the literature. One can cite the Principal Component Analysis (PCA)(Loutas et al., 2019), Isometric Feature Mapping (ISOMAP) (Ali and Saidi, 2018) and Auto-Encoder (AE) (Lin and Tao, 2019). Among these techniques, the AE can perform transformations with non-linear activation functions. Moreover, it provides a high level of fusion performance thanks to the learning task of the neural networks which do not require complex tuning parameters. Therefore, in this work, the auto-encoder network is proposed to fuse the health indicator observations extracted from each sensor. The general structure of the auto-encoder consists of three-layer types that are: an input layer, a hidden layer (encoding layer) and an output layer (decoding layer), as shown in Figure 3.4.

As the health indicators are extracted from different sensors, it is necessary to normalize them into a nominal scale (Nguyen and Medjaher, 2019) before the fusion step with the auto-encoder network. Hence, the following equation 3.1 is used to normalize the health

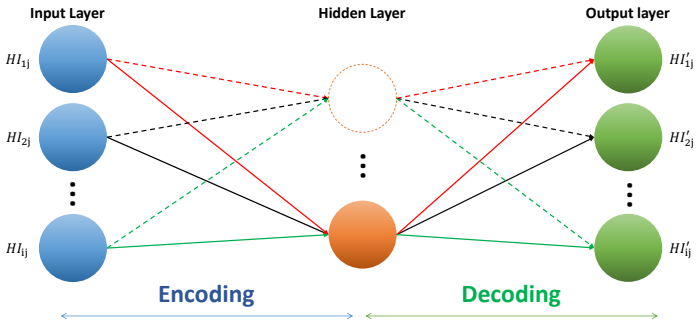

Figure 3.4: Illustration of Auto-Encoder network structure.

indicators to their dispersion.

$$HI_h = \frac{(HI_h - \bar{HI}_h)}{StD(HI_h)} \tag{3.1}$$

where HI_h is the h^{th} observation of the health indicator and StD is the standard deviation of the global observations.

Next, the auto-encoder receives the normalized health indicators as the inputs for the encoding task as expressed by equation 3.2.

$$O_1 = [HI_{(1)}, HI_{(2)}, HI_{(3)}, ..., HI_{(h)}] \tag{3.2}$$

Then, the encoding task is performed through the activation function.

$$O_2 = f(w_n \times O_1 + b) \tag{3.3}$$

where f is the activation function, w and b are the weights and bias of network, respectively, with n representing the number of hidden units and also the reduction size. For an illustration, if $n = 3$, all health indicator observations will be reduced into 3 dimensions, as expressed by equation 3.3.

In the third layer, and by using equation 3.4, the reconstructed task is launched.

$$O_3 = g(w'_n \times O_2 + b') \tag{3.4}$$

where w' and b' are the transposed weights and bias values used for decoding the data

and g is the activation function which can be the same or different than the one used in the encoding phase.

The output of the decoding phase O_3 is then injected into a loss function that characterizes the difference between the AE output with the input data. Training an AE network aims to minimize this loss function by updating the weights and the bias of the encoding and decoding phases using the gradient-descent back-propagation algorithm. The performance of the AE is evaluated by the Mean Square Error (MSE) between the input and the output layers.

In this study, through the proposed AE, multiple HIs extracted from different signals are embedded into three-dimensional space to facilitate the graphical visualization of the fault patterns for further FDD tasks.

3.3.1.3 Patterns recognition and evaluation of their peripheral thresholds

The last step of the indirect monitoring aims to learn the failure patterns for online fault detection and diagnostics. For this purpose, the observations of the fused health indicators are taken as a training database (Ω_p). This database is used to learn the classifier model how to map each observation of (Ω_p) to its corresponding class s (e.g. $s = 0$ corresponds to the healthy class and $s = 1$ correspond to a faulty class 1). Note that this technique is a supervised learning which requires prior samples of the healthy and the faulty classes.

In literature, there exists several machine learning classifiers. One can cite the most popular ones such as Discriminant Analysis (DA) (Cho and Jiang, 2018), Support vector machine (SVM) (Fatima et al., 2015), K-Nearest Neighbor (K-NN) (Madeti and Singh, 2018), Decision Tree (DT) (Samantaray, 2009), Naive Bayes (NB) (Mukherjee and Sharma, 2012), and Adaptive Neuro-Fuzzy Inference System (ANFIS) (Jang, 1993). All of these classifiers can perform good classification with a high level of accuracy results depending on the separability between the different health states to be trained. Thanks to the proposed processing methodology, the different health states of the system can be clearly separated with negligible dispersion between the HI observations and therefore it offers promising diagnostic results.

In this study, to highlight the performance and robustness of the proposed methodology, different classifiers, e.g. DA, SVM, K-NN, DT, NB and ANFIS, will be considered. Among them, the K-NN model is the most classic and popular one thanks to its simplicity of implementation and fast computing time.

After classification of the different types of the axis drifts, the peripheral threshold for each class (P_{thr}) is evaluated. This value is served to consider whether a new observation

belongs to an identified class or not with a predetermined significance level. To calculate it, we firstly identify the centroïd of each class, then evaluate the Euclidean distances, noted D_{HI}, from each HI observation belonging to this class to its centroïd. Then, inspired by the empirical 99.7% rule used in statistics, the peripheral threshold for each class is defined by:

$$P_{thr} = \bar{D_{HI}} + 3 \times \sigma(D_{HI}) \tag{3.5}$$

where $\bar{D_{HI}}$ and $\sigma(D_{HI})$ are respectively the mean and the standard deviation values of the distances from each observation to its class's centroïd. Comparing the distances of a new observation to the centroïd of each existing class with its P_{thr}, the monitoring system can decide whether it is necessary to refer to the result of the direct monitoring mode to identify the label for this observation or not. This procedure will be detailed in the next subsection.

3.3.2 Online phase: detection and diagnostics of robot axes drifts

This phase of the proposed methodology performs an online continuous indirect monitoring of the robot motions. It uses the classifier model trained in the offline phase for early fault detection and diagnostics of the known types of the robot axis drifts. It also allows automatically labeling uncertain observations and updating the classifier with the information from the direct monitoring. The information fusion algorithm for an effective online detection and diagnostics of the robot axis drifts will be presented in Subsection 3.3.2.1. Then, the direct monitoring process will be detailed in Subsection 3.3.2.2 to clarify how to localize the origin of the axis drifts with the encoder measurements.

3.3.2.1 Information fusion procedure for online diagnostics

Algorithm 1 presents the procedure for reliable online detection and diagnostics of the robot axis drifts.From the beginning of a machining process (at each observation time) the proposed algorithm loads the actual vectors C and P_{thr} that consist of the centroïds and the peripheral thresholds, respectively, of the existing classes characterizing all the current known types of robot axis drifts. In the same time, the data acquired from multiple sensor sources placed at the tool level are injected into the signal processing pipeline presented in Subsection 3.3.2.1 to construct the HI for each type of signal. These HIs are then fused using the AE model trained in the offline phase (3.3.2.2) to obtain a new 3D observation point.

Algorithm 1 Online detection and diagnostics of robot axis drifts

At each observation instant:

1: Load the vectors C and P_{thr}
2: Collect new data from indirect monitoring
3: Construct the HI for each type of signals
4: Fuse HIs from different sensor sources
5: **for** $j = 1$ to $length(P_{thr})$ **do**
6: Calculate the distance ($D_{HI}(j)$)
7: **if** $D_{HI}(j) \leq P_{thr}(j)$ **then**
8: Use the trained classifier for this new HI observation
9: Break **for loop**, go to **Step 1** of next observation instant
end if
end for
10: Launch the direct monitoring
11: Use the result of the direct monitoring to label the HI observations from indirect monitoring
12: Retrain the classifier
13: Update the vectors C and P_{thr}

Next, the distance $D_{HI}(j)$, from the observation point to the centroïds of each existing class j, is evaluated and compared with the peripheral threshold of this class, $P_{thr}(j)$ (Figure 3.5). If at least a distance from the observation to the centroïd of one existing class is lower than its peripheral threshold ($D_{HI}(E_2) < P_{thr}(E_2)$ in subFigure 3.5(a)), the trained classifier will be applied on this new HI observation to infer its class, i.e. diagnostics of the known axis drift. Otherwise, if $D_{HI}(j) > P_{thr}(j)$ for all j (subFigure 3.5(b)), the direct monitoring mode will be launched. After a necessary elapsed time needed to collect sufficient amount of encoder measurements, the direct monitoring can correctly localize the origin of the new axis drifts. This information is then used to label the relevant HI observations obtained from indirect monitoring. Based on this, the classifier will be retrained and the vectors C and P_{thr} will be updated accordingly.

3.3.2.2 Direct monitoring using encoder measurements

The direct monitoring way uses the already installed encoder sensors in each servo-motor of the robot to track its motions. It accesses to the robot control system to acquire the set-points of each axis positioning values recognized by the robot's internal sensors. However, this task requires some elapsed time of few minutes to access and collect an essential

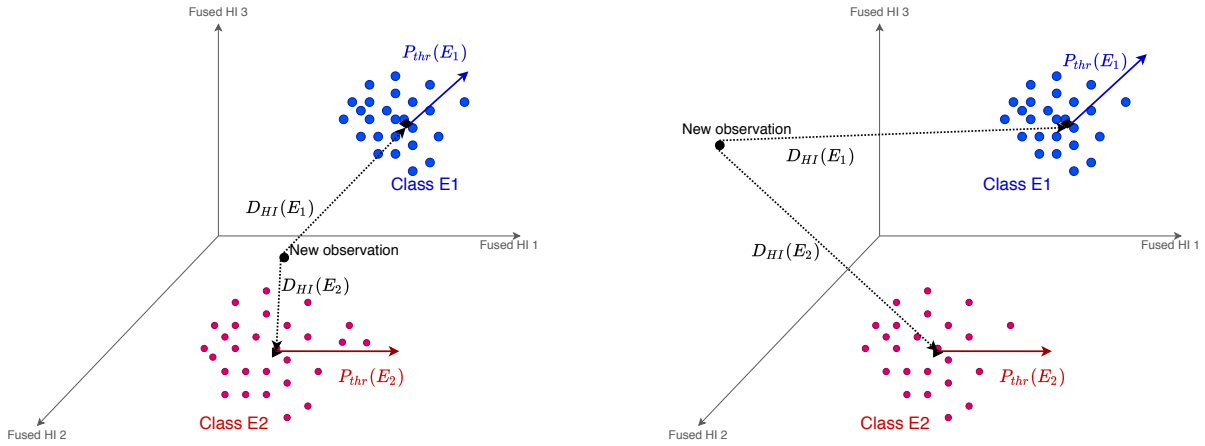

a) $D_{HI}(E_1) > P_{thr}(E_1)$, $D_{HI}(E_2) < P_{thr}(E_2)$ b) $D_{HI}(E_1) > P_{thr}(E_1)$, $D_{HI}(E_2) > P_{thr}(E_2)$

Figure 3.5: Illustration of the comparison between D_{HI} and P_{thr}.

amount of encoder measurements for the evaluation of the corresponding HI.

$$HI_i = (\texttt{RMS}(error_i)/\texttt{StD}(error_i))^2 \tag{3.6}$$

where $error_i$ is the trajectory errors presented in the i-th axis during the elapsed time of the direct monitoring. For an illustration, Figure 3.6 shows the trajectory errors of the six axes of the robot caused by the drifts of the first axis.

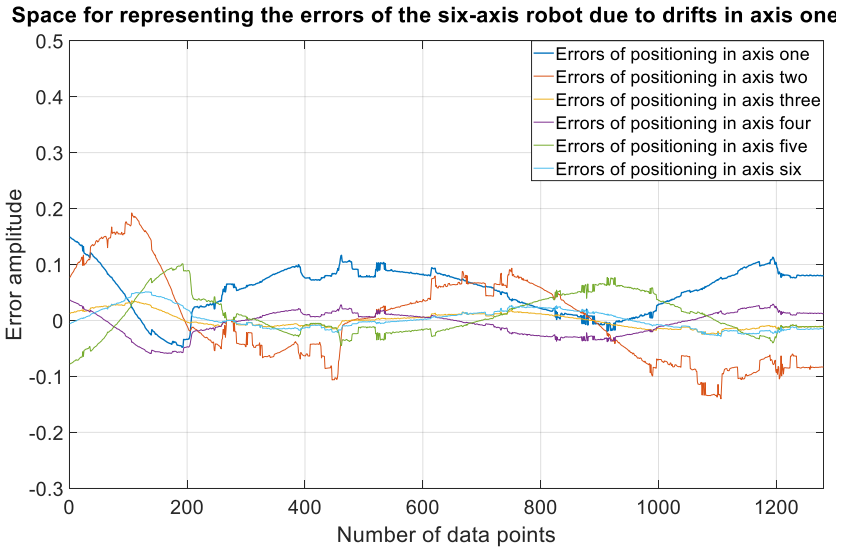

Figure 3.6: Trajectory errors of the robot six axis caused by drifts in the first axis.

Once the errors are calculated, the RMS and StD expressed by equations 3.7 and 3.8 can

be combined to build an effective health indicator (equation 3.6) that directly detects the deviation origin of the robot axes.

$$\texttt{RMS}(error_i) = \sqrt{\frac{1}{n}\sum_{j=1}^{n} error_{ij}^2} \tag{3.7}$$

$$\texttt{StD}(error_i) = \sqrt{\frac{1}{n}\sum_{j=1}^{n} (error_{ij} - \overline{error_i})^2} \tag{3.8}$$

where i and j represent the axis and observation number respectively, n is the total number of observations during the elapsed time of the direct monitoring, and $\overline{error_i}$ is the mean value of the deviations in the i-th axis.

From equations (3.7) and (3.8), one can see that the StD value is equal to RMS when the mean value of errors is 0. In this case, the HI, expressed by equation (3.6), will be equal to 1. Hence, one can conclude that in the nominal case (no deviations) the proposed health indicator is close to 1 because the mean value of the errors tends to zero. In the presence of deviations, the health indicator will be significantly different from 1. For mathematical demonstrations of these properties, please consult Appendix B.

From the statistical analysis of multiple empirical observations, the authors propose to fix the anomaly threshold to 2, i.e. if $HI_i > 2$, then a drift in the i-th axis is detected. For an illustration, Table 3.2 presents the two observations of HI_i values corresponding to the i-th axis in the case where there exists drifts in the first axis.

HI_1	HI_2	HI_3	HI_4	HI_5	HI_6
5.82	1.00	1.08	1.05	1.06	1.05
6.5	1.3	1.03	1.2	1.05	1.3

Table 3.2: Two observations of HI_i when there exists the drifts in the first axis.

One can see that the direct observation of error trajectories in Figure 3.6 does not allow detecting the origin of drifts, while the HI_i values presented in Table 3.2 clearly identify the source of the drifts. Indeed, two HI observations of the first axis are greater than 2 (they are 5.82 and 6.5), while the HIs values of other axes are close to 1. By this result, it is possible to use the HI value,s grater than 2, to label new observations of the indirect monitoring if this latter technique presents new drifts in the robot axes motions.

3.4 Case study for online fault diagnostics

This section investigates the performance of the proposed methodology on the METALLICADOUR research and transfer center. It consists of a multi-axis robot with six degrees of freedom used to perform machining operations and to collect failure patterns corresponding to multiple single and combined drifts.

The details of this platform will be presented in Subsection 3.4.1. Then, Subsection 3.4.2 shows the performance of the direct monitoring used to localize the origin of the drifts and for which the failure patterns have not been learned by the classifier in indirect monitoring. Next, the performance of the indirect monitoring method for diagnostics of robot axis drifts, which failure patterns have already been learned, will be investigated in Subsection 3.4.3. Finally, Subsection 3.4.4 is dedicated to consider how the information fusion process performs online fault detection and diagnostics of known and unknown robot axis drifts.

3.4.1 Description of the machining platform

Figure 3.7 illustrates the global overview of the platform which consists of an ABB IRB 6660 six-axis robot known for its high-rigidity of machining metallic work-pieces with good quality. This robot is composed of six servomotors powered and controlled by an IRC5 control system. At the sixth axis of the robot, a High-Speed Machining (HSM) spindle is placed and equipped with a flat-end mill unit (of 10 mm diameter) for milling aluminum work-pieces. In this case study, the designed work-piece has a labyrinth form with a depth of 5 mm, as shown in Figure 3.7. This shape allows taking into account all the robot arm motions leading to perform system-level monitoring. Besides, the machining parameters are set as follows: spindle speed of 9000 rpm with 648 mm/mn of feed rate.

Table 3.3 summarizes the set-up parameters of two groups of experiments. The first group aims to process seven experiments that correspond to the nominal condition of the robot (E1), where no drift occurs, and six faulty states representing the single drifts of the six robot axis (E2, E3, ... E6), respectively. The second group of experiments is used to investigate the combined drifts of the robot arms under the same machining condition. For example, E1 & E4 is the case where there exists the combined drifts in the first and fourth axes. Note that the drifts are created by injecting errors in the axis rotation range during the process, i.e. $\pm 0.01^\circ$ of the actual position. Different error degrees from low to high can be performed while keeping tolerant values that should not be exceeded. These latter values can be determined according to standards used in the domain or given by experts. The development engineers at METALLICADOUR center recommend drifts in the range of $[\pm 0.06^\circ, \pm 0.18^\circ]$ from the nominal position. Also, note that the calculation of the drift

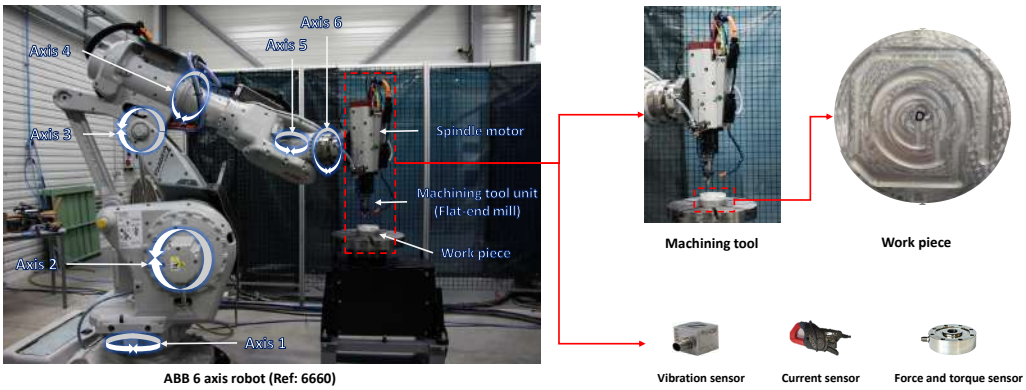

Figure 3.7: Overall schema of the test bench.

degree is mainly related to the distance between the center of the workpiece and the center of the axis, which also needs an expert to evaluate the criterion threshold alarm.

First group of experiments					
Speed (rpm)	Feed rate (mm/mn)	Cutting depth (mm)	Health state	Error degree (°)	Acquisition parameters
9000	648	5	E1: Healthy state	.	Hardware: IRC5/NI
			E2: Drifts in axis one	+0.065	F_s (IRC5): 41.6 Hz
			E3: Drifts in axis two	+0.120	F_s (NI): 25.6 KHz
			E4: Drifts in axis three	+0.080	File format: (.csv)
			E5: Drifts in axis four	+0.085	Duration: 60/file
			E6: Drifts in axis five	+0.120	
			E7: Drifts in axis six	+0.155	
Second group of experiments					
Speed (rpm)	Feed rate (mm/mn)	Cutting depth (mm)	Health state	Error degree (°)	Acquisition parameters
9000	648	5	E1: Healthy state	.	Hardware: IRC5/NI
			E1 & E4: Drifts in axis one and four	+0.012/-0.04	F_s (IRC5): 41.6 Hz
			E2 & E4: Drifts in axis two and four	+0.120/+0.04	F_s (NI): 25.6 KHz
			E3 & E6: Drifts in axis three and six	-0.04/+0.155	File format: (.csv)
			E4 & E5: Drifts in axis four and five	+0.155/-0.04	Duration: 60/file
			E2 & E5: Drifts in axis two and five	-0.040/+0.04	
			E4 & E6: Drifts in axis four and six	-0.080/+0.18	

Table 3.3: Summary of experimental tests.

Concerning the indirect monitoring process, the three-phase current sensors are placed at the IRC5 inverter output while the three-axis vibration, force and torque sensors are installed at the spindle tool level. The acquisition of these measurements is done by National Instrument (NI) devices with Labview acquisition software at a sampling frequency of 25.6 kHz. The recorded data are stored in (.csv) files with a duration of 5 s/file.

For the direct monitoring process, the servomotors of the robot are already equipped with encoders (one encoder for each servomotor). As the robot has six-axis, the total

number of encoders equal to six. The measurements of each encoder are recorded by the IRC5 controller with a sampling frequency of 41.6 Hz and stored in (.xlsx) files.

3.4.2 Investigation on the performance of direct monitoring

As mentioned in the case study description, for direct monitoring, the encoders are installed on the rotating shaft of each servomotor and used to collect data during each experiment controlled by the IRC5 system. The encoder measurements represent the rotating position values of the robot arms. Following the method proposed in Subsection 3.3.2.2, these values are used to construct the health indicators of the robot axes to directly assess the drift origins. Table 3.4 shows the obtained observations of HI_i through two groups of experiments. The first column indicates the origin of the drifts while the remaining six columns present the HIs values of the 6 robot axes.

First group of experiments						
Drift origin	HI_1	HI_2	HI_3	HI_4	HI_5	HI_6
Axis 1	**2.80**	1.00	1.00	1.05	1.06	1.05
Axis 2	1.06	**2.57**	1.00	1.06	1.06	1.00
Axis 3	1.04	1.03	**9.00**	1.02	1.05	1.00
Axis 4	1.06	1.03	1.02	**13.7**	1.03	1.00
Axis 5	1.00	1.02	1.03	1.25	**4.02**	1.5
Axis 6	1.13	1.01	1.01	1.14	1.12	**121**

Second group of experiments						
Drift origin	HI_1	HI_2	HI_3	HI_4	HI_5	HI_6
Axis 1 & axis 4	**5.52**	1.03	1.00	**34.2**	1.08	1.00
Axis 2 & axis 4	1.04	**10.3**	1.10	**10.5**	1.03	1.13
Axis 3 & axis 6	1.07	1.01	**2.10**	1.08	1.00	**6.30**
Axis 4 & axis 5	1.00	1.10	1.00	**2.91**	**2.60**	1.05
Axis 2 & axis 5	1.02	**4.20**	1.00	1.03	**2.75**	1.02
Axis 4 & axis 6	1.07	1.00	1.00	**9.82**	1.07	**177**

Table 3.4: HIs values of six robot axes when there exists single and combined drifts.

From Table 3.4, one can notice that the constructed health indicators allow clearly identifying which axis is the origin of the robot arm deviations. This identification is indicated when the health indicator values are greater than 2. For example, considering the first line in the first group of experiments, when the drift is injected into the first axis, the obtained values of the calculated health indicator from the second to the sixth axis are close to 1 (which means no drift) while the value of the first axis is equal to 2.80. This

latter value indicates that the axis one deviated from its nominal trajectory during the process.

Moreover, even in the case of combined drifts, in the second group of experiments, the constructed health indicators allow isolating the deviated axes during the process. For example, considering the first line in the second group of experiments, when the drifts are injected simultaneously into the first and fourth axes, the obtained values of the health indicators of these axes are respectively 5.52 and 34.2 while the ones of the remaining axes are close to 1.

3.4.3 Investigation on the performance of indirect monitoring for the cases where the failure patterns have already been learned

For indirect monitoring, the recorded measurements of all sensors placed at the tool level (current, vibration, force and torque) are injected into the processing algorithm to extract features and build the fused health indicators. The tuning parameters of the AE network for HI fusion are summarized in Table 3.5. Figure 3.8 presents the distribution of the fused health indicators. From this figure, one can see that the proposed methodology allows clearly separating the different types of the robot axes deviations with a negligible dispersion between the observations. These positive results will allow significantly improving the performance of the classifier models for an automatic diagnostic of the origin of the robot trajectory deviations.

Hidden unit	Epoch	loss function	Encoder function	Decoder function
3	1000	MAE	Logsig	Purelin

Table 3.5: Turning parameters of the AE network.

For an automatic detection and diagnostics of the origin of the robot drifts, the fused HIs are fed into a classifier model. To highlight the performance of the fused HIs, various common classifiers (SVM, LR, NB, DT, ANFIS and K-NN) are considered. Their accuracy, using the health indicators extracted separately from each measurement with the one handling the fused health indicators, are compared.

There are in total ($100 \times 14 \times 4 \times 3$) observations of HIs from 4 sensors, that correspond to 100 samples for each type of signal in each experiment (14 experiments have been investigated). The fused health indicator observations will contain (1400×3) samples where 3 is the dimensional size of the fused HIs.

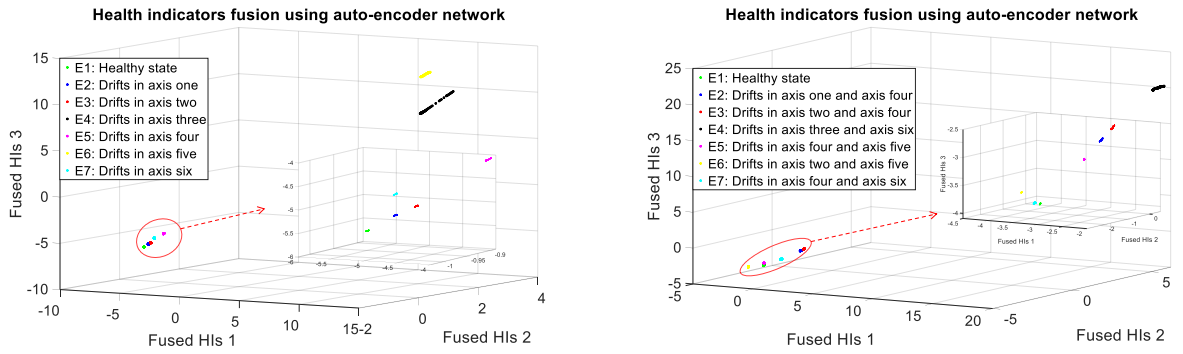

a) Fused health indicators of the first group of experiments.

b) Fused health indicators of the second group of experiments.

Figure 3.8: Distribution of the fused HIs under different machining conditions.

To evaluate the robustness of the indirect monitoring method when the failure patterns of the robot axis drifts have been already learned, for each experiment the train and test set randomly take 50% of the total observations. The trained classifiers are then used to diagnose the origin of the robot drifts when considering the observations in the test set without prior knowledge about the operating condition and the fault type. The accuracy scores of these trained classifiers for diagnostic of the robot axis drifts are summarized in Table 3.6.

First group of experiments					
Classifier model	Current HIs	Vibration HIs	Force HIs	Torque HIs	Fused HIs
SVM	97.33	95.90	100	100	**100**
LR	98.67	97.57	100	100	**100**
NB	99.71	94.35	100	100	**100**
DT	96.79	94.86	100	100	**100**
ANFIS	95.15	94.11	100	100	**100**
KNN	99.74	95.64	100	100	**100**
Second group of experiments					
Classifier model	Current HIs	Vibration HIs	Force HIs	Torque HIs	Fused HIs
hline SVM	100	100	96.62	98.87	**100**
LR	100	100	97.51	97.79	**100**
NB	100	100	98.06	98.18	**100**
DT	100	100	97.70	96.29	**100**
ANFIS	100	100	98.80	96.50	**100**
KNN	100	100	98.20	97.94	**100**

Table 3.6: Accuracy score (%) of classifiers for diagnostic of the robot axis drifts.

From Table 3.6, the performance of the fused health indicators obtained from the sensors

placed at the tool level is highlighted with an accuracy score of 100% for all classifier models and all groups of experiments. In other words, when the failure patterns have been already learned, the proposed indirect monitoring method allows diagnosing exactly the origin of the robot arm deviation. Considering the HI extracted from only one sensor, one can notice that in the first group of experiments, where only the operating condition variation (speed) is investigated, the force and torque indicators can diagnose well the origin of the drifts with 100% accuracy while the current and vibration indicators cannot perform good results. Besides, in the second group of experiments, when injecting combined drifts on the robot axes, the current and the vibration indicators give better diagnostics (100% accuracy) instead of the force and torque indicators. These differences of results can be explained by the effects of the sensor positions on the quality of the indirect monitoring process. In fact, it is preferred to place the current sensor at the inverter or the supply controller of the robot to collect all useful information about current signals used and/or supplied at the system level. Also, the vibration sensors need to be placed as near as possible to the machining unit, while the force and torque sensors should be placed at the sixth axis level of the robot.

Besides, as the accuracy scores of all classifier models are 100% for all groups of experiments when using the fused HIs, hereafter the authors propose to use the K-NN model, the most classic and simplest one, to learn the failure patterns in the offline phase and to diagnose the axes drifts in the online phase.

3.4.4 Investigation on the performance of the information fusion process

This section aims to investigate the performance of information fusion between direct and indirect monitoring for online detection and diagnostics of robot axes drifts. For this purpose, the first group of experiments is used to learn the pattern failures of single drifts in the offline phase, while the second one is used to illustrate how the information fusion process (Algorithm 1 presented in Subsection 3.3.2.1) works to detect and diagnose the unknown drifts (combined drifts) in the online phase.

Firstly, the data collected from the first experiment of the second group, corresponding to the healthy state (E1), are used to verify whether the proposed methodology can correctly group the E1 observations into the already existing classes (first group of experiments). Considering Table 3.7, its second and third columns present the centroïd position and the peripheral threshold of the existing classes that have been already trained in the offline phase by using the data acquired from the first group of experiments. The last column in Table 3.7 shows the distance from a new observation of the class E1 (second experiment group) to the centroïd of each existing class (first experiment group). One

Class	Centroïd position	P_{thr}	D_{HI}
E1: Healthy state	(-5.65, -0.92, -5.65)	0.32	0.10
E2: Drifts in axis one	(-5.31, -0.91, -5.31)	0.70	5.09
E3: Drifts in axis two	(-5.16, -0.89, -5.16)	1.14	7.4
E4: Drifts in axis three	(7.72, 3.03, 7.72)	111.13	211.63
E5: Drifts in axis four	(-4.1, -0.89, -4.10)	0.50	23.82
E6: Drifts in axis five	(13.72, 0.78, 13.72)	42.59	300.66
E7: Drifts in axis six	(-4.54, -1.02, -4.54)	1.42	17.15

Table 3.7: Parameters of the existing classes and the one from a new observation.

can see that, as $D_{HI}(E1) < P_{thr}(E1)$, the trained K-NN model is applied to infer the class for the new observation. It correctly identifies that this observation belongs to the healthy state (E1). Similarly, for other observations from the first experiment of the second group, the trained K-NN model can attain the best score with an accuracy of 100%. For an illustration, Figure 3.9 shows the distribution of the existing classes and of the new observations (new class 1) from the first experiment of the second group. One can see that the new healthy group is close to the existing healthy state (E1) and far from the other faulty classes (E2, ..., E7) characterizing the drifts of each axis.

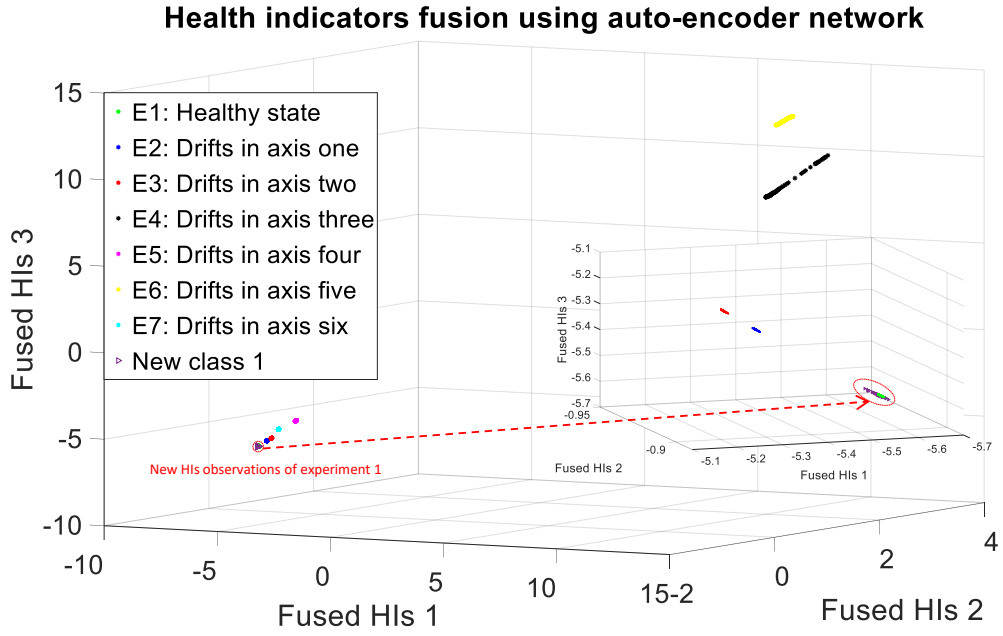

Figure 3.9: Distribution of the existing classes and the new observations.

Secondly, the data collected from the other experiments in the second group, corre-

sponding to the combined drifts and for which the failure patterns are unknown, are used to verify whether the proposed methodology can detect these anomaly points and then launch the direct monitoring. Considering Table 3.8, the second column shows the peripheral threshold, P_{thr}, of the existing classes (E1, E2, ..., E7) presented in the first column. The remaining columns indicate the distances from an observation of the unknown classes (E1 & E4, E2 & E4, ..., E4 & E6) to the centroïd of the existing classes. One can see that all of these distances are greater than the P_{thr} of the existing classes. Moreover, Figure 3.10 illustrates the graphical distribution of the fused HIs corresponding to each experiment of the second group starting for the second one. Each new class does not belong to any of the peripheral threshold of the existing ones. Hence, the proposed methodology considers them as anomaly points and uses the information of the direct monitoring method to label them. The ability of the direct monitoring to correctly localize the drift origins has been highlighted in Subsection 3.4.2.

	P_{thr}	E1 & E4	E2 & E4	E3 & E6	E4 & E5	E2 & E5	E4 & E6
E1:	0.32	83.55	79.29	477.54	89.48	78.68	81.84
E2:	0.7	50.37	74.97	472.38	82.59	73.04	75.69
E3:	1.14	79.39	73.42	469.91	79.64	70.81	73.16
E4:	111.13	291.51	277.78	296.81	233.47	260.56	251.17
E5:	0.5	73.67	63.80	454.56	58.54	55.86	55.68
E6:	42.59	404.76	382.86	345.83	353.60	378.04	369.50
E7:	1.42	73.14	64.98	462.18	66.10	59.75	61.01

Table 3.8: Distances from the combined drifts to the centroïds of existing classes.

To better understand the process of information fusion, let's consider a particular example consisting of the combined drift (E1 & E4) occurring for the first time. At this moment, the monitoring system is operating under the indirect mode. Hence, the measurements from the sensors placed at the tool level are collected and injected into the signal processing pipeline to create the fused HIs. Then, the distances, D_{HI}, from this fused HIs observation to the centroïds of the existing classes are evaluated to compare them with their peripheral thresholds P_{thr}. As $D_{HI} > P_{thr}$ for all classes (comparing the third and the second columns of Table 3.8), the monitoring system switches to the direct mode (but still records the data from the indirect monitoring). After the elapsed time of 2 minutes to access the robot controller and to get the minimum amount of encoder measurements, the monitoring system can assess the health indicator for each robot axis: $HI_1 = 5.52$, $HI_2 = 1.03$, $HI_3 = 1.00$, $HI_4 = 34.2$, $HI_5 = 1.08$, $HI_6 = 1.00$. As HI_1 and HI_4 are greater than 2, the monitoring system can correctly identify the origin of this combined drifts, E1 & E4, and then launches an alarm. Besides, based on the direct monitoring result, the monitoring system labels the observations recorded from the indirect monitoring during the elapsed time of 2 minutes as E1 & E4. Then, it retrains the classifier of the indirect

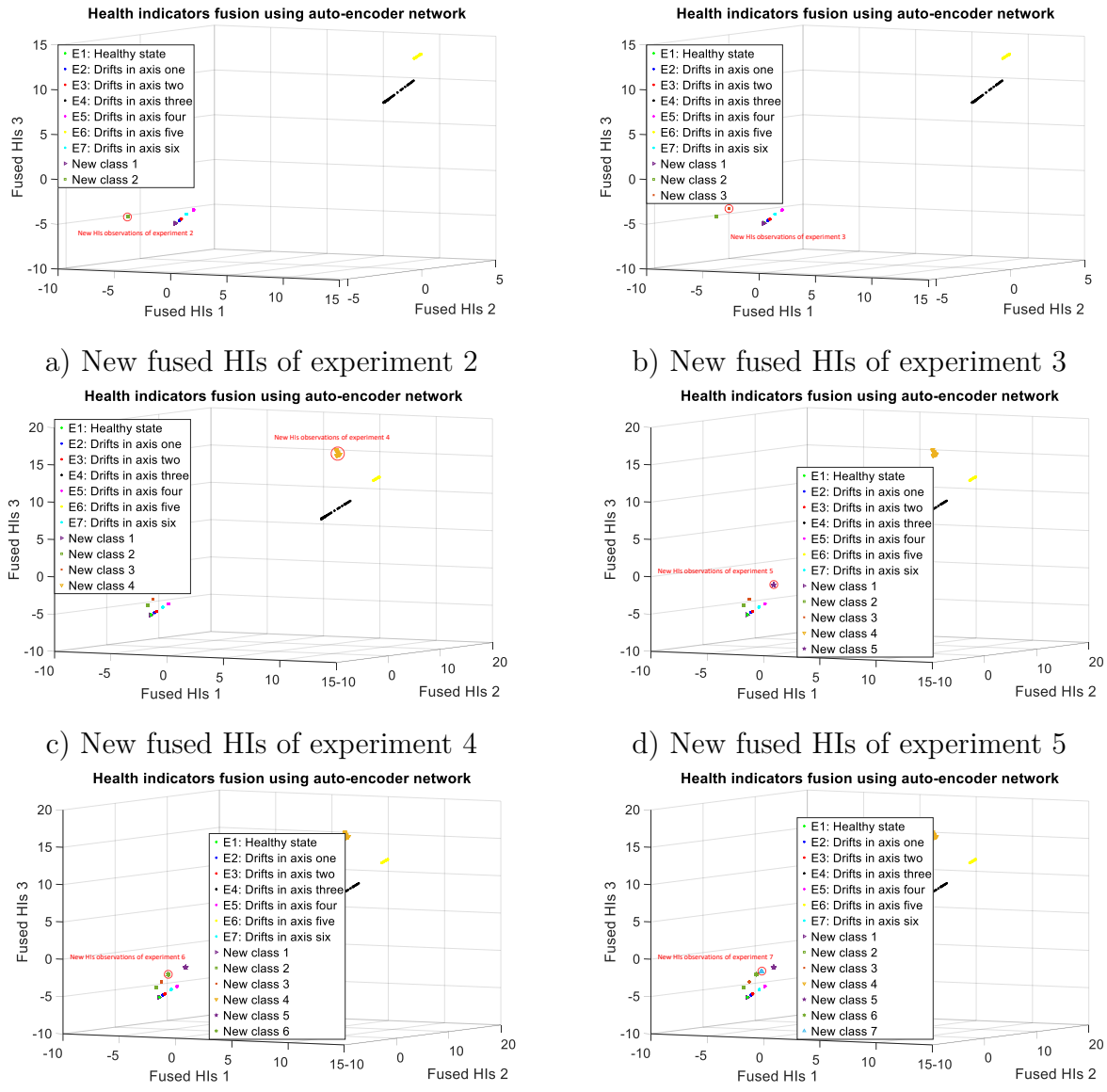

a) New fused HIs of experiment 2

b) New fused HIs of experiment 3

c) New fused HIs of experiment 4

d) New fused HIs of experiment 5

e) New fused HIs of experiment 6

f) New fused HIs of experiment 7

Figure 3.10: Illustration of the fused HIs of the second group of experiments.

monitoring with the new observations and new labels, and updates the P_{thr} of each class. The result shows that the P_{thr} of the old classes (E1, E2, ..., E7) do not change while the P_{thr} of the new class E1 & E4 is 0.3.

After updating the classifier and P_{thr}, the monitoring system returns to the indirect mode. Now, assuming that the combined drift (E1 & E4) occurs for the second time. Then, the distances from this new observation to the centroïds of the existing classes (E1, E2, E3, E4, E5, E6, E7, and E1 & E4) are evaluated and respectively equal to 33.82, 32.53, 32.13,

118, 29.8, 163.88, 29.59, and 0.04. One can see that $D_{HI}(E1\ \&\ E4) = 0.04$ is lower than $P_{thr}(E1\ \&\ E4) = 0.3$, hence the classifier is applied on this observation to infer its label. The result shows then that the monitoring system can correctly diagnose this combined drift without switching to the direct mode.

3.5 Conclusion

A new and more efficient online fault diagnostics approach that allows automatically updating the unknown fault types has been presented in this chapter. It is based on the information fusion of indirect and direct monitoring techniques and is dedicated to deal with the challenges posed for fault diagnostics of systems with dynamic behaviors. The proposed methodology is applied to diagnose the origin of the drifts in the robot axes movement. In detail, it uses indirect measurements from sensors placed at the tool level to early detect and diagnose the axis drifts, whose failure patterns have been already learned. Besides, it has also the ability to automatically label the unknown drifts thanks to the information from the direct monitoring process using the robot encoder measurements. To illustrate the applicability of the proposed methodology, a real case study using an ABB IRB 6660 robot with six degrees of freedom was used. The obtained results highlight the flexibility and effectiveness of the monitoring system using both direct and indirect techniques. Indeed, thanks to the performance and the robustness of the fused health indicators constructed from multiple tool-level-sensor signals, the classifier in indirect mode can diagnose the known types of drifts with the best accuracy score up to 100%. For uncertain observations, that are outside of all peripheral thresholds of the existing classes, the monitoring system can automatically detect them and use the result of direct monitoring mode to label these observations. It also updates the indirect mode's classifier to quickly and correctly diagnose these types of faults when they occur again.

As a synthesis, the concept of information fusion of direct and indirect monitoring methods is a good candidate to overcome the significant drawback of fault diagnostic based on pattern recognition techniques. Although the performance of the proposed methodology has only been verified through machining axis robots, its principles can be generalized for other dynamic systems in further studies.

In reality, the behavior of dynamic systems is usually monitored and adjusted by a control system. This controller aims to adjust the output of the system to desired inputs (setpoints). Its activities can be coupled to the diagnostics module so that the monitoring of the systems is enhanced. However, for prognostics, the set-points made by these controllers can lead to additional challenges. Indeed, the prognostics model attempts to predict the system's health state in the future based on its current condition and also the information

related to future operating conditions. Its results are impacted by the control activities. For this reason, it is necessary to develop a new efficient prognostics approach that allows taking into account the variations caused by the control activities. This problem will be addressed in the next chapter.

Chapter 4

New approach for failure prognostics of controlled process

Contents

4.1 Introduction

The previous chapter presented an efficient online fault diagnostics approach that allows automatically updating the unknown fault types of the dynamical systems thanks to the additional information provided by the monitoring part in its controller. However, the set-points made by these controllers can lead to additional challenges for prognostics procedure. Indeed, under the control activities that attempt to adjust the system's output to the desired inputs, future conditions of the system become unpredictable. For this reason, it is necessary to develop a prognostics approach that allows taking into account the variations caused by the control activities.

Hence, this chapter proposes a new efficient hybrid approach based on the combination of machine learning models that allows adapting long-term predictions by using accurate short-term predictions. This combination not only captures the changes in long-term degradation trend over time, but also takes into account the variations of system states in short term. It deals with the challenges of prognostics in closed-loop controlled systems in general, and heat-exchangers for the first concrete case study in particular. To do this, Section 4.2 gives an overall view of the challenges in prognostics of heat-exchangers in the pulp mill industry, and therefore highlights the necessity to develop a new adaptive prognostic approach. This proposed approach is described in Section 4.3. Next, Section 4.4 is dedicated to highlight its performance through real data from a real pulp and mill manufacturing. Finally, some conclusions and perspectives of this work are presented in section 4.5.

4.2 Fault prognostics of controlled pulp mill process

The pulp and paper manufacturing is one of the most important industries in the world (Akbari et al., 2018, Barla, 2007). This manufacturing process consists of different operations, including wood preparation, pulping, chemical and heat recovery, bleaching, and paper-making (Bajpai, 2015). Each system of these activities is dependent on the others making the manufacturing process more complex. Among them, according to the statistics of experts, the black-liquor evaporator (heat-exchanger) is the critical system in the pulp and mill processes (Steinhagen et al., 1993). Its main role is to increase the concentration of the black-liquor by evaporating the water through a high level of heat transfer. The concentrated black-liquor is needed to improve the combustion in the kraft recovery boiler (Naqvi et al., 2010) and convert the generated vapor from this boiler into other forms of energy such electrical supply source (Pettersson and Harvey, 2010). In practice, the rate of heat transfer is significantly affected by the fouling phenomena, which exists in heat-exchanger tubes and increases over time (Ardsomang et al., 2013, Markowski et al., 2013). As a first solution to remedy to the fouling evolution, controller systems such as proportional–integral–derivative (PID) controller is integrated. It main functionality is to evaluate the error between the desired physical quantities associated to the fouling withing the measured one, and based on this error, inject a correction set-points to adjust the fouling level (Melo et al., 2015). The set-points generated by the controller allow to slow down the evolution of fouling in the heat exchangers. However, it is necessary to carry out a systematic maintenance in order to clean the heat exchanger tubes leading to high costs to the manufacturing. Hence, to avoid unnecessary maintenance actions, one need to implement an efficient monitoring of the fouling evolution and an accurate prognostics of the Time-to-Clean (TTC) of the heat-exchanger tubes.

In literature, despite the rapid growth in developing prognostics approaches, the prediction of fouling of black liquor heat exchangers is still an unexplored area. In this regard, the first conducted works addressed the adjustment of different input/output parameters related to heat exchangers to reduce discrepancies between their nominal and current behaviors, thereby limiting the fouling evolution over time. For example, the authors in (Hong et al., 2002) proposed adjusting the operation parameters to control the fouling evolution. Similarly, in (Boo et al., 2013), the authors implemented an algorithm that allowed the automatic control of the parameters causing the fouling initiation. The next studies used physical and/or chemical processes to reduce the fouling phenomenon in the heat exchanger. The work published in (Kang and Liu, 2015) proposes the integration of a heat pump between the condenser and the heat exchanger to reduce its energy consumption and therefore slowdown fouling creation. In (Wang et al., 2016), the authors proposed a chemical substance, such as CO_2 hydrate slurries, to increase the density flow in the heat exchanger as a solution to avoid crude creation in the heat tubes. All of these strategies, which aimed at reducing fouling evolution, were not able to exactly identify the origin of the fouling because of the complex architecture of the process. For this purpose, research has evolved into fouling detection and diagnostics. Thus, the authors in (Oh et al., 2020) proposed a residual-based fault diagnostics technique that uses heat transfer as a health indicator (HI) to detect abnormal changes in the heat exchanger and learn a classifier model for diagnostics. Another work reported in (Guelpa and Verda, 2020) exploits the mass flow rate and the temperature of both sides of the heat exchanger to build an HI, which is then used to learn a diagnostic model to localize the fouling origin.

The aforementioned works address monitoring issues for fouling reduction, detection, and diagnostics. Regarding fouling prognostics, and to our humble knowledge, the first study in the domain was conducted by the University of Tennessee in the USA through a simplified heat-exchanger test bench (Ardsomang et al., 2013, Welz et al., 2014), where the authors created the fouling phenomenon by adding a kaolin clay product to the water of the heat tubes. This test bench provided a linear trend of fouling evolution under two operational conditions. The obtained results of prognostics show a high level of nonlinear predictions, creating a large range of errors between the real and predicted fouling levels. Moreover, the effects of closed-loop controllers and the real variations of systems connected to the heat exchanger are not taken into account in their case study. Therefore, to make fouling prognostics more accurate, different practical and scientific issues should be addressed. The first issue relies on predicting fouling evolution while handling controller activities that can instantaneously respond to changes in operational conditions and adapt to the current fouling level. These activities consequently cause a change in the system degradation trend over time and therefore lead to inaccuracy in the prognostics results. The second issue concerns the requirement of developing accurate prognostics approaches in the long-term horizon for efficient maintenance scheduling while taking into account the instantaneous changes in system behavior.

In this regard, the prognostics approach should satisfying the following requirements:

- Capture of the changes in degradation trend over time caused by the operational condition variations and the controller set-points;
- Estimate the overall degradation process of the system until its failure threshold;
- Ensure a good accuracy of prognostics results in the short and long-term horizon for planning maintenance actions.

According to these requirements, the proposed approach is developed based on the adaptation of long-term predictors to the instantaneous changes of system behaviors, which are captured by different short-term predictors. Its main contributions are summarized as follows:

- Adaptation of a long-term predictor to the instantaneous changes in heat-exchanger behaviors captured by different short-term predictors;
- Proposition of a fusion procedure to estimate the fouling dynamic evolution, until its critical threshold, in heat exchangers;
- Improvement of fouling prognostic results in both short- and long-term horizons.

4.3 Proposed new hybrid approach

As previously mentioned, the main contribution of this chapter is to develop an adaptive prognostics approach that deals with the challenges of prognostics in closed-loop controlled systems in general, and heat-exchangers in particular. This approach is based on the information fusion of long- and short-term predictions to improve the reliability of prognostics results in long-term horizon. It inherits the advantages of both long- and short-term predictors and overcomes the drawbacks of each one considered separately. Its pros and cons are summarized in table 4.1.

	Advantages	Disadvantages
Long-term predictor	Provide information in long-term Capture degradation trend (from nominal to failure states)	Require an elapsed time to start Discrete inspection Infeasible in case of encoder failure.
Short-term predictor	Provide more accurate results	Require additional sensor Require many historical scenarios to learn failure patterns.
Fusion of long & short -term predictors	Automatically update long-term predictor by short-term predictions Enhance reliability of results in long-term horizon	Require more time and computation resource to train multiple predictors

Table 4.1: Pros and cons of the proposed methodology.

Figure 4.1 illustrates how long- and short-term predictors were performed based on machine Learning (ML) models. In long-term prediction, the first machine learning (ML_1) model is used to predict multi-step ahead system health states. It takes the HI observations from time $t = 0$ to actual time $t = t_c$ for the prediction of the system health state at $t = t_c + 1$ (figure 4.1.1). Then, this predicted state is used as input to estimate the next observation and so forth. This kind of prediction procedure provides information in long-term, from the nominal conditions of the system to its failure, and makes an overview of the degradation trend. However, the disadvantage of this approach is the accumulation of the error predictions when using the predicted value as the next input. In fact, the predicted value can contain a certain error that accumulates and increases over time. Hence, this approach only captures the trend of the degradation process and leads to a loss of information on the degradation state. Indeed, when training the model, its parameters are fixed to approximate all the observations ahead of the trajectory; and therefore the smoothed curves, i.e. the degradation trend, are generated.

In short-term prediction, the second model (ML_2), that consists of multiple short-term predictors ($ML_{2.1}$, $ML_{2.2}$, $ML_{2.3}$, etc.), is used to sequentially predict the system states after short-time periods t_1, t_2, t_3, etc. These predictors use the fusion of system monitoring data, from $t = 0$ to $t = t_c$, for forecasting only one value of the degradation state after the defined short-time period (figure 4.1.2). For example, the first predictor $ML_{2.1}$ forecasts the degradation state at 6 hours after while the second $ML_{2.2}$, the third $ML_{2.3}$ and the fourth $ML_{2.4}$ ones provide the estimated degradation state at 12, 18 and 24 hours after, respectively. The obtained results by these predictors are more accurate than the long-term prediction results. However, these predictors require a new observation for the only one prediction value and consequently do not provide an overview of the degradation trend.

Inspiring from the strengths of both prediction techniques, the proposed approach, that relies on fusing the obtained predictions, uses long-term predictor (ML_1) to capture the evolution trend of the fouling phenomenon. Then, to deal with delays of system behavior changes caused by the effect of the closed-loop controller, the different short-term predictors

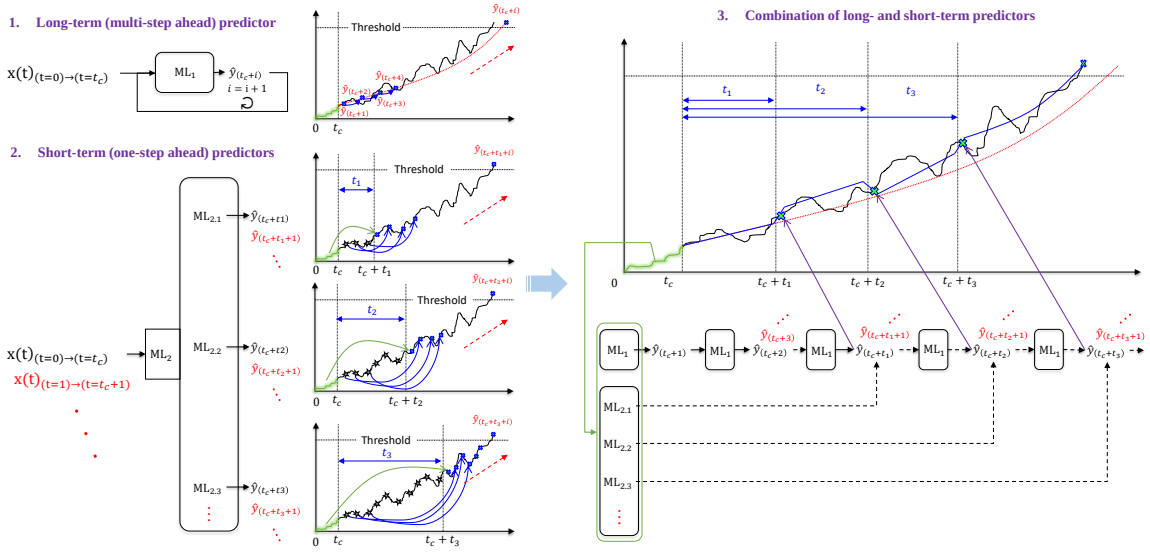

Figure 4.1: Illustration of the long- & short-term predictors working process.

($ML_{2.i}$) are built with the fused data. These latter models aim to correct the prediction errors of the long-term model by updating its predictions in short-term for enhancing the reliability of prognostics results in long-term horizon presented in figure 4.1.3.

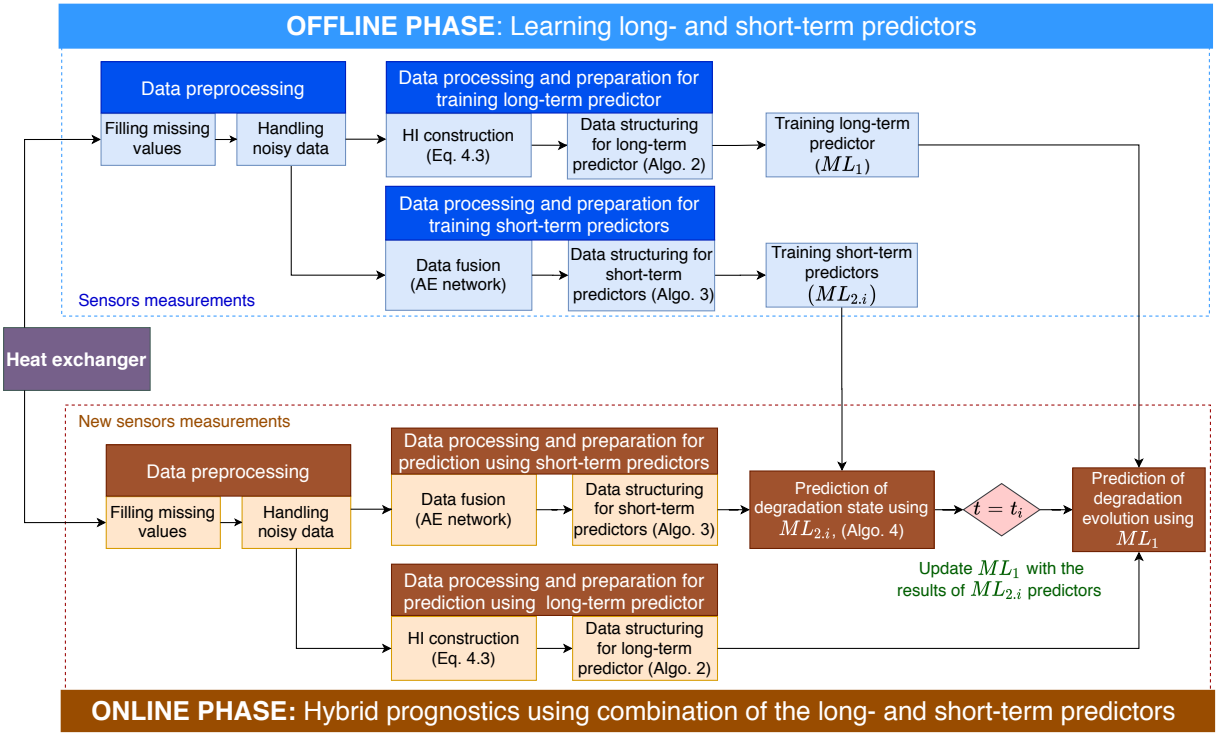

Figure 4.2: Flow chart of the proposed prognostics approach.

The flow chart of the proposed approach is presented in figure 4.2. It is principally composed of two phases, offline and online phase. The details of the offline phase, that exploits multiple sensor measurements to build health indicators, prepare data for training long- and short-term predictors and are presented in subsection 4.3.1. In the online phase (subsection 4.3.2), the proposed approach uses the long-term predictor to forecast the degradation trend. Then, the information of the degradation states after the defined periods, t_1, t_2, etc., is updated by the short-term predictors, $ML_{2.i}$. Finally, subsection 4.3.3 is dedicated to discuss the choice of the suitable models for long- and short-term predictors.

4.3.1 Offline phase: Learning long- and short-term predictors

This phase aims to process the recorded raw data of the sensors to train long- and short-term predictors. For this purpose, the collected measurements are injected into a treatment procedure consisting of the following steps:

- Data preprocessing;
- Data preparation for training
  - long-term predictor: construction of Health indicators (HIs) based on physical characteristics of the system's degradation phenomenon;
  - short-term predictors: fusion of sensor signals using Auto-Encoder (AE) network.

4.3.1.1 Data preprocessing

In condition monitoring, it is necessary to visualize and analyze the raw data to identify their errors before using them for prognostic models construction (Jia et al., 2017). In this study, the acquired data suffer from missing values and noise.

To remedy missing values, we propose to use a non-linear interpolation technique (Xu et al., 2019, Akima, 1970) that is suitability for non-stationary data. The performance of this technique is illustrated in figure 4.3. On the left side, one can see the raw measurements with missing values, while the right side shows the obtained results after using the non-linear interpolation.

Next, to handle noisy data, that are caused by environment effects and sensors having poor quality, we propose to use the AE network. Its performance, that allows fusing and reconstructing data, is proven in numerous studies (Lin and Tao, 2019).

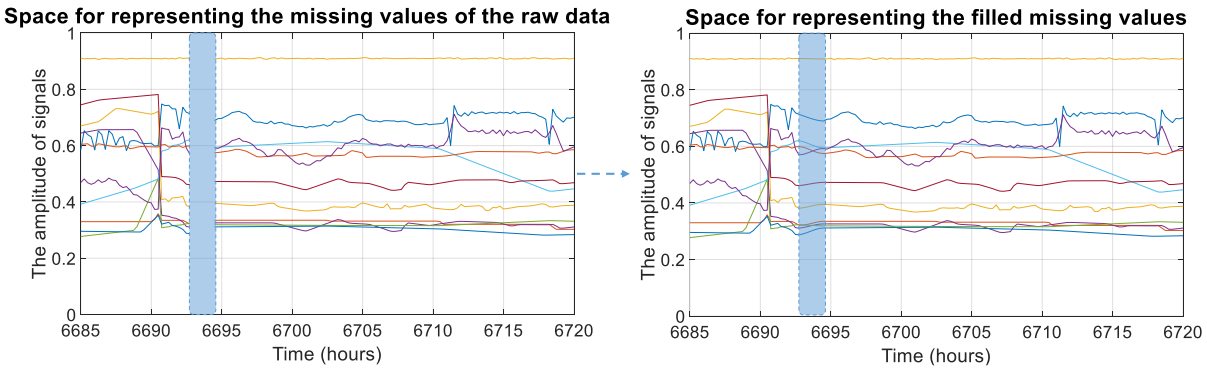

Figure 4.3: Imputing missing data using a non-linear interpolation.

In this work, the completed data $x(t)$ (after handling the missing values) with m dimensions of measurements are injected into the AE input layer for fusion. This step, named encoding phase, is performed by using one hidden layer, that allows fusing data and consequently reducing their dimensions to one representative vector. Next, the encoded data is injected into the decoding phase to reconstruct the m-dimensional input data, $\hat{x}(t)$. The difference between the input data $x(t)$ and their reconstructed one $\hat{x}(t)$ is used as a loss function to train the AE model. Technically, this procedure updates the weights and the bias of the encoding and decoding layers using the gradient-descent back-propagation algorithm to minimize the Mean Square Error (MSE) between $x(t)$ and $\hat{x}(t)$. The outputs of the AE, $\hat{x}(t)$, capture major signals in the inputs but is considered more reliable as it has the ability to eliminate noises inherent in the inputs.

4.3.1.2 Data preparation for training prognostics models

This step is simultaneously performed by two tasks: 1) data preparation for training the long-term predictor and 2) data preparation for training the short-term predictors. In the first task, the preprocessed measurements are used to build health indicators representing the different fouling evolution trends based on their physical characteristics. These HIs allows effectively tracking fouling evolution over time, and therefore can be used as the input of long-term predictor. In the second task, all preprocessed measurements are fused using an auto-encoder network to reduce the noise and the dimensionality of the data. This technique allows benefiting all existing sensor measurements and compressing them for effectively learning the short-term predictors.

Task 1: Data preparation for training the long-term predictor

The main objective of this task aims to extract features and build HI that allows

capturing the degradation trends in long-term of the system. In practice, the construction of a such HI strictly depends on the behavior and on the characteristics of the targeted system. For fouling issue, there exists several techniques in literature to represent the evolution of fouling in heat-exchangers (concentrators). One of these techniques is the use of the input(s), output(s) temperatures and pressures of the concentrators to estimate their heat transfer rate (Ardsomang et al., 2013). Indeed, this rate is highly affected by the fouling in the heat tubes. Therefore, the variation in the overall heat transfer rate is a good indicator characterizing the fouling. For this purpose, the heat transfer rate is evaluated by equation 4.1.

$$Q = U \times A \times \Delta T_{lm} \tag{4.1}$$

with

$$\Delta T_{lm} = \frac{(T_2 - t_2) - (T_1 - t_1)}{\ln[(T_2 - t_2)/(T_1 - t_1)]} \tag{4.2}$$

where Q is the heat transfer rate between two fluids (hot and cold) in the heat-exchanger, U is the overall heat transfer coefficient, A is the heat transfer surface area and ΔT_{lm} is the logarithmic mean temperature difference (t_1, t_2), calculated from the input and output temperatures (T_1, T_2) of both fluids. More details about the heat-exchanger design parameters could be found in (Kresta et al., 2015). Then, the HI expression, i.e. fouling index representing the resistance to heat transfer, can be defined according to the following equation:

$$HI = \frac{Q}{\Delta T_{lm}} \tag{4.3}$$

From equation 4.3, the evaporated water, which is represented by Q, is strongly correlated with the health indicator, while the difference between the steam temperature and heavy black liquor (ΔT_{lm}) represents the driving force of heat exchange. Figure 4.4 illustrates different trajectories of the HI obtained by using equation 4.3.

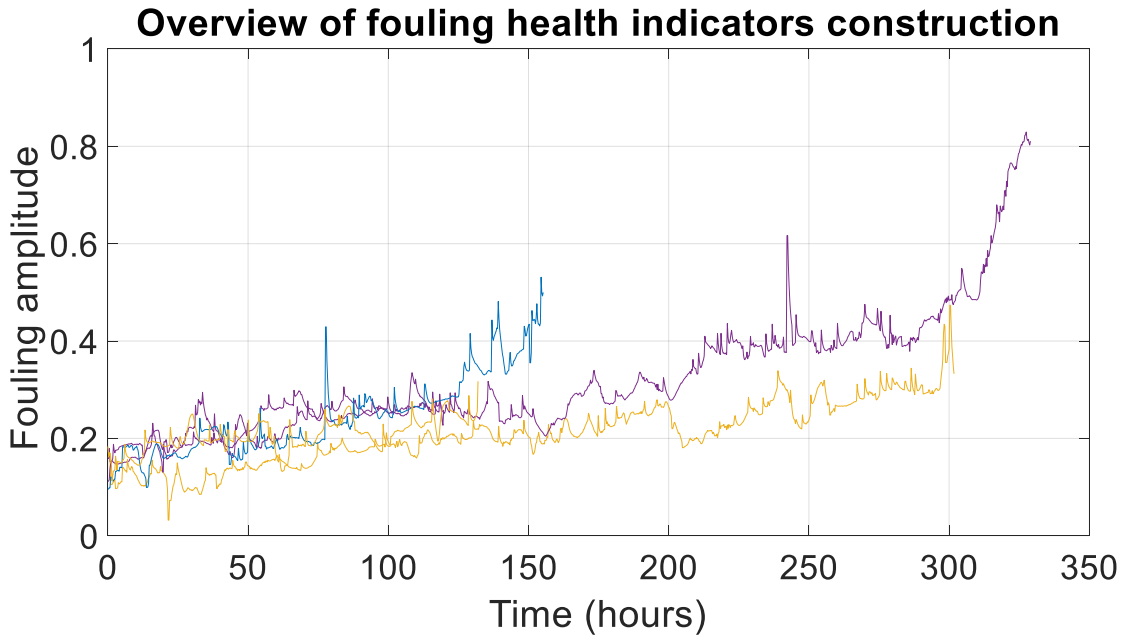

Figure 4.4: Three trajectory examples of the fouling HI over time.

The obtained HI trajectories are then structured in the exploitable format for training the long-term predictor using the algorithm 2. Let's assume that there are j historical HI trajectories (sequences) representing the degradation trends of the system, from its nominal condition to its end of life. These trajectories are stored and then divided into two parts, l_trn and l_tgt that correspond to the long-term training inputs and the long-term target outputs, respectively. The training inputs represent the actual observations of the system health state, while the target outputs consist of the desired values to be predicted and represent the system health states in the future.

Algorithm 2 Data structuring for long-term predictor

Initialization:
Set the number of sequences, j
Create empty cells l_trn, l_tgt
for $i = 1$ *to* j **do**
  Calculate the length l of the trajectory HI_i
  Save all of the observations of HI_i from 1 to $(l-1)$ in l_trn_i cell
  Save all of the observations of HI_i from 2 to l in l_tgt_i cell

Task 2: Data preparation for training the short-term predictors

In addition to the ability of noise elimination, the AE model is also used for dimen-

sionality reduction. Technically, using the encoding layer, it allows fusing all preprocessed sensor measurements (presented on the left side of Figure 4.5) and consequently learn the presentation of one dimension for the fused data (shown on the right side of Figure 4.5).

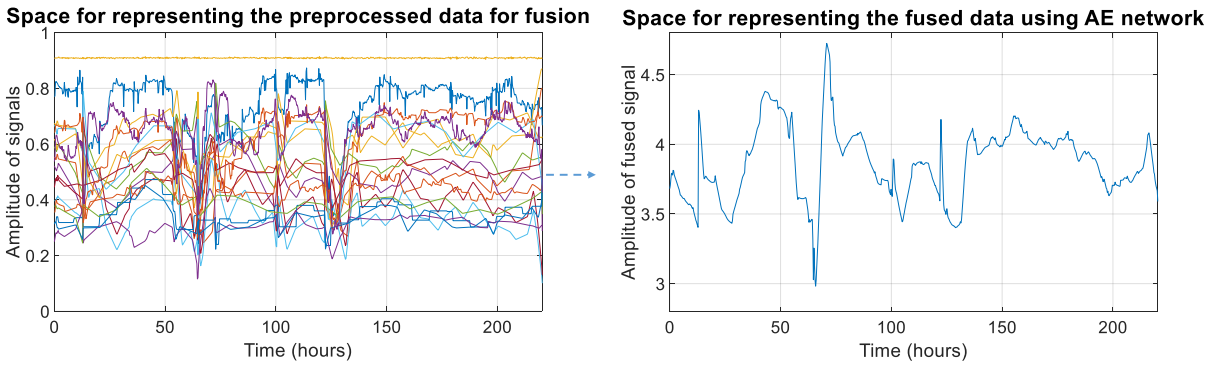

Figure 4.5: Data fusion using auto-encoder neural network.

The fused data obtained at the output of the encoding layer are then structured in the exploitable format for training the short-term predictors using algorithm 4.1. Specifically, the constructed cells $train_{h+1}$ and $target_{h+1}$ of each fused data sequence S_i should be stored in the same column vector variables s_trn and s_tgt, respectively. Note that the short-term prediction requires to know the essential observation period for the training inputs, denoted by $strain$, and the starting prediction instant, denoted by $starget$. For illustration, the essential observation period can be set as 24 hours while the starting prediction instant may occur at 30 hours (6 hours after the essential observation period).

Algorithm 3 Data structuring for short-term predictors

Initialization:
Set the number of sequences, j
Set the essential observation period, $strain$
Set the starting prediction instant, $starget$
Create empty variables s_trn, s_tgt
for $i = 1$ *to* j **do**
    Load the total sequence S_i
    Calculate the length l of S_i
    for $h = 0$ *to* $(l - starget - 1)$ **do**
        Save S_i from the instant $(h + 1)$ to $(strain + h)$ in $train_{h+1}$ cell
        Save the target value at the instant $(starget + h)$ in $target_{h+1}$ cell
    Save all $train_{h+1}$ cells in s_trn
    Save all $target_{h+1}$ cells in s_tgt

Training the long- and short-term predictors:
Once the data structure for the long- and the short-term predictors are prepared, they are injected into the prediction models to learn how to map each observation of the training inputs to their corresponding target outputs. We propose to use the existing ML models, for example NARX and LSTM, to separately learn the short and long term predictions in the offline phase. As these training procedures do not belong to the main contributions of this chapter and were presented in the literature, it is not necessary to describe them in this section. Next, the principal contribution of the chapter, which concerns the development of a hybrid prognostics approach based on the combination of the results of the long- and short-term predictors, will be detailed in section 4.3.2.

4.3.2 Online phase: Combination of the long- and short-term predictors

This subsection aims to propose a new effective hybrid approach for online prognostics based on the long- and short-term predictors trained in the offline phase. The proposed approach inherits the advantages and overcomes the disadvantages of the existing long- and short-term predictors. It uses the results provided by the short-term model to update the predictions by the long-term model.

Algorithm 4 describes how the proposed hybrid prognostics approach works. In summary, the first machine learning model ML_1, i.e. long term predictor, starts forecasting the degradation trend using the actual observations of the system from time $t = 0$ to the current time $t = t_c$. Simultaneously, the first short-term predictor, $ML_{2.1}$, also use the same observations to predict the system health state at $t = t_c + t_1$, where t_1 is the forecast horizon of the first predictor. This result is used by the long-term predictor, ML_1, as its input at $t = t_c + t_1$ to update the forecasting degradation evolution. The updating process is sequentially performed m times where m is the number of short-term predictors. In this case study, four short-term predictors, $ML_{2.1}$, $ML_{2.2}$, $ML_{2.3}$, and $ML_{2.4}$, are built and used to predict the system state at $t = t_c + t_1$, $t = t_c + t_2$, $t = t_c + t_3$ and $t = t_c + t_4$, respectively. For instance, that means when the predictions of ML_1 reaches the instant $t = t_c + t_1$, it replaces its predicted value at that time by the one obtained with $ML_{2.1}$ and update the predictions ahead until the instant $t = t_c + t_2$ where the $ML_{2.1}$ is investigated to update for the second time the degradation trend, etc. The obtained trajectory is used to evaluate the remaining useful life of the system, which is named Time-To-Clean (TTC) in this case study. The TTC is determined by the time from the current moment until the time when the degradation trajectory reaches a critical threshold (Thr) given by the expert of the system.

Algorithm 4 Online prognostics procedure

INITIALIZATION:
Set the critical threshold, Thr
Set the update times for long-term predictors, t_1, t_2, t_3 and t_4
Create empty cell named global predictions, GP
Set the number of prognostics points, n, in long term horizon ($n = 1000$)
Create a counter h to track the number of prediction times and set $h = 1$.
PREDICTION PROCEDURE:
Load monitoring data from $t = 0$ to $t = t_c$
Forecast the degradation trend by ML_1
Save the results in a vector $Pred$ consisting n values
for $j = 1$ *to* n **do**
    $Pred_j$
    for $i = 1$ *to* 4 **do**
        if $j = t_i$ **then**
            Predict the system state at $t_c + t_i$ by $\mathrm{ML}_{2.i}$
            Replace $Pred_j$ by this result
            Update the degradation evolution by ML_1
Save the predicted observations of $Pred$ from 1 to n in cell h of GP
Evaluate the failure time
Save the failure time in cell h of D
Upgrade the update time t_1, t_2, t_3, and t_4 by one unit time
Increase the counter h and repeat **PREDICTION PROCEDURE**.

4.3.3 Discussion on the choice of models for long- and short-term predictors

The previous subsections presented only a generic prognostics framework for closed-loop controlled systems. Indeed, for a particular system, it is necessary to choose the appropriate machine learning models, that can respond well to the system's special characteristics.

Considering fouling phenomena of the heat-exchanger tubes, it is necessary to build a model that is capable to capture the change of the fouling evolution trend under the closed-loop controller effects.

The build model is required to learn the global degradation trends taking into account non-stationary operating conditions from multiple historical scenarios. Hence, this chapter proposes to use two artificial neural networks, Long-Short Term Memory (LSTM) and Nonlinear Auto-Regressive Exogenous Model (NARX), that allows finding complex relationships between input and output variables without prior knowledge.

In detail, thanks to the capacity of learning the degradation trend over long-time sequences, the LSTM network is a promising candidate for long-term predictor. It uses the predicted sequential values of the previous prediction steps as an input, and therefore may capture useful information from the past trend. Moreover, its memory gate allows taking only the useful information with regard of the global degradation trend, while the forget gate can decide which unnecessary information to discard to further improve the predictions in long-term-horizon. In addition, it is better than RNN in dealing with the vanishing/exploding gradient issue and can remember longer sequences than GRU (Rezaeianjouybari and Shang, 2020). This procedure is illustrated in Figure 4.6.

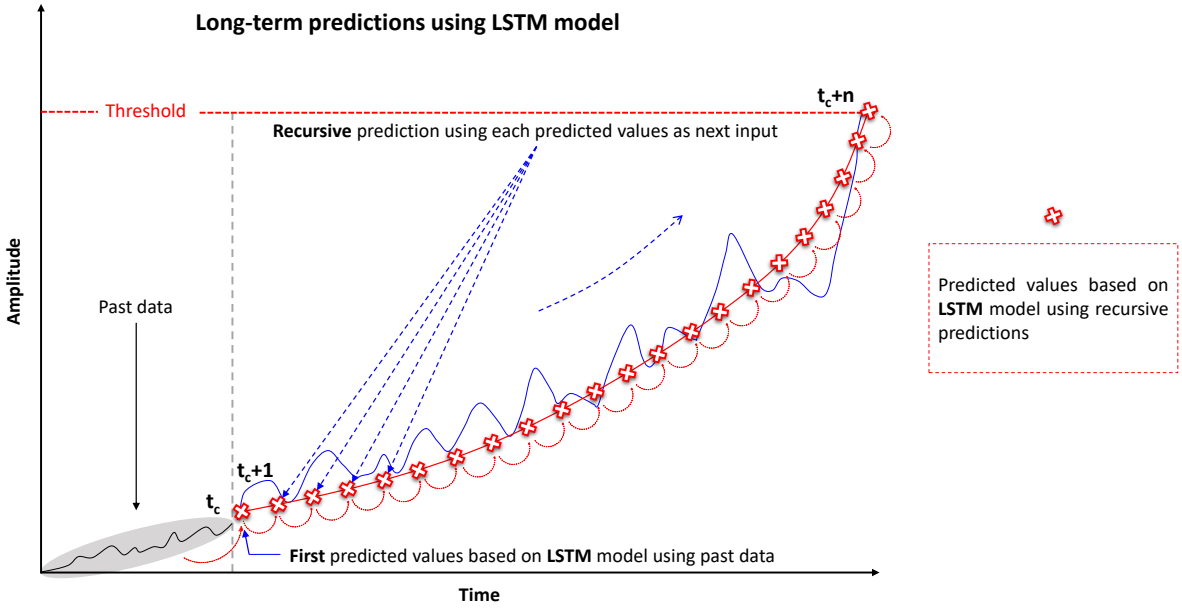

Figure 4.6: Long-term prediction based on LSTM model.

Besides, the NARX model is appropriate to build short-term predictors. It is a simple neural network based on the concept of causality that connects the predicted value, e.g. fouling level, to the premises of the monitoring data at a defined time (Shih and Lee, 1995). The main advantages of this model are the simple learning process, which does not require complex setting parameters, and its fast computing time when exploiting data. In detail, it uses past monitoring data to estimate only one value in the future, which is usually more precise than long-term predictions. As the proposed approach uses four short-term predictors, four NARX models are built. These models use the monitoring data to predict the system health state after the following periods: $t_1 = 6$, $t_2 = 12$, $t_3 = 18$ and $t_4 = 24$ hours, as illustrated in Figure 4.7.

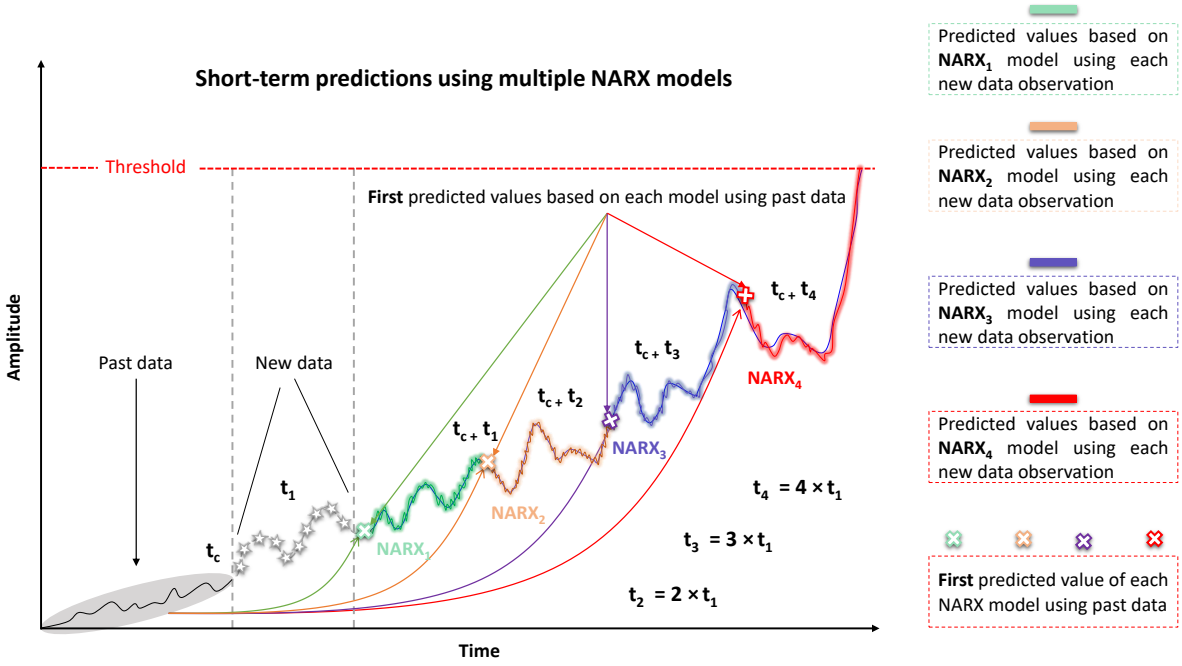

Figure 4.7: Short-term prediction based on NARX models.

More details on the main structures and functionality of the LSTM and NARX models can be consulted in (Wu et al., 2018b, Chan et al., 2015), respectively.

4.4 Case study application and results

In order to verify the effectiveness and the applicability of the proposed hybrid prognostics approach, real data of pulp and paper industry located in Canada are investigated. The aim of the proposed study is to anticipate unexpected fouling of the heat-exchanger tubes by forecasting its evolution and predicting more accurately its TTC. Therefore, the fouling is monitored using several sensors such as temperature and pressure placed at different locations of the plant. By using these sensors, the data are first recorded and cleaned for the processing task. This latter step uses all measurements for fusion and builds efficient health indicators that reflect well the fouling behaviors. Then, the obtained results are injected into the proposed algorithm for prognostics purpose.

The details of this case study will be presented in Subsection 4.4.1. Then, Subsection 4.4.2 aims to discuss the performance of the long- and short-term predictors. Finally, Subsection 4.4.3 is dedicated to investigate the performance of the proposed hybrid prognostics approach.

4.4.1 System description

The Kraft pulping process consists of several steps including wood chips cooking, pulp washing, bleaching and pulp drying. This latter action provides black liquor that is principal material in the energy conversion process. The global overview of this process is represented in Figure 4.8.

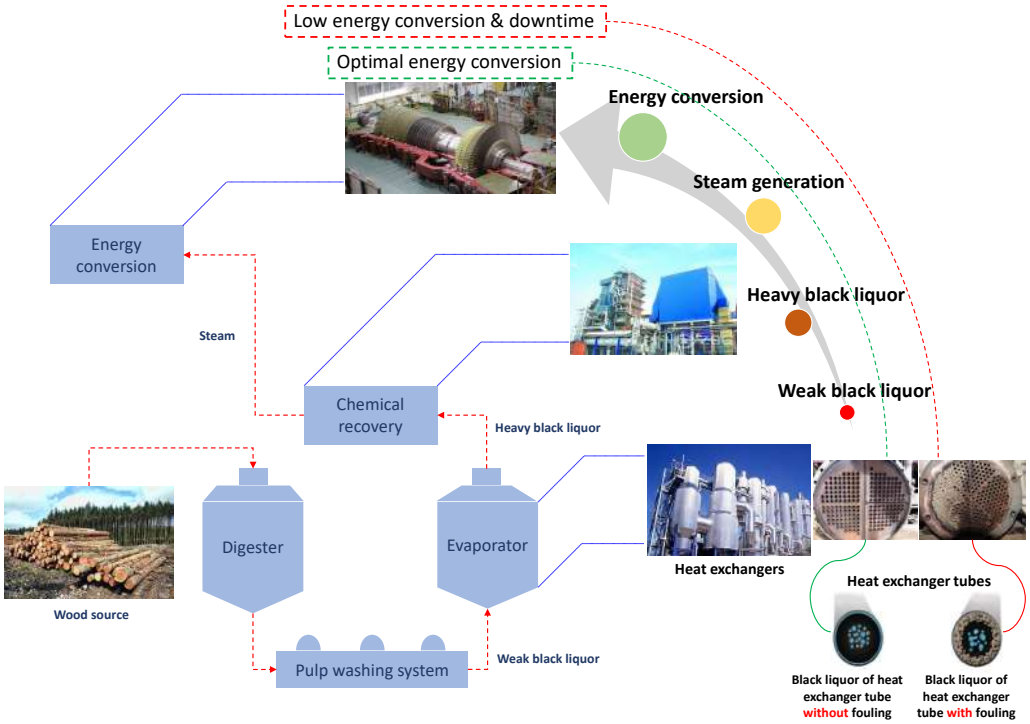

Figure 4.8: Illustration of fouling problem in pulp and mill manufacturing process.

Specially, the organic and inorganic solids dissolved in the black liquor are injected into a concentrator to further concentrate the weak black liquor from approximately 15–18% of dissolved solids up to 65–70% of solids. The output of the concentrator (heavy black liquor) is sent to the recovery boiler system, where vapor (steam) is formed by heating the heavy black liquor. The vapor formed in the recovery cycle is used as a source to be converted into another form of power for energy conservation. However, during the process, fouling is created and consists of unwanted material that appears on the inner surface of the heat-exchanger tubes. Over time, this fouling increases and affects the performance of the exchanger, and the quality of the black liquor cannot reach the standard level to be sent to the recovery boiler. Technically, when the heat exchanger tubes are in a nominal state (without fouling), the performance of the energy conversion process can attain the optimal level. Otherwise, with a high fouling level, its performance significantly decreases and can lead to downtime.

Figure 4.8 shows the important impact of the fouling phenomenon in a heat exchanger on the energy conversion process. Hence, to track this phenomenon well, various sensors are placed on the system. A brief summary of these variables is presented in Table 4.2. . In this case study, these sensors were used to collect raw data during 8 months at a sampling frequency of 1 sample/15 min under different operating conditions. Each sample of the data represents the mean value of all measurements in 15 min.

Variable	Description	Unit
V1	Flow of liquor feeding the concentrator	l/s
V2	B.P.R. of liquor feeding the concentrator	K
V3	Solid concentration of liquor feeding the concentrator	%
V4	B.P.R. of liquor leaving the concentrator	K
V5	Solid concentration of liquor leaving the concentrator	%
V6	B.P.R. of liquor from concentrator's flash tank	K
V7	Solid concentration of liquor from concentrator's flash tank	%
V8	Temperature of vapor from concentrator	K
V9	Pressure of fresh steam sent to the concentrator	kg/ms^2
V10	Temperature differential steam-liquor	K
V11	Temperature of liquor from concentrator	K
V12	Temperature of liquor sent to storage tank	K
V13	Temperature of fresh steam before desuperheating	K
V14	Temperature of vapor from concentrator	K
V15	Liquor flow from concentrator's flash tank	l/s
V16	Liquor level in the concentrator	%
V17	Flow of fresh steam to the concentrator	kg/s
V18	Pressure of concentrator's flash tank	kg/ms^2

Table 4.2: Summarize of monitoring measurements.

Then, the HIs (constructed by Task 1 in Subsection 2.1.2) and the fused data (obtained by Task 2 in Subsection 2.1.2), are divided into two groups, training and test sets, taken randomly. The training group contains 17 trajectories for learning the prediction models while the test group has 3 trajectories for the online prognostics of fouling. To avoid the remarks redundancy, only the results of the second test trajectory are insightfully investigated in next subsection, while the ones obtained when using the first and third test trajectories can be consulted in Appendix A.

4.4.2 Performance of the long- and short-term predictors

As the performance of the proposed hybrid adaptive prognostics approach strictly depends on the choice of predictor models, this section is dedicated to investigate the plausibility of choosing LSTM and NARX for long- and short-term predictions, respectively. The appropriate tuning parameters of these models are summarized in Table 4.3. They are chosen through numerous empirical tests. Specifically, each set of parameters is tested many times to observe the robustness and performance of the correspondent model, and then based on these observations, the best one is chosen. Note that the LSTM performance is significantly affected by the changes of the optimizer (ADAM, SGDM, RMSprop) and the size of hidden units. Besides, the NARX is very simple and requires to adjust only the number of hidden layers.

LSTM network					
Parameters	Hidden units	Epochs	Optimizer	Learning rate	L2 regularization
values/methods	100	100	Adam	0.001	10^{-4}

NARX network				
Parameters	Hidden size	Hidden units	Epochs	Optimizer
values/methods	5	100	1000	Levenberg-Marquardt

AE network						
Parameters	Hidden size	Epochs	Loss function	Training algorithm	Encoder	Decoder
values/methods	1	500	MAE	GDM	Logsig	Purelin

Table 4.3: Parameter tuning of the prediction models.

Figure 4.9 compares the obtained results in long-term predictions using LSTM with other existing models such as NARX, ARIMA, and GRU. One can see that the LSTM is the best one for tracking changes in the evolution trend of the fouling. It allows predicting the TTC to be close to the actual one (the result is only 3 hours earlier than the actual TTC). Besides, the other models (NARX, ARIMA and even GRU in the family of recurrent neural networks like LSTM) provide non-accurate results with the differences of 9.3, 13, and 23 hours from the actual TTC, respectively.

Figure 4.10 shows the prediction results in short-term horizon of 6 hours using NARX or LSTM model. One can see that in this case, the NARX model provides more accurate results than the LSTM one. Indeed, the difference between the predicted and the actual values when using the NARX is only 15 minutes while the one provided by the LSTM is 3 hours. However, as the NARX model only provides good results in short-term horizon (6 hours in this case), it does not provide enough time for planning maintenance actions. Hence, it is necessary to perform the prognostics in long-term horizon.

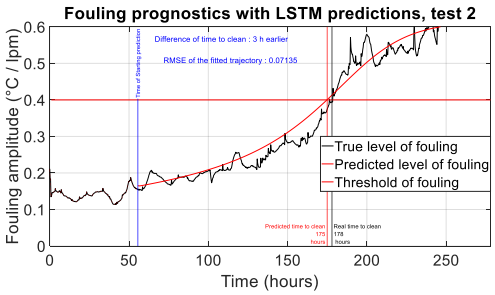

a) Long-term predictions with the LSTM model

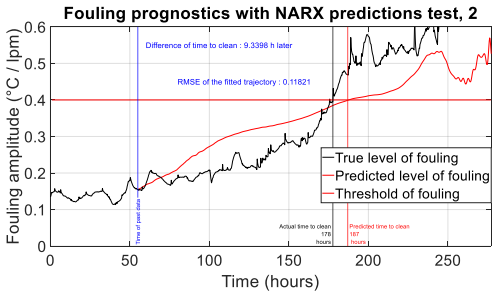

b)Long-term predictions with the NARX model

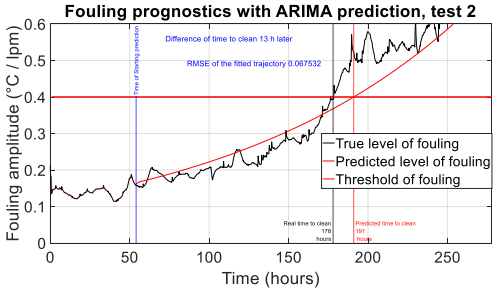

c) Long-term predictions with the ARIMA model

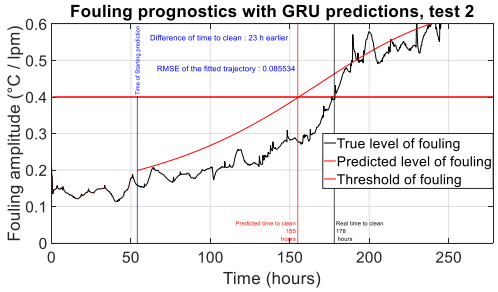

d) Long-term predictions with the GRU model

Figure 4.9: Fouling prognostics using long-term predictions considering data $test_2$.

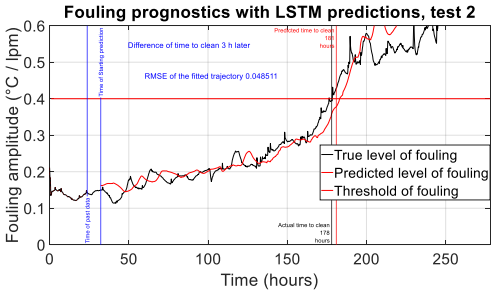

a) Short-term predictions with the LSTM model.

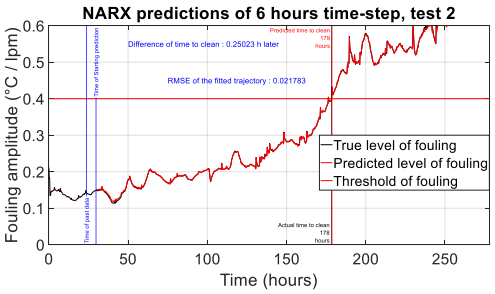

b) Short-term predictions with the NARX model.

Figure 4.10: Fouling prognostics using short-term predictions considering data $test_2$.

4.4.3 Performance of the proposed approach

In this section, the proposed hybrid prognostics approach is applied to improve the accuracy prediction in long-term horizon. It uses four NARX models for short-term predictions and one LSTM model for long-term prediction. In detail, for each time-step $(t_c + t_i)$ the four NARX models use the preprocessed raw data after fusion step to predict the fouling level

at 6 hours, 12 hours, 18 hours and 24 hours later (see figure 4.11), respectively. Besides, the LSTM model predicts the fouling trend using the constructed HIs, and then use the NARX outputs to refine the fouling state.

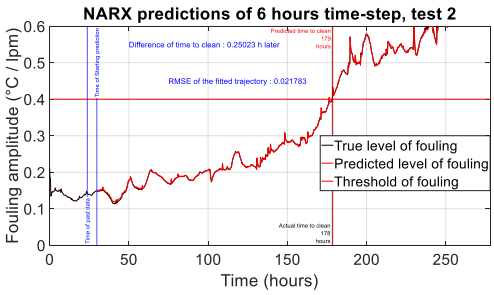

a) $NARX_1$ predictions of 6 hours time-step

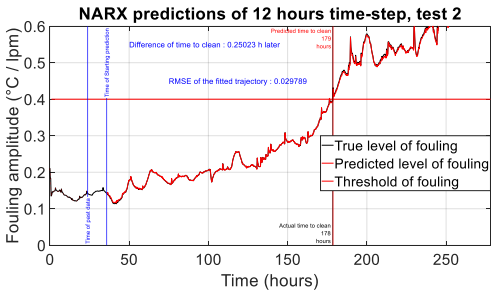

b) $NARX_2$ predictions of 12 hours time-step

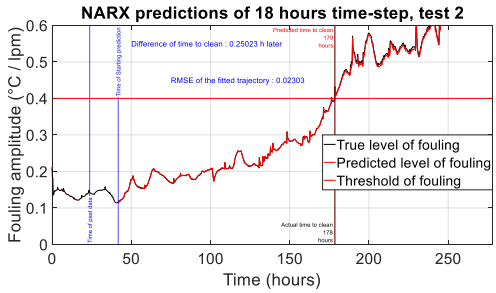

c) $NARX_3$ predictions of 18 hours time-step

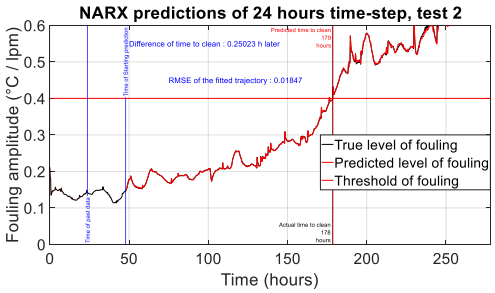

d) $NARX_4$ predictions of 24 hours time-step

Figure 4.11: Fouling prognostics with NARX models considering data $test_2$.

For illustration of the performance of the proposed approach, figure 4.12 compares the fouling trend prediction obtained when using only long-term predictor based on LSTM with the ones of the proposed approach. In figure 4.12, the blue curve represents the fouling trend obtained when using only the long-term predictor based on LSTM model. Besides, the red curve represents the one obtained when using the proposed adaptive approach. In this figure, on the zoomed parts, the fouling curve represented by black color has been reduced due to a controller action or condition change. In this case, the blue curve continues its trajectory without taking into account this change, while the proposed method is able to capture this change in the fouling evolution represented by red curve.

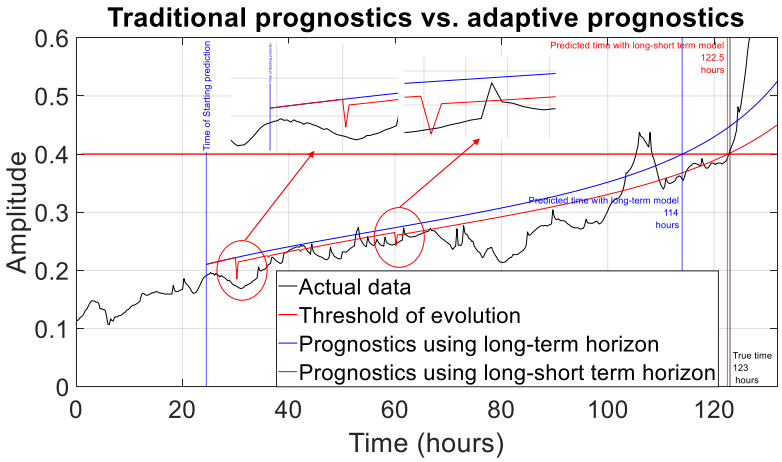

Figure 4.12: Classic long-term predictor vs. the proposed adaptive one for prognostics.

Furthermore, the proposed approach, that integrates the results of 4 NARX models in LSTM long-term predictor, also provides accurate results of fouling levels even for a long-term horizon (figure 4.13).

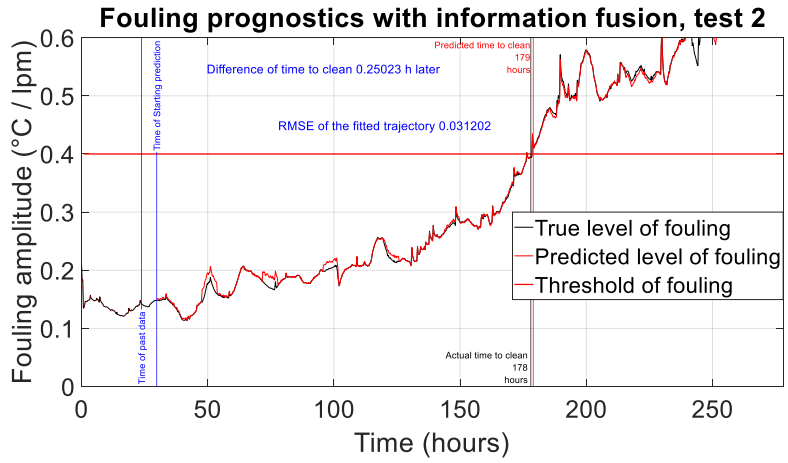

Figure 4.13: Fouling prognostics using the proposed approach considering data test_2.

Figure 4.14 compares the probability density distribution of the predicted TTC values at different times using the proposed approach with other existing models (when investigating the data test_2). One can see that the proposed approach is better than the existing ones. Indeed, the mean values of predicted TTC obtained when using the ARIMA,GRU and only LSTM models are respectively 192, 212 and 185 while the one of the proposed approach is 178, same value as the real TTC. In addition, the confidence interval given by the proposed approach is smaller than the one of the ARIMA and GRU models.

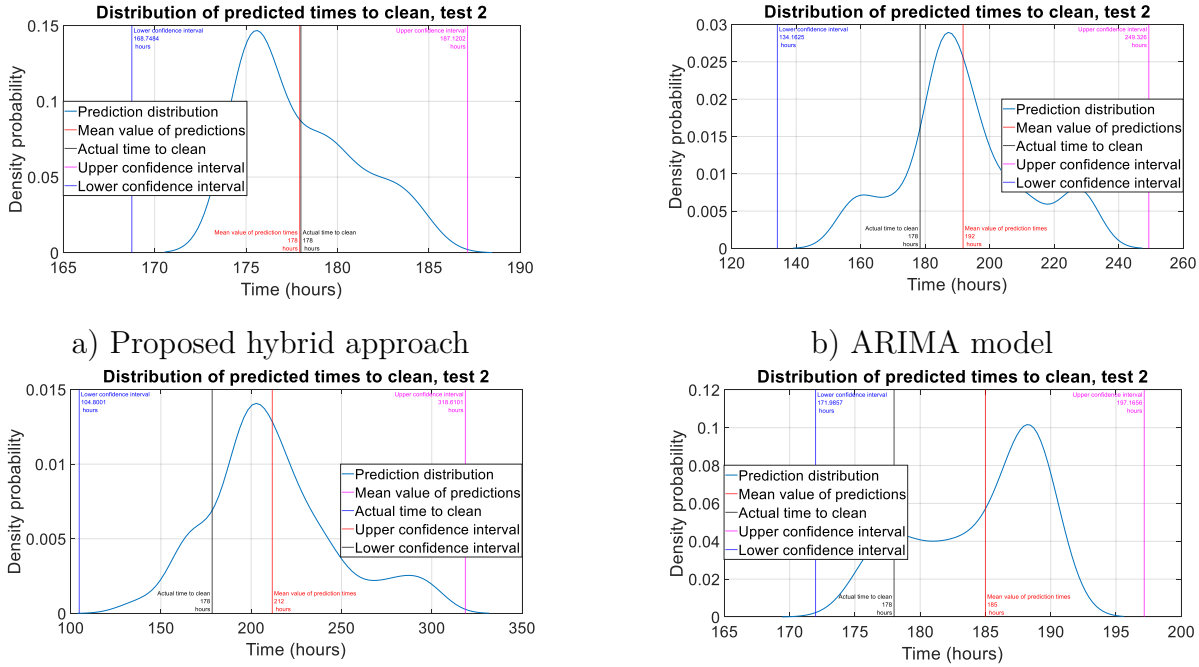

a) Proposed hybrid approach

b) ARIMA model

c) GRU model

d) LSTM model

Figure 4.14: Probability density distribution of the predicted TTC values, $test_2$.

In order to confirm the effectiveness of the proposed approach, we further evaluate its performance on a range of popular prognostics metrics widely used in the literature and compare to those of existing approaches, including LSTM, GRU, and ARIMA (table 4.4). The investigated metrics consist of accuracy (Acc), precision (Pre), mean absolute percentage error (MAPER), root mean square error (RMSE), and prognostics horizon (PH). Among them, the Acc, Pre, MAPER, and RMSE are measures of the goodness of the predictions, while the PH is defined as the difference between the time when the predictions first meet the specified performance criteria and the end of life time (Saxena et al., 2010). In this case study, the parameter α for PH calculation is set to 10%; and the Acc is evaluated following the formula presented in (Benkedjouh et al., 2015). Note that the greater the values of Acc and PH, the better the prognostics algorithm; and otherwise for Pre, MAPER, and RMSE.

Table 4.4 shows that the proposed approach is the best according to all of the considered metrics. This is convincing evidence highlighting the effectiveness and robustness of our approach.

The superiority of the proposed approach have been proven in table 4.4, it provide high level of prediction accuracy with good fitting of the fouling trajectories. It is helpful for making decisions, e.g. scheduling maintenance actions. Because, the systematic mainte-

	LSTM	GRU	ARIMA	Proposed approach
Acc	0.9	0.81	0.82	**0.95**
Pre	14.26	27.33	17.7	**8.2**
MAPER	15.26	22.66	19.55	**5.9**
RMSE	21.7	38.43	28.93	**8.93**
PH (*Hours*)	78	58	69	**105**

Table 4.4: Results of prognostics metrics.

nance scheduling . Because, the systematic scheduling of the cleaning of the heat exchanger tubes is very expensive, when one decides to track the fouling up to the critical phase to do the cleaning. In fact, if a systematic maintenance of one week is planned for the cleaning, with the prognosis of the fouling, this action can be reduced to one cleaning per two weeks for example, which is very beneficial for the company. Moreover, with the monitoring of the fouling, it is possible to operate on the different parameters of the exchanger input in order to optimize the energy conversion process.

4.5 Conclusion

A new adaptive prognostics approach, based on the combination of long- and short-term predictors, has been presented in this chapter. This approach allowed the prediction of fouling in the heat exchangers and the time-to-clean of their tubes, leading to an optimization of the energy conversion of the black liquor. More precisely, a long-term fouling dynamic evolution was captured by using a long short-term memory model. Then, the adaptation to changes due to controller activities was addressed by deploying four nonlinear auto-regressive exogenous models that predicted the fouling level in discrete short-term horizons. Finally, an improvement in the accuracy of the fouling prognostics, and therefore the prediction of cleaning time, was achieved by a fusion procedure that exploits each short-term predictor to update the predictions of the long-term model. The efficiency and robustness of the approach were verified through real industrial data collected from a pulp and mill manufacturing system. The obtained results clearly highlighted an accuracy of 95% within a prognostic horizon of 105 hours. These results confirm the relevance of the approach in taking into account the behavior changes due to the control system variations and in predicting the fouling evolution. The results can be useful for scheduling the cleaning actions of heat exchanger tubes and optimizing the black liquor conversion process.

Conclusions, limitations & perspectives

Conclusions

This research work was conducted within the framework of a European project, SMART, aiming to support small and medium-sized companies in improving their productivity, reducing their maintenance costs, and thus increasing their competitiveness. One of the levers for achieving these goals was to develop intelligent autonomous systems from the viewpoint of system health management. Hence, in this manuscript, we addressed the topics of data-driven prognostics and health management of engineering systems, including three principal tasks: fault detection, diagnostics, and failure prognostics.

In the first chapter, we reported the literature works related to the three above mentioned topics. We started by categorizing different techniques for health indicators construction, fault detection, fault diagnostics, and failure prognostics; and then pointed out the challenges and the key issues to be addressed. In detail, it was seen that for fault detection, various and different health indicators were proposed to detect faults of only specified components with limited number of monitoring parameters under few operating conditions. These limitations were due to the lack of a reliable and effective health indicator, which did not allow taking into account diversities of component fault types, various monitoring parameters, and different operating conditions. Regarding fault diagnostics, we have presented a brief review of methods based on pattern recognition techniques, which are the most widely used in data-driven framework. This type of method consisted of two phases: learning the states of the system (healthy, faulty) and then diagnosing online the faults. However, it could not diagnose new faults that had not been recognized in the learning phase. For the prognostics aspect, we discussed different approaches and techniques developed to anticipate failures. To our humble knowledge, few existing works took into account instantaneous changes of operation parameters caused by controller activities to improve long-term predictions of system residual lifetime. Finally, we filled the literature gaps by positioning and proposing our contributions that remedy the challenges of each topic.

The second chapter focused on the construction of an efficient and robust health indicator for fault detection. This health indicator was applied to detect multiple fault types of different systems, such as critical components of rotating machines, i.e. unbalanced supply, rotor bar, bearing, gear, as well as machining tool of manufacturing systems. Besides, apart from the detection of several types of faults, it was able to extract fault signatures

from numerous measurement types such as current, voltage, vibration, force, and torque signals under various operating conditions (speed, load level, machining parameters). The effectiveness and performance of the proposed indicator were demonstrated by its application in three case studies including rotating motors of railways, gearbox of wind turbine, and multi-axis machining robot. The obtained results from these demonstrators showed clearly that the proposed health indicator can detect faults of a large range of components.

The third chapter aimed to consider the challenges posed for fault diagnostics of dynamic systems such as multi-axis robots. Especially, it addressed an interesting research question: how to diagnose the origin of robot axis drifts where these drifts have not been learned before. For this purpose, a new online diagnostics method for localizing the origin of drifts of the multi-axis robot has been presented. This method was based on the fusion of information from two monitoring methods: direct and indirect. The direct monitoring used sensors already installed in the different parts of the system (six servo motors) while the indirect monitoring used sensors installed in a unique point of the system (machining tool). In the off-line phase, the data obtained from the indirect monitoring were processed to build a diagnostic model using the health indicator presented in Chapter 2. In the off-line phase, the measurements from the tool-level sensors were used to indirectly track the robot motions, and thus we could early detect and diagnose the axis drifts, whose fault patterns were already learned in the offline phase. For unknown anomaly observations from the tool-level sensors, the direct monitoring approach using the robot encoder measurements was launched to localize the origin of the axis drifts. Using this result, the relevant observations from the indirect monitoring were labeled and thus, the classifier for online diagnostics of the robot axis drifts was updated. This proposed methodology was applied to a real machining multi-axis robot to highlight its performance and efficiency. It was clearly shown that it is possible to diagnose online the origin of new faults even if these latter faults have not been learned previously.

The fourth chapter was dedicated to prognostics issues of system failure in a controlled industrial process that can lead to negative impacts in long-term predictions. To remedy this problem, we proposed a new adaptive prognostics approach based on the combination of machine learning predictors. The first machine learning model was used to predict the system's health state in long-term horizon. Besides, the second machine learning model, which was composed of several sub-models, was used to predict the system in discrete short instants. Next, the predictions obtained by the short-term models were used to update online the long-term predictor to reduce uncertainties and to improve the prognostics accuracy. The proposed approach was tested on real manufacturing data of pulp and mill industry. Particularly, this approach was used for prognostics of fouling in heat exchanger tubes and predicted their time to clean. The obtained results clearly highlighted an accuracy of 95% within a prognostic horizon of 105 hours. These results confirm the relevance of the approach in taking into account the behavior changes due to

the control system variations and in predicting the fouling evolution. They can be useful for scheduling the cleaning actions of the heat-exchanger tubes and optimizing the energy conversion process.

Contribution publications

A major part of this research work's contributions has been presented in several international conferences and published in high quality journals. Particularly, the methodology for construction of the new health indicator for fault detection has been published in the following journal:

- Soualhi, M., Nguyen, K. T., Soualhi, A., Medjaher, K., & Hemsas, K. E. (2019). Health monitoring of bearing and gear faults by using a new health indicator extracted from current signals. Measurement, 141, pages: 37-51.

Besides, the application of the proposed robust new health indicator for faults detection and diagnostics of different systems has been disclosed in the following publications:

- Soualhi, M., Nguyen, K., Medjaher, K., Lebel, D., & Cazaban, D. (May 06, 2019). Health indicator construction for system health assessment in smart manufacturing. In Prognostics and System Health Management Conference (PHM-Paris) (pp. 45-50) in the institute of electrical and electronics engineers (IEEE).
- Soualhi, M., Nguyen, K. T., & Medjaher, K. (2020). Pattern recognition method of fault diagnostics based on a new health indicator for smart manufacturing. Mechanical Systems and Signal Processing (MSSP), 142, 106680.

Regarding the contribution of fault diagnostics for dynamic systems such as multi-axis robots drifts, which is based on information fusion of direct and indirect monitoring ways, we have presented an article in the international conference of IFAC world congress 2020 and submitted a paper for Information Fusion journal:

- Soualhi, M., Nguyen, K., Medjaher, K., Lebel, D., & Cazaban, D. (July 11, 2020). Data-driven diagnostics of positioning deviations in multi-axis robots for smart manufacturing. IFAC-PapersOnLine.
- Soualhi, M., Nguyen, K. T., & Medjaher, K. Information fusion of direct and indirect monitoring for online detection and diagnostics of multi-axis robot drifts. Submitted to Information fusion journal (IF).

Finally, the prognostics approach based of the combination of long- and short-term predictors is published in Applied Energy journal:

- Soualhi, M., El Koujok, M. Nguyen, K., Medjaher, A., Ragab, H., Ghezzaz. A., Amazouz & O., Mohamed-Salah (2020, October). Adaptive Prognostics in a Controlled Industrial Process Based on Long- and Short-Term Predictors. Applied Energy (APEN).

Limitations

Although the results obtained in this thesis contribute to address the challenges of prognostics and health management induced by the Industry 4.0 (e.g., complex systems, dynamic behaviors, self monitoring and control process), there exists some limitations in each fault detection, diagnostic and prognostics contribution.

Fault detection

The proposed monitoring methodology and the new health indicator have been successfully applied to detect faults in several systems. However, with regard to their effectiveness, they have the following limitations:

- Regarding the proposed health indicator, its performance was depending on the quantity of data segments to be processed. The selection of the right value is still done manually through experimental results. Consequently, it is time consuming.
- The effectiveness of the proposed health indicator was tested in different operating conditions but these latter conditions were addressed separately.

Fault diagnostics

Diagnostics of multi-axes robot drifts is a new research field for condition monitoring. In this regard, we attempt to propose a new methodology to localize the origin of the robot drifts. However, it still exists some locks detailed below:

- For unknown fault types, the performance of the proposed methodology strictly depends on the result of direct monitoring mode, which can be infeasible if there exists a failure of one of the encoders.

- The indirect monitoring strategy used an auto-encoder network to fuse the different measurement types without taking into account the characteristic of each measurement. This can lead to imprecise result if one of the measurements does not represent well the system behavior.

Failure prognostics

The combination of short- and long-term predictors is a promising solution for the prognostics of system health states in long-term horizon. This combination provides some advantages, but has some limitations:

- Regarding the prognostics approach, the development was concentrated on the predicting tool but no deep study is conducted in data analysis step for the construction of the health indicator which is a crucial element for accurate prognostics.
- The proposed approach used four short-term predictors. This choice was taken based on an expert knowledge and with manual implementation. This takes a lot of time for the regularization of the model hyper-parameters.

Perspectives

The limitations mentioned above are the trigger points of the future works that will be developed to further improve our contributions. The following perspectives provide insights into these improvement suggestions.

Fault detection

To further enhance the performance of the proposed monitoring methodology of fault detection, the following aspects should be addressed:

- Development of an automatic selection procedure to optimize hyper-parameters, e.g. length of signal segmentation.
- Investigation of real-time variations in the operating conditions.
- Construction of generic prototype for system condition monitoring and its applicability in other case studies such as hydraulic, electronic, photo-voltaic, etc.

Fault diagnostics

The following propositions could be considered to overcome certain limitations:

- Implementation of an automatic feature selection procedure for health indicators fusion in the indirect monitoring.
- Development of additional monitoring techniques/sensors that overcome the direct monitoring errors if there exists a failure of one of the encoders.

Failure prognostics

In the last part of research work of this thesis, we propose some ideas to improve the proposed prognostics approach:

- Development of a systematic and automatic guidance tool for model selection of short-term predictors.
- Development of optimization algorithms for tuning the hyper-parameters of the prediction models.
- Integration of the prognostics results into the controllers for system reconfiguration and resilience.

As final and perspective of the overall thesis, one needs to exploit the proposed work to build a prognostics and health management monitoring prototype with a real implementation in an industry 4.0 production line.

Appendix

Appendix A

Health indicators construction for fault detection

The first appendix of this thesis aims to illustrate the obtained results of fault detection by using the proposed new health indicator on the other different operating conditions, corresponding to speed and load variations on LASPI test bench, and load level variation on AMPERE test bench, respectively. For this purpose, Figure A.1 shows the fault detection results on the LASPI platform with the three-phase current and voltage signals. Then, Figure A.2 presents the results obtained with AMPERE test bench when considering the three-phase current and voltage signals and also the three axis vibration signals.

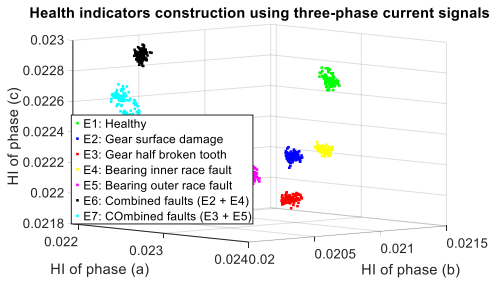

a) Current signals, 35 Hz, 0%

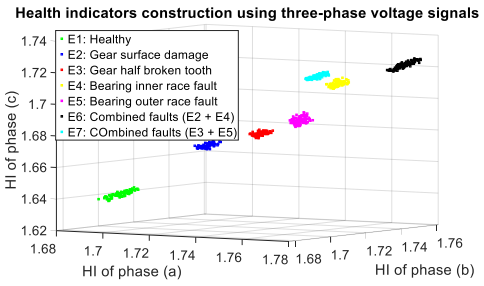

e) Voltage signals, 35 Hz, 0%

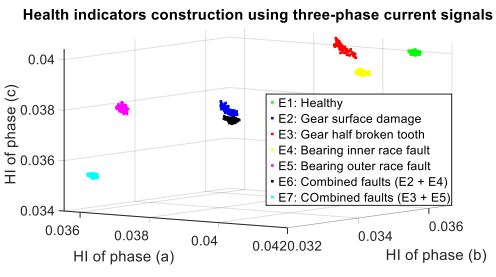

c) Current signals, 35 Hz, 75%

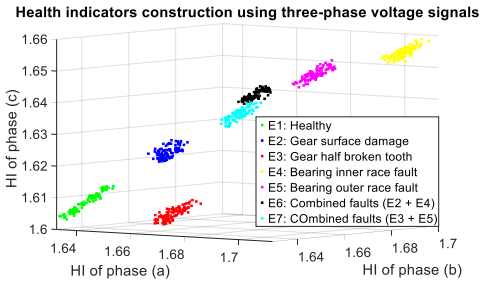

e) Voltage signals, 35 Hz, 75%

Figure A.1: Proposed HI on LASPI platform.

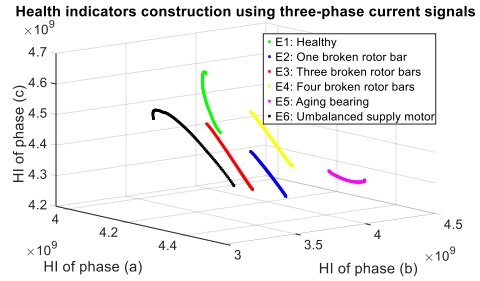

a) Current signals, 25 Hz, 0%

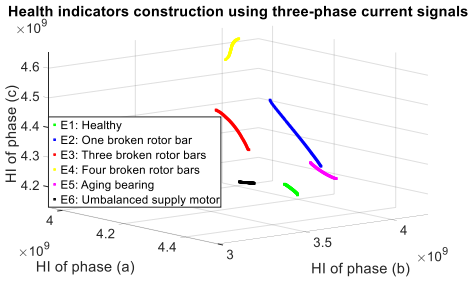

b) Current signals, 25 Hz, 25%

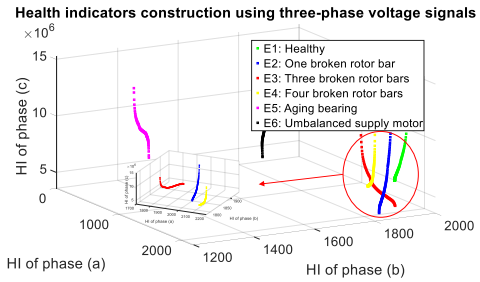

c) Voltage signals, 25 Hz, 0%

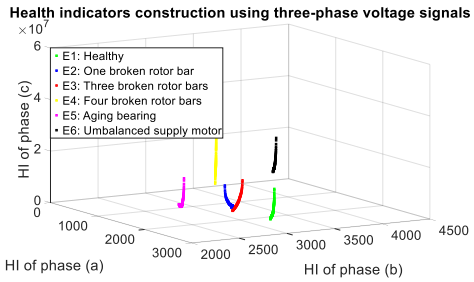

d) Voltage signals, 25 Hz, 25%

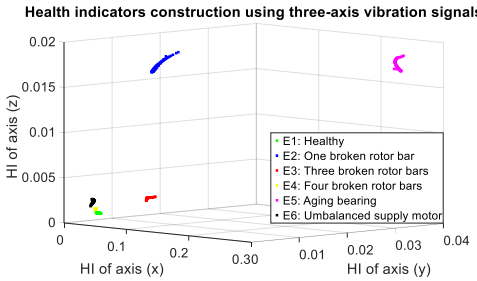

e) Vibration signals, 25 Hz, 0%

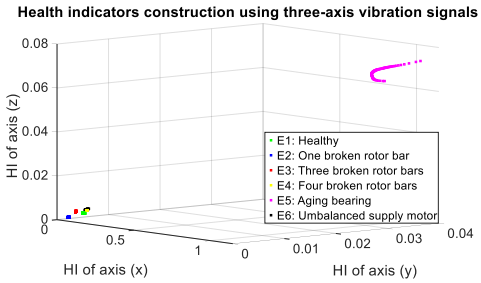

f) Vibration signals, 25 Hz, 25%

Figure A.2: Proposed HI on AMPERE platform.

One more again, the proposed health indicators allow separating the different health states of the system and can detect faults using different monitoring parameters and also under different operating conditions.

Appendix B

Mathematical demonstration of the direct monitoring HI

In Chapter 3 we have explained the functionality of the proposed health indicator used to localize the origin of the robot axes drifts. Below, we present the mathematical signification of the health indicator and make a coherence between the theoretical and the experimental results.

First, the HI is evaluated by the ratio between the RMS and the StD of the error values. Theoretically, in case where no drift occurs in the robot axes motions, the errors between the nominal and actual positions of the robot axes may be equal to 0 and may be constant. Hence, the value of the StD is 0 and thus the HI will not exist. However, in practice, the errors cannot be constant and equal to 0 even if there is not any drift in the robot axes because of noises during the data acquisition processes or the errors of measurement equipment. Hence, as we use real experimental data, the StD is always different to 0 and the determination condition of HI is satisfied.

Next, we will demonstrate that the health indicator of i-th axis of the robot is always greater or equal to 1: $HI_i \geq 1$. For this purpose the mean expression of the errors between the nominal and current positions of the i-th axis is re-written by equation B.1.

$$\overline{error_i} = \frac{1}{n}\sum_{j=1}^{n} error_{ij} \tag{B.1}$$

By replacing $\overline{error_i}$ with the equation B.1; the health indicator expression is re-written as follows:

$$HI_i = \left(\frac{\sqrt{\frac{1}{n}\sum_{j=1}^{n} error_{ij}^2}}{\sqrt{\frac{1}{n}\sum_{j=1}^{n}\left(error_{ij} - \frac{1}{n}\sum_{j=1}^{n} error_{ij}\right)^2}} \right)^2 \tag{B.2}$$

After developing equation B.2, one can obtain the expression in equation B.5:

$$HI_i = \left(\frac{\sqrt{\frac{1}{n}\sum_{j=1}^{n} error_{ij}^2}}{\sqrt{\frac{1}{n}\sum_{j=1}^{n} error_{ij} - \left(\frac{1}{n}\sum_{j=1}^{n} error_{ij}\right)^2}} \right)^2 \tag{B.3}$$

$$HI_i = \left(\frac{\sqrt{\frac{1}{n}\sum_{j=1}^{n} error_{ij}^2 + \left(\frac{1}{n}\sum_{j=1}^{n} error_{ij}\right)^2 - \left(\frac{1}{n}\sum_{j=1}^{n} error_{ij}\right)^2}}{\sqrt{\frac{1}{n}\sum_{j=1}^{n} (error_{ij})^2 - \left(\frac{1}{n}\sum_{j=1}^{n} error_{ij}\right)^2}} \right)^2 \tag{B.4}$$

$$HI_i = \left(\sqrt{1 + \frac{\left(\frac{1}{n}\sum_{j=1}^{n} error_{ij}\right)^2}{\frac{1}{n}\sum_{j=1}^{n} error_{ij}{}^2 - \left(\frac{1}{n}\sum_{j=1}^{n} error_{ij}\right)^2}} \right)^2 \tag{B.5}$$

$$HI_i = \sqrt{1 + \frac{(\overline{error_i})^2}{Var(error_i)}} \geq 1 \tag{B.6}$$

From equation B.6, the numerator represents the square of the mean value and is always greater than 0. Also, the denominator represents the variance of $error_i$ and thus always is greater than 0. Hence, the $HI_i \geq 1$.

After this notation, we will prove that the HI is equals to 1 when no drifts occur, and greater than 1 in the presence of drifts. For this purpose Figure B.1 is used for an illustration of the error trajectory observations in the six-axis of the robot when drifts occurred in axis six.

1. $HI_i \approx 1$ **when there is not any drift in the robot axis** i**-th**

   From equation B.5, the HI expression is dependent to the random variable $error_{ij}$. When the robot axes did not show any drifts, the square of the mean error values fluctuates around 0 with a dispersion due to noises caused by the sensitivity of the sensors. Indeed, every type of sensor has the relevant particular characteristics such as precision interval (Cheng et al., 2008). Besides, in the case of being impacted by the derivation source in another axis, the errors measured in the axis i will significantly

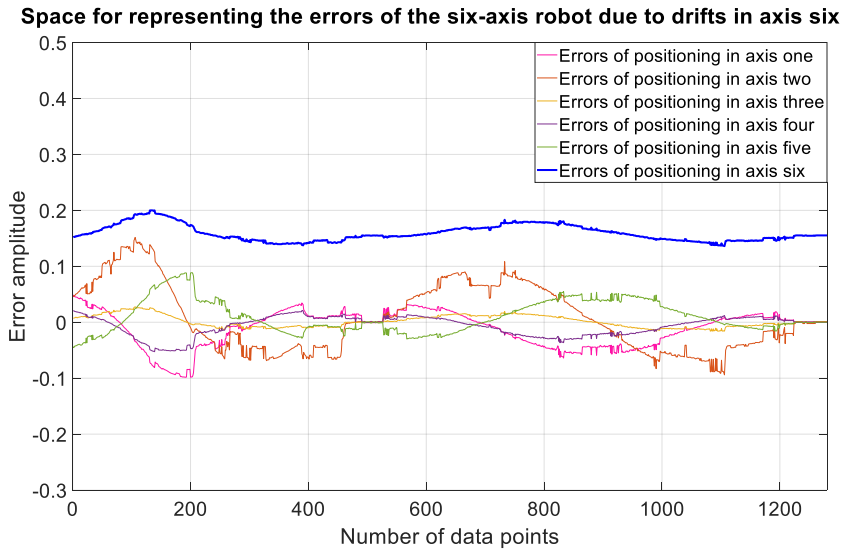

Figure B.1: Trajectory errors of the robot six axis caused by drifts in the sixth axis.

fluctuate, then its variance is quite large. Hence, in this case:

$$(\overline{error_i})^2 \approx 0; \text{and} (\overline{error_i})^2 << Var(error_i)$$

Hence, we have: $HI_i \approx 1$

Considering Figure B.1 where the derivation source is the axis 6, one can see that the error observations from axis 1 to the axis 5 fluctuate around 0 but with some dispersion as mentioned above. For example, the mean value of the error observations of axis one equals to 2.4424e-05 while the variance equals 0.007. In this case the HI equals to 1.0035 and shows that there is no drifts in axis 1.

2. $HI_i >> 1$ **when there is a derivation in the robot axis** i**-th**

If the derivation source localizes in the robot axis i, the mean value of the error observations is significantly greater than 0 with a negligible dispersion. This is due to sensor noise which is not significant compared to the drift variations, and also due to the precision interval of data collection. In this case, we have:

$$(\overline{error_i})^2 \neq 0; \text{ and } (\overline{error_i})^2 >> Var(error_i)$$

Hence, we have: $HI_i >> 1$

Considering Figure B.1, the mean value of the errors in the axis 6 is 0.0233 and its variance equals 0.001. Hence, using these values in the HI in equation B.6, we obtain the HI_6 value that is 23.3532, significantly greater than 1.

Appendix C

Information fusion of ML models for fouling prognostics

The appendix below presents the remaining results obtained using the test trajectories, $test_1$ and test3, to highlights the robustness of the proposed approach. For this purpose, figure C.1 and figure C.2 illustrate the predictions using the four short-term horizons based on the NARX models. In parallel, the prediction results and their distributions in long-term horizon using the LSTM network are shown in figure C.3 and figure C.4. Finally, the results of the proposed approach are highlighted in figure C.5 and figure C.6.

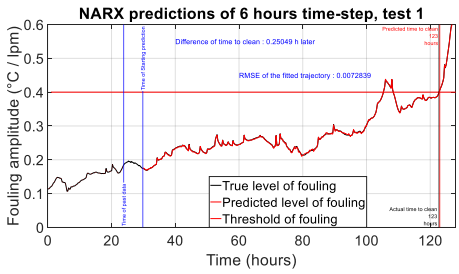

a) $NARX_1$ predictions, 6 hours

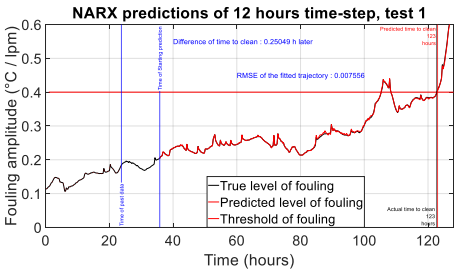

b) $NARX_2$ predictions, 12 hours

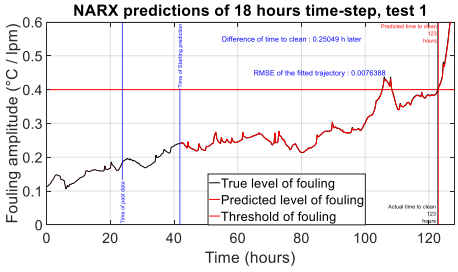

c) $NARX_3$ predictions, 18 hours

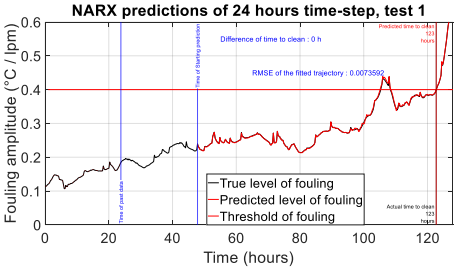

d) $NARX_4$ predictions, 24 hours

Figure C.1: Fouling prognostics using NARX models with data $test_1$.

From figures C.4 and C.6, it can be seen that the difference between the mean value of the overall predictions and the real TTC of $test_1$ using the LSTM model (figures C.4) is 5 hours earlier comparing to the one obtained with the proposed approach (figures C.6)

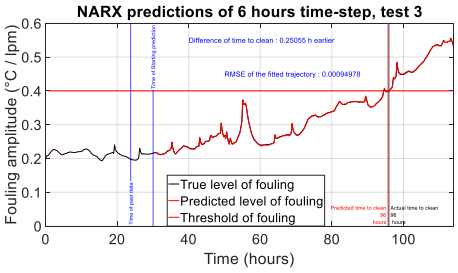

a) $NARX_1$ predictions, 6 hours

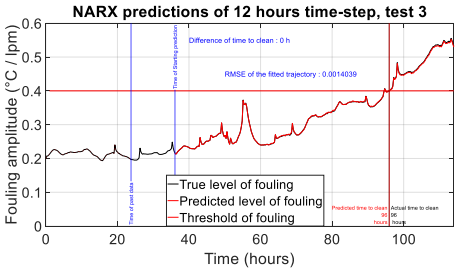

b) $NARX_2$ predictions, 12 hours

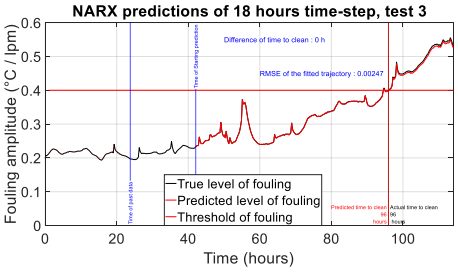

c) $NARX_3$ predictions, 18 hours

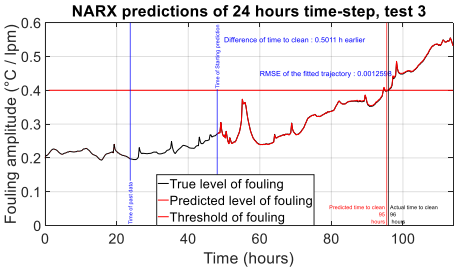

d) $NARX_4$ predictions, 24 hours

Figure C.2: Fouling prognostics using NARX models with data $test_3$.

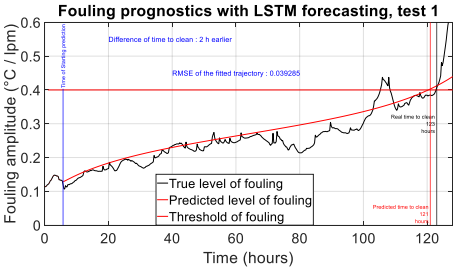

a) LSTM forecasting with data $test_1$

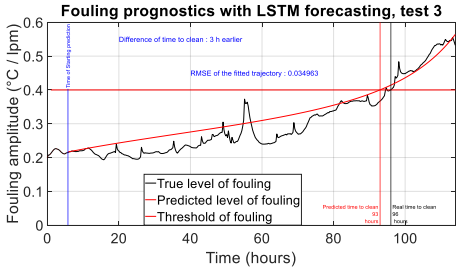

b) LSTM forecasting with data $test_3$

Figure C.3: Fouling prognostics using long-term predictions.

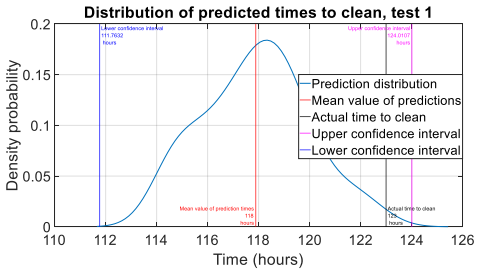

a) Predicted values distribution of $test_1$

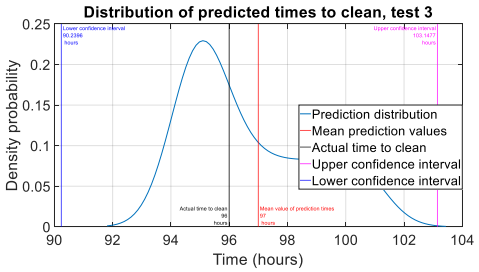

b) Predicted values distribution of $test_3$

Figure C.4: Distribution of the predicted TTC values using LSTM.

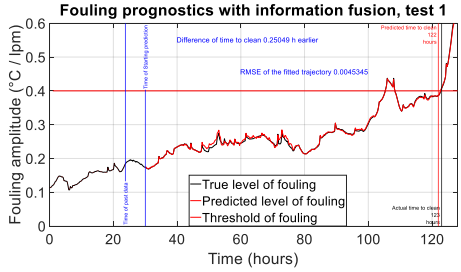

a) Fouling prognostics using all NARX models with data $test_1$

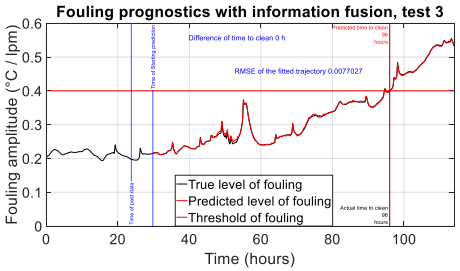

b) Fouling prognostics using all NARX models with data $test_3$

Figure C.5: Fouling prognostics using the proposed approach.

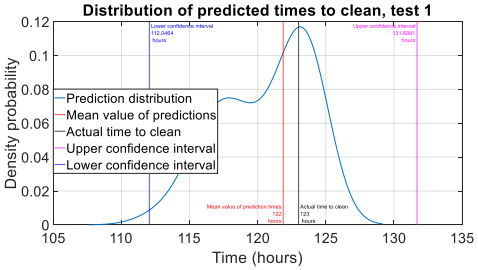

a) Predicted values distribution of $test_1$

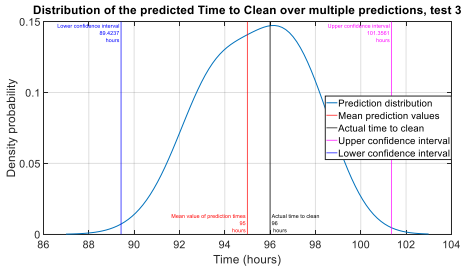

b) Predicted values distribution of $test_3$

Figure C.6: Distribution of the predicted TTC values using NARX-LSTM.

which equals to 1 hour. Besides, in $test_3$, the difference is one hour later when using the LSTM and one hour earlier with the proposed approach.

Bibliography

AFNOR (2001). Nf en 13306 x 60-319–terminologie de la maintenance. *Cited in page 22*

Aggarwal, S. and Chugh, N. (2019). Signal processing techniques for motor imagery brain computer interface: A review. *Array*, 1:100003. *Cited in page 16*

Ahamed, N., Pandya, Y., and Parey, A. (2014). Spur gear tooth root crack detection using time synchronous averaging under fluctuating speed. *Measurement*, 52:1–11. *Cited in page 19*

Akbari, M., Oyedun, A. O., Jain, S., and Kumar, A. (2018). Options for the conversion of pulp and paper mill by-products in western canada. *Sustainable Energy Technologies and Assessments*, 26:83–92. *Cited in page 90*

Akima, H. (1970). A new method of interpolation and smooth curve fitting based on local procedures. *Journal of the ACM (JACM)*, 17(4):589–602. *Cited in page 95*

Al Hage, J., El Najjar, M. E., and Pomorski, D. (2017). Multi-sensor fusion approach with fault detection and exclusion based on the kullback–leibler divergence: Application on collaborative multi-robot system. *Information Fusion*, 37:61–76. *Cited in page 70*

Ali, J. B. and Saidi, L. (2018). A new suitable feature selection and regression procedure for lithium-ion battery prognostics. *International Journal of Computer Applications in Technology*, 58(2):102–115. *Cited in page 70*

Ammouri, Hamade, R. (2011). Indirect tool-wear maps for tool condition monitoring in dry metal drilling operations. In *Advances in Sustainable Manufacturing*, pages 115–120. Springer. *Cited in page 19*

Ardsomang, T., Hines, J. W., and Upadhyaya, B. R. (2013). Heat exchanger fouling and estimation of remaining useful life. In *Annual Conference of Prognostics and Health Management Society*, pages 1–9. Estados Unidos ˆ eKnoxville Knoxville. *Cited in pages 90, 91, and 97*

Atamuradov, V., Medjaher, K., Camci, F., Zerhouni, N., Dersin, P., and Lamoureux, B. (2020). Machine health indicator construction framework for failure diagnostics and prognostics. *Journal of Signal Processing Systems*, pages 1–19. *Cited in page 19*

Atamuradov, V., Medjaher, K., Dersin, P., Lamoureux, B., and Zerhouni, N. (2017). Prognostics and health management for maintenance practitioners-review, implementation and tools evaluation. *International Journal of Prognostics and Health Management*, 8(060):1–31. *Cited in pages 16 and 27*

Bajpai, P. (2015). Basic overview of pulp and paper manufacturing process. In *Green Chemistry and Sustainability in Pulp and Paper Industry*, pages 11–39. Springer. *Cited in page 90*

Baraldi, P., Cadini, F., Mangili, F., and Zio, E. (2013a). Model-based and data-driven prognostics under different available information. *Probabilistic Engineering Mechanics*, 32:66–79. *Cited in page 28*

Baraldi, P., Compare, M., Sauco, S., and Zio, E. (2013b). Ensemble neural network-based particle filtering for prognostics. *Mechanical Systems and Signal Processing*, 41(1-2):288–300. *Cited in pages 30 and 33*

Baraldi, P., Mangili, F., and Zio, E. (2013c). Investigation of uncertainty treatment capability of model-based and data-driven prognostic methods using simulated data. *Reliability Engineering & System Safety*, 112:94–108. *Cited in page 28*

Barla, P. (2007). Iso 14001 certification and environmental performance in quebec's pulp and paper industry. *Journal of environmental economics and management*, 53(3):291–306. *Cited in page 90*

Bektas, O., Jones, J. A., Sankararaman, S., Roychoudhury, I., and Goebel, K. (2019). A neural network filtering approach for similarity-based remaining useful life estimation. *The International Journal of Advanced Manufacturing Technology*, 101(1-4):87–103. *Cited in page 32*

Benbouzid, M. E. H. (2000). A review of induction motors signature analysis as a medium for faults detection. *IEEE transactions on industrial electronics*, 47(5):984–993. *Cited in page 16*

Benkedjouh, T., Medjaher, K., Zerhouni, N., and Rechak, S. (2015). Health assessment and life prediction of cutting tools based on support vector regression. *Journal of Intelligent Manufacturing*, 26(2):213–223. *Cited in page 110*

Bensaad, D., Guillet, F., Soualhi, A., and El Badaoui, M. (2017). Kurtosis analysis as a cycle-ratio function in gear and bearing fault detection. *International Journal of Condition Monitoring*, 7(2):36–40. *Cited in page 19*

Berrueta, L. A., Alonso-Salces, R. M., and Héberger, K. (2007). Supervised pattern recognition in food analysis. *Journal of chromatography A*, 1158(1-2):196–214. *Cited in page 24*

Boo, C., Elimelech, M., and Hong, S. (2013). Fouling control in a forward osmosis process integrating seawater desalination and wastewater reclamation. *Journal of Membrane Science*, 444:148–156. *Cited in page 91*

Byington, C. S., Watson, M., and Edwards, D. (2004). Data-driven neural network methodology to remaining life predictions for aircraft actuator components. In *2004 IEEE Aerospace Conference Proceedings (IEEE Cat. No. 04TH8720)*, volume 6, pages 3581–3589. IEEE. *Cited in page 30*

Cai, H., Jia, X., Feng, J., Li, W., Pahren, L., and Lee, J. (2020). A similarity based methodology for machine prognostics by using kernel two sample test. *ISA transactions*. *Cited in page 32*

Cao, L. and Gu, Q. (2002). Dynamic support vector machines for non-stationary time series forecasting. *Intelligent Data Analysis*, 6(1):67–83. *Cited in page 28*

Chan, R. W., Yuen, J. K., Lee, E. W., and Arashpour, M. (2015). Application of nonlinear-autoregressive-exogenous model to predict the hysteretic behaviour of passive control systems. *Engineering Structures*, 85:1–10. *Cited in page 103*

Chang, M.-H., Kang, M., and Pecht, M. (2017). Prognostics-based led qualification using similarity-based statistical measure with rvm regression model. *IEEE Transactions on Industrial Electronics*, 64(7):5667–5677. *Cited in page 33*

Chen, C., Vachtsevanos, G., and Orchard, M. E. (2012). Machine remaining useful life prediction: An integrated adaptive neuro-fuzzy and high-order particle filtering approach. *Mechanical Systems and Signal Processing*, 28:597–607. *Cited in page 30*

Chen, C., Zhang, B., Vachtsevanos, G., and Orchard, M. (2010). Machine condition prediction based on adaptive neuro–fuzzy and high-order particle filtering. *IEEE Transactions on Industrial Electronics*, 58(9):4353–4364. *Cited in page 30*

Chen, S., Wen, P., Zhao, S., Huang, D., Wu, M., and Zhang, Y. (2018). A data fusion-based methodology of constructing health indicators for anomaly detection and prognostics. In *2018 International Conference on Sensing, Diagnostics, Prognostics, and Control (SDPC)*, pages 570–576. IEEE. *Cited in page 32*

Chen, X. W. and Nof, S. Y. (2007). Error detection and prediction algorithms: Application in robotics. *Journal of Intelligent and Robotic Systems*, 48(2):225–252. *Cited in page 65*

Chen, Z. and Li, W. (2017). Multisensor feature fusion for bearing fault diagnosis using sparse autoencoder and deep belief network. *IEEE Transactions on Instrumentation and Measurement*, 66(7):1693–1702. *Cited in pages 17 and 22*

Cheng, J., Yang, Y., and Yu, D. (2010). The envelope order spectrum based on generalized demodulation time–frequency analysis and its application to gear fault diagnosis. *Mechanical systems and signal processing*, 24(2):508–521. *Cited in page 20*

Cheng, S., Azarian, M., and Pecht, M. (2008). Sensor system selection for prognostics and health monitoring. In *International Design Engineering Technical Conferences and Computers and Information in Engineering Conference*, volume 43277, pages 1383–1389. *Cited in page 124*

Chinnam, R. B. and Baruah, P. (2003). Autonomous diagnostics and prognostics through competitive learning driven hmm-based clustering. In *Proceedings of the International Joint Conference on Neural Networks, 2003.*, volume 4, pages 2466–2471. IEEE. *Cited in page 26*

Cho, S. and Jiang, J. (2018). Optimal fault classification using fisher discriminant analysis in the parity space for applications to npps. *IEEE Transactions on Nuclear Science*, 65(3):856–865. *Cited in page 72*

Coglianese, C. (2019). Confronting complexity with regulatory excellence: Recommendations in the wake of the philadelphia refinery explosion. *U of Penn Law School, Public Law Research Paper*, (20-08). *Cited in page 1*

Deloux, E. (2008). *Politiques de maintenance conditionnelle pour un système à dégradation continue soumis à un environnement stressant.* PhD thesis, UNIVERSITE DE NANTES. *Cited in page 2*

Deutsch, J. and He, D. (2017). Using deep learning-based approach to predict remaining useful life of rotating components. *IEEE Transactions on Systems, Man, and Cybernetics: Systems*, 48(1):11–20. *Cited in page 29*

Deutsch, J., He, M., and He, D. (2017). Remaining useful life prediction of hybrid ceramic bearings using an integrated deep learning and particle filter approach. *Applied Sciences*, 7(7):649. *Cited in page 30*

Diez-Olivan, A., Del Ser, J., Galar, D., and Sierra, B. (2019). Data fusion and machine learning for industrial prognosis: Trends and perspectives towards industry 4.0. *Information Fusion*, 50:92–111. *Cited in page 64*

dos Santos, H. F. R., Weitzel, L., and Sobral, A. P. B. (2019). Prognostics of an industrial gas turbine: A time series forecasting data driven approach. *Revista de Sistemas de Informação da FSMA*, (24):19–30. *Cited in page 28*

Eker, O. F., Camci, F., Guclu, A., Yilboga, H., Sevkli, M., and Baskan, S. (2011). A simple state-based prognostic model for railway turnout systems. *IEEE Transactions on Industrial Electronics*, 58(5):1718–1726. *Cited in page 27*

El Koujok, M., Ragab, A., Ghezzaz, H., and Amazouz, M. (2020). A multi-agent-based methodology for known and novel faults diagnosis in industrial processes. *IEEE Transactions on Industrial Informatics.* *Cited in page 24*

Elangovan, M., Sugumaran, V., Ramachandran, K., and Ravikumar, S. (2011). Effect of svm kernel functions on classification of vibration signals of a single point cutting tool. *Expert Systems with Applications*, 38(12):15202–15207. *Cited in page 19*

Elsheikh, A., Yacout, S., and Ouali, M.-S. (2019). Bidirectional handshaking lstm for remaining useful life prediction. *Neurocomputing*, 323:148–156. *Cited in page 34*

EN, B. (2017). 13306: 2017: Maintenance—maintenance terminology. *BSI Standards Publication*. *Cited in page 10*

Fan, J., Yung, K.-C., and Pecht, M. (2015). Predicting long-term lumen maintenance life of led light sources using a particle filter-based prognostic approach. *Expert systems with applications*, 42(5):2411–2420. *Cited in page 28*

Farrar, C. R. and Worden, K. (2012). *Structural health monitoring: a machine learning perspective*. John Wiley & Sons. *Cited in page 25*

Fatima, S., Mohanty, A., and Naikan, V. (2015). Multiple fault classification using support vector machine in a machinery fault simulator. In *Vibration Engineering and Technology of Machinery*, pages 1021–1031. Springer. *Cited in page 72*

Fusco, R., Sansone, M., Filice, S., Carone, G., Amato, D. M., Sansone, C., and Petrillo, A. (2016). Pattern recognition approaches for breast cancer dce-mri classification: a systematic review. *Journal of medical and biological engineering*, 36(4):449–459. *Cited in page 24*

Gebraeel, N., Lawley, M., Liu, R., and Parmeshwaran, V. (2004). Residual life predictions from vibration-based degradation signals: a neural network approach. *IEEE Transactions on industrial electronics*, 51(3):694–700. *Cited in page 29*

Gebraeel, N. Z., Lawley, M. A., Li, R., and Ryan, J. K. (2005). Residual-life distributions from component degradation signals: A bayesian approach. *IiE Transactions*, 37(6):543–557. *Cited in page 27*

Goebel, K., Saha, B., Saxena, A., Celaya, J. R., and Christophersen, J. P. (2008). Prognostics in battery health management. *IEEE instrumentation & measurement magazine*, 11(4):33–40. *Cited in pages 13 and 26*

Gope, D., Gope, P. C., Thakur, A., and Yadav, A. (2015). Application of artificial neural network for predicting crack growth direction in multiple cracks geometry. *Applied Soft Computing*, 30:514–528. *Cited in page 29*

Gotlih, J., Brezocnik, M., Balic, J., Karner, T., Razborsek, B., and Gotlih, K. (2017). Determination of accuracy contour and optimization of workpiece positioning for robot milling. *Advances in Production Engineering & Management*, 12(3). *Cited in page 64*

Gouriveau, R., Medjaher, K., and Zerhouni, N. (2016). *From prognostics and health systems management to predictive maintenance 1: Monitoring and prognostics*. John Wiley & Sons. *Cited in pages 12, 16, 24, 27, and 41*

Guelpa, E. and Verda, V. (2020). Automatic fouling detection in district heating substations: Methodology and tests. *Applied Energy*, 258:114059. *Cited in page 91*

Guo, Y. and Ammula, S. (2005). Real-time acoustic emission monitoring for surface damage in hard machining. *International Journal of Machine Tools and Manufacture*, 45(14):1622–1627. *Cited in page 19*

Han, M. and Pan, J. (2015). A fault diagnosis method combined with lmd, sample entropy and energy ratio for roller bearings. *Measurement*, 76:7–19. *Cited in page 19*

Harrou, F., Sun, Y., Taghezouit, B., Saidi, A., and Hamlati, M.-E. (2018). Reliable fault detection and diagnosis of photovoltaic systems based on statistical monitoring approaches. *Renewable energy*, 116:22–37. *Cited in page 19*

Harvey, T., Wood, R., and Powrie, H. (2007). Electrostatic wear monitoring of rolling element bearings. *Wear*, 263(7-12):1492–1501. *Cited in page 19*

Heimes, F. O. (2008). Recurrent neural networks for remaining useful life estimation. In *2008 international conference on prognostics and health management*, pages 1–6. IEEE. *Cited in page 34*

Hong, S., Bae, T.-H., Tak, T., Hong, S., and Randall, A. (2002). Fouling control in activated sludge submerged hollow fiber membrane bioreactors. *Desalination*, 143(3):219–228. *Cited in page 91*

Hsu, C.-S. and Jiang, J.-R. (2018). Remaining useful life estimation using long short-term memory deep learning. In *2018 IEEE International Conference on Applied System Invention (ICASI)*, pages 58–61. IEEE. *Cited in page 29*

Hu, Y., Baraldi, P., Di Maio, F., and Zio, E. (2015). A particle filtering and kernel smoothing-based approach for new design component prognostics. *Reliability Engineering & System Safety*, 134:19–31. *Cited in page 28*

Jang, J.-S. (1993). Anfis: adaptive-network-based fuzzy inference system. *IEEE transactions on systems, man, and cybernetics*, 23(3):665–685. *Cited in page 72*

Jardine, A. K., Lin, D., and Banjevic, D. (2006). A review on machinery diagnostics and prognostics implementing condition-based maintenance. *Mechanical systems and signal processing*, 20(7):1483–1510. *Cited in page 20*

Javed, K., Gouriveau, R., Li, X., and Zerhouni, N. (2018). Tool wear monitoring and prognostics challenges: a comparison of connectionist methods toward an adaptive ensemble model. *Journal of Intelligent Manufacturing*, 29(8):1873–1890. *Cited in page 33*

Javed, K., Gouriveau, R., and Zerhouni, N. (2017). State of the art and taxonomy of prognostics approaches, trends of prognostics applications and open issues towards maturity at different technology readiness levels. *Mechanical Systems and Signal Processing*, 94:214–236. *Cited in page 27*

Jia, X., Zhao, M., Di, Y., Yang, Q., and Lee, J. (2017). Assessment of data suitability for machine prognosis using maximum mean discrepancy. *IEEE transactions on industrial electronics*, 65(7):5872–5881. *Cited in page 95*

Jin, X., Yu, X., Wang, X., Bai, Y., Su, T., and Kong, J. (2020). Prediction for time series with cnn and lstm. In *Proceedings of the 11th International Conference on Modelling, Identification and Control (ICMIC2019)*, pages 631–641. Springer. *Cited in page 34*

Jouin, M., Gouriveau, R., Hissel, D., Péra, M.-C., and Zerhouni, N. (2013). Prognostics and health management of pemfc–state of the art and remaining challenges. *International Journal of Hydrogen Energy*, 38(35):15307–15317. *Cited in page 10*

Jouin, M., Gouriveau, R., Hissel, D., Péra, M.-C., and Zerhouni, N. (2016). Particle filter-based prognostics: Review, discussion and perspectives. *Mechanical Systems and Signal Processing*, 72:2–31. *Cited in page 28*

Kang, L. and Liu, Y. (2015). Multi-objective optimization on a heat exchanger network retrofit with a heat pump and analysis of co2 emissions control. *Applied Energy*, 154:696–708. *Cited in page 91*

Kannatey-Asibu, E., Yum, J., and Kim, T. (2017). Monitoring tool wear using classifier fusion. *Mechanical Systems and Signal Processing*, 85:651–661. *Cited in page 24*

Khelif, R., Chebel-Morello, B., Malinowski, S., Laajili, E., Fnaiech, F., and Zerhouni, N. (2016). Direct remaining useful life estimation based on support vector regression. *IEEE Transactions on industrial electronics*, 64(3):2276–2285. *Cited in pages 28 and 34*

Khlaief, A., Nguyen, K., Medjaher, K., Picot, A., Maussion, P., Tobon, D., Chauchat, B., and Cheron, R. (2019). Feature engineering for ball bearing combined-fault detection and diagnostic. In *2019 IEEE 12th International Symposium on Diagnostics for Electrical Machines, Power Electronics and Drives (SDEMPED)*, pages 384–390. IEEE. *Cited in pages 17 and 19*

Kresta, S. M., Etchells III, A. W., Dickey, D. S., Atiemo-Obeng, V. A., et al. (2015). *Advances in industrial mixing: a companion to the handbook of industrial mixing*. John Wiley & Sons. *Cited in page 97*

Kumar, A., Tseng, F., Guo, Y., and Chinnam, R. B. (2008). Hidden-markov model based sequential clustering for autonomous diagnostics. In *2008 IEEE International Joint Conference on Neural Networks (IEEE World Congress on Computational Intelligence)*, pages 3345–3351. IEEE. *Cited in page 26*

Kuric, I., Tlach, V., Ságová, Z., Císar, M., and Gritsuk, I. (2018). Measurement of industrial robot pose repeatability. In *MATEC Web of Conferences*, volume 244, page 01015. EDP Sciences. *Cited in page 64*

Lamraoui, M., El Badaoui, M., and Guillet, F. (2015). Chatter detection in cnc milling processes based on wiener-svm approach and using only motor current signals. In *Vibration Engineering and Technology of Machinery*, pages 567–578. Springer. *Cited in page 19*

Lee, J., Bagheri, B., and Kao, H.-A. (2015a). A cyber-physical systems architecture for industry 4.0-based manufacturing systems. *Manufacturing letters*, 3:18–23. *Cited in page 41*

Lee, J., Bagheri, B., and Kao, H.-A. (2015b). A Cyber-Physical Systems architecture for Industry 4.0-based manufacturing systems. *Manufacturing Letters*, 3:18–23. *Cited in page 64*

Lee, J., Wu, F., Zhao, W., Ghaffari, M., Liao, L., and Siegel, D. (2014). Prognostics and health management design for rotary machinery systems—reviews, methodology and applications. *Mechanical systems and signal processing*, 42(1-2):314–334. *Cited in page 13*

Lei, Y., He, Z., Zi, Y., and Hu, Q. (2007). Fault diagnosis of rotating machinery based on multiple anfis combination with gas. *Mechanical systems and signal processing*, 21(5):2280–2294. *Cited in pages 25 and 29*

Lei, Y., Kong, D., Lin, J., and Zuo, M. J. (2012). Fault detection of planetary gearboxes using new diagnostic parameters. *Measurement Science and Technology*, 23(5):055605. *Cited in page 19*

Lei, Y., Li, N., Guo, L., Li, N., Yan, T., and Lin, J. (2018). Machinery health prognostics: A systematic review from data acquisition to rul prediction. *Mechanical Systems and Signal Processing*, 104:799–834. *Cited in pages 27, 29, and 30*

Lezama, J., Schweitzer, P., Weber, S., Tisserand, E., and Joycux, P. (2014). Arc fault detection based on temporal analysis. In *2014 IEEE 60th Holm Conference on Electrical Contacts (Holm)*, pages 1–5. IEEE. *Cited in page 19*

Li, J., Li, X., and He, D. (2019). A directed acyclic graph network combined with cnn and lstm for remaining useful life prediction. *IEEE Access*, 7:75464–75475. *Cited in page 29*

Li, X., Ding, Q., and Sun, J.-Q. (2018a). Remaining useful life estimation in prognostics using deep convolution neural networks. *Reliability Engineering & System Safety*, 172:1–11. *Cited in page 29*

Li, Y., Liang, X., Lin, J., Chen, Y., and Liu, J. (2018b). Train axle bearing fault detection using a feature selection scheme based multi-scale morphological filter. *Mechanical systems and signal processing*, 101:435–448. *Cited in page 21*

Liao, L. and Köttig, F. (2014). Review of hybrid prognostics approaches for remaining useful life prediction of engineered systems, and an application to battery life prediction. *IEEE Transactions on Reliability*, 63(1):191–207. *Cited in page 27*

Liao, L. and Köttig, F. (2016). A hybrid framework combining data-driven and model-based methods for system remaining useful life prediction. *Applied Soft Computing*, 44:191–199. *Cited in page 30*

Lin, P. and Tao, J. (2019). A novel bearing health indicator construction method based on ensemble stacked autoencoder. In *2019 IEEE International Conference on Prognostics and Health Management (ICPHM)*, pages 1–9. IEEE. *Cited in pages 70 and 95*

Liu, D., Luo, Y., Liu, J., Peng, Y., Guo, L., and Pecht, M. (2014). Lithium-ion battery remaining useful life estimation based on fusion nonlinear degradation ar model and rpf algorithm. *Neural Computing and Applications*, 25(3-4):557–572. *Cited in page 33*

Liu, J., Vitelli, V., Zio, E., and Seraoui, R. (2015). A novel dynamic-weighted probabilistic support vector regression-based ensemble for prognostics of time series data. *IEEE Transactions on Reliability*, 64(4):1203–1213. *Cited in page 32*

Liu, Y.-C., Chang, Y.-J., Liu, S.-L., and Chen, S.-P. (2019). Data-driven prognostics of remaining useful life for milling machine cutting tools. In *2019 IEEE International Conference on Prognostics and Health Management (ICPHM)*, pages 1–5. IEEE. *Cited in page 28*

Lo, N. G., Soualhi, A., Frinì, M., and Razik, H. (2018). Gear and bearings fault detection using motor current signature analysis. In *2018 13th IEEE Conference on Industrial Electronics and Applications (ICIEA)*, pages 900–905. IEEE. *Cited in page 19*

Loutas, T., Eleftheroglou, N., Georgoulas, G., Loukopoulos, P., Mba, D., and Bennett, I. (2019). Valve failure prognostics in reciprocating compressors utilizing temperature measurements, pca-based data fusion and probabilistic algorithms. *IEEE Transactions on Industrial Electronics*. *Cited in page 70*

Lu, C., Chen, J., Hong, R., Feng, Y., and Li, Y. (2016). Degradation trend estimation of slewing bearing based on lssvm model. *Mechanical Systems and Signal Processing*, 76:353–366. *Cited in page 28*

Lu, D., Qiao, W., and Gong, X. (2017). Current-based gear fault detection for wind turbine gearboxes. *IEEE Transactions on Sustainable Energy*, 8(4):1453–1462. *Cited in pages 19 and 41*

Madani, A., Ong, J. R., Tibrewal, A., and Mofrad, M. R. (2018). Deep echocardiography: data-efficient supervised and semi-supervised deep learning towards automated diagnosis of cardiac disease. *NPJ digital medicine*, 1(1):1–11. *Cited in page 25*

Madeti, S. R. and Singh, S. (2018). Modeling of pv system based on experimental data for fault detection using knn method. *Solar Energy*, 173:139–151. *Cited in page 72*

Malhi, A., Yan, R., and Gao, R. X. (2011). Prognosis of defect propagation based on recurrent neural networks. *IEEE Transactions on Instrumentation and Measurement*, 60(3):703–711. *Cited in page 29*

Markowski, M., Trafczynski, M., and Urbaniec, K. (2013). Identification of the influence of fouling on the heat recovery in a network of shell and tube heat exchangers. *Applied energy*, 102:755–764. *Cited in page 90*

Martinez-Luengo, M., Kolios, A., and Wang, L. (2016). Structural health monitoring of offshore wind turbines: A review through the statistical pattern recognition paradigm. *Renewable and Sustainable Energy Reviews*, 64:91–105. *Cited in page 24*

Medjaher, K., Tobon-Mejia, D. A., and Zerhouni, N. (2012). Remaining useful life estimation of critical components with application to bearings. *IEEE Transactions on Reliability*, 61(2):292–302. *Cited in page 14*

Medjaher, K., Zerhouni, N., and Baklouti, J. (2013). Data-driven prognostics based on health indicator construction: Application to pronostia's data. In *2013 European Control Conference (ECC)*, pages 1451–1456. IEEE. *Cited in page 17*

Mehala, N. and Dahiya, R. (2008). A comparative study of fft, stft and wavelet techniques for induction machine fault diagnostic analysis. In *Proceedings of the 7th WSEAS international conference on computational intelligence, man-machine systems and cybernetics, Cairo, Egypt*, volume 2931. *Cited in page 20*

Melo, T., Silva, J., and da Rocha Neto, J. (2015). Development of a multivariable control system on an experimental platform dedicated to the study of fouling phenomena. In *2015 IEEE International Instrumentation and Measurement Technology Conference (I2MTC) Proceedings*, pages 1314–1319. IEEE. *Cited in page 90*

Meng, T., Jing, X., Yan, Z., and Pedrycz, W. (2020). A survey on machine learning for data fusion. *Information Fusion*, 57:115–129. *Cited in page 70*

Mobley, R. K. (2002). *An introduction to predictive maintenance*. Elsevier. *Cited in page 15*

Mukherjee, S. and Sharma, N. (2012). Intrusion detection using naive bayes classifier with feature reduction. *Procedia Technology*, 4:119–128. *Cited in page 72*

Naqvi, M., Yan, J., and Dahlquist, E. (2010). Black liquor gasification integrated in pulp and paper mills: A critical review. *Bioresource technology*, 101(21):8001–8015. *Cited in page 90*

Ng, Y. S. and Srinivasan, R. (2010). Multi-agent based collaborative fault detection and identification in chemical processes. *Engineering Applications of Artificial Intelligence*, 23(6):934–949. *Cited in page 22*

Nguyen, K. T. and Medjaher, K. (2019). A new dynamic predictive maintenance framework using deep learning for failure prognostics. *Reliability Engineering & System Safety*, 188:251–262. *Cited in page 70*

Nguyen, K. T. P. and Medjaher, K. (2020). An automated health indicator construction methodology for prognostics based on multi-criteria optimization. *ISA Transactions*. *Cited in page 16*

Oh, H., Lee, W.-Y., Won, J., Kim, M., Choi, Y.-Y., and Han, S.-B. (2020). Residual-based fault diagnosis for thermal management systems of proton exchange membrane fuel cells. *Applied Energy*, 277:115568. *Cited in page 91*

Ondel, O., Boutleux, E., and Clerc, G. (2006). A method to detect broken bars in induction machine using pattern recognition techniques. *IEEE Transactions on industry applications*, 42(4):916–923. *Cited in pages 24 and 41*

Orchard, M. E. and Vachtsevanos, G. J. (2009). A particle-filtering approach for on-line fault diagnosis and failure prognosis. *Transactions of the Institute of Measurement and Control*, 31(3-4):221–246. *Cited in page 28*

Ozevin, D., Cox, J., Hardman, W., Kessler, S., and Timmons, A. (2014). Fatigue crack detection at gearbox spline component using acoustic emission method. Technical report, University of Illinois at Chicago Chicago United States. *Cited in page 19*

Pettersson, K. and Harvey, S. (2010). Co2 emission balances for different black liquor gasification biorefinery concepts for production of electricity or second-generation liquid biofuels. *Energy*, 35(2):1101–1106. *Cited in page 90*

Pezzani, C. M., Fontana, J. M., Donolo, P. D., De Angelo, C. H., Bossio, G. R., and Silva, L. I. (2018). Svm-based system for broken rotor bar detection in induction motors. In *2018 IEEE ANDESCON*, pages 1–6. IEEE. *Cited in page 41*

Qiao, G. and Weiss, B. A. (2018). Quick health assessment for industrial robot health degradation and the supporting advanced sensing development. *Journal of manufacturing systems*, 48:51–59. *Cited in pages 64 and 65*

Quiroz, J. C., Mariun, N., Mehrjou, M. R., Izadi, M., Misron, N., and Radzi, M. A. M. (2018). Fault detection of broken rotor bar in ls-pmsm using random forests. *Measurement*, 116:273–280. *Cited in page 41*

Rabiei, E., Droguett, E. L., and Modarres, M. (2016). A prognostics approach based on the evolution of damage precursors using dynamic bayesian networks. *Advances in mechanical engineering*, 8(9):1687814016666747. *Cited in page 27*

Ragab, A., El-Koujok, M., Poulin, B., Amazouz, M., and Yacout, S. (2018). Fault diagnosis in industrial chemical processes using interpretable patterns based on logical analysis of data. *Expert Systems with Applications*, 95:368–383. *Cited in page 24*

Ragab, A., Yacout, S., Ouali, M.-S., and Osman, H. (2019). Prognostics of multiple failure modes in rotating machinery using a pattern-based classifier and cumulative incidence functions. *Journal of Intelligent Manufacturing*, 30(1):255–274. *Cited in page 32*

Rahman, M. M. and Uddin, M. N. (2017). Online unbalanced rotor fault detection of an im drive based on both time and frequency domain analyses. *IEEE Transactions on Industry Applications*, 53(4):4087–4096. *Cited in page 21*

Rai, V. and Mohanty, A. (2007). Bearing fault diagnosis using fft of intrinsic mode functions in hilbert–huang transform. *Mechanical Systems and Signal Processing*, 21(6):2607–2615. *Cited in page 20*

Ramasso, E. (2014). Investigating computational geometry for failure prognostics. *International Journal on Prognostics and Health Management*. *Cited in page 32*

Ramasso, E. and Saxena, A. (2014). Performance benchmarking and analysis of prognostic methods for cmapss datasets. *International Journal on Prognostics and Health Management*. *Cited in page 34*

Ren, L., Dong, J., Wang, X., Meng, Z., Zhao, L., and Deen, J. (2020). A data-driven auto-cnn-lstm prediction model for lithium-ion battery remaining useful life. *IEEE Transactions on Industrial Informatics*. *Cited in page 29*

Rezaeianjouybari, B. and Shang, Y. (2020). Deep learning for prognostics and health management: State of the art, challenges, and opportunities. *Measurement*, 163:107929. *Cited in page 102*

Rigamonti, M. M., Baraldi, P., Zio, E., et al. (2016). Echo state network for the remaining useful life prediction of a turbofan engine. In *annual conference of the prognostics and health management society 2015*, pages 255–270. *Cited in page 29*

Saha, B., Goebel, K., Poll, S., and Christophersen, J. (2008). Prognostics methods for battery health monitoring using a bayesian framework. *IEEE Transactions on instrumentation and measurement*, 58(2):291–296. *Cited in page 30*

Sahai, A. K., Rath, N., Sood, V., and Singh, M. P. (2020). Arima modelling & forecasting of covid-19 in top five affected countries. *Diabetes & Metabolic Syndrome: Clinical Research & Reviews*, 14(5):1419–1427. *Cited in page 28*

Saidi, L., Ali, J. B., Bechhoefer, E., and Benbouzid, M. (2017). Wind turbine high-speed shaft bearings health prognosis through a spectral kurtosis-derived indices and svr. *Applied Acoustics*, 120:1–8. *Cited in page 20*

Sait, A. S. and Sharaf-Eldeen, Y. I. (2011). A review of gearbox condition monitoring based on vibration analysis techniques diagnostics and prognostics. In *Rotating Machinery, Structural Health Monitoring, Shock and Vibration, Volume 5*, pages 307–324. Springer. *Cited in pages 17 and 21*

Samantaray, S. (2009). Decision tree-based fault zone identification and fault classification in flexible ac transmissions-based transmission line. *IET generation, transmission & distribution*, 3(5):425–436. *Cited in page 72*

Saon, S., Hiyama, T., et al. (2010). Predicting remaining useful life of rotating machinery based artificial neural network. *Computers & Mathematics with Applications*, 60(4):1078–1087. *Cited in page 29*

Saxena, A., Celaya, J., Saha, B., Saha, S., and Goebel, K. (2010). Metrics for offline evaluation of prognostic performance. *International Journal of Prognostics and health management*, 1(1):4–23. *Cited in page 110*

Saxena, A., Goebel, K., Simon, D., and Eklund, N. (2008). Damage propagation modeling for aircraft engine run-to-failure simulation. In *2008 international conference on prognostics and health management*, pages 1–9. IEEE. *Cited in page 34*

Sbarufatti, C., Corbetta, M., Manes, A., and Giglio, M. (2016). Sequential monte-carlo sampling based on a committee of artificial neural networks for posterior state estimation and residual lifetime prediction. *International Journal of Fatigue*, 83:10–23. *Cited in page 27*

Segreto, T., Karam, S., Teti, R., and Ramsing, J. (2015). Feature extraction and pattern recognition in acoustic emission monitoring of robot assisted polishing. *Procedia CIRP*, 28:22–27. *Cited in page 65*

Sevilla, P., Herrera-Ruiz, G., Robles-Ocampo, J., and Jáuregui-Correa, J. (2011). Tool breakage detection in cnc high-speed milling based in feed-motor current signals. *The International Journal of Advanced Manufacturing Technology*, 53(9-12):1141–1148. *Cited in page 19*

Sharma, V. and Parey, A. (2016). Gear crack detection using modified tsa and proposed fault indicators for fluctuating speed conditions. *Measurement*, 90:560–575. *Cited in page 19*

Shih, R.-F. and Lee, L.-S. (1995). Use of fuzzy cause-effect digraph for resolution fault diagnosis for process plants. 1. fuzzy cause-effect digraph. *Industrial & engineering chemistry research*, 34(5):1688–1702. *Cited in page 102*

Skima, H., Medjaher, K., Varnier, C., Dedu, E., and Bourgeois, J. (2016). A hybrid prognostics approach for mems: From real measurements to remaining useful life estimation. *Microelectronics Reliability*, 65:79–88. *Cited in page 30*

Skrickij, V., Bogdevičius, M., and Junevičius, R. (2016). Diagnostic features for the condition monitoring of hypoid gear utilizing the wavelet transform. *Applied Acoustics*, 106:51–62. *Cited in page 19*

Soualhi, A., Clerc, G., Razik, H., and Rivas, F. (2013). Long-term prediction of bearing condition by the neo-fuzzy neuron. In *2013 9th IEEE International Symposium on Diagnostics for Electric Machines, Power Electronics and Drives (SDEMPED)*, pages 586–591. IEEE. *Cited in page 29*

Soualhi, A., Medjaher, K., and Zerhouni, N. (2014). Bearing health monitoring based on hilbert–huang transform, support vector machine, and regression. *IEEE Transactions on Instrumentation and Measurement*, 64(1):52–62. *Cited in pages 27 and 33*

Soualhi, A., Medjaher, K., Zerhouni, N., and Razik, H. (2016). Early detection of bearing faults by the hilbert-huang transform. In *2016 4th International Conference on Control Engineering & Information Technology (CEIT)*, pages 1–6. IEEE. *Cited in pages 17, 21, and 41*

Steinhagen, R., Müller-Steinhagen, H., and Maani, K. (1993). Problems and costs due to heat exchanger fouling in new zealand industries. *Heat transfer engineering*, 14(1):19–30. *Cited in page 90*

Sun, D., Lee, V. C., and Lu, Y. (2016). An intelligent data fusion framework for structural health monitoring. In *2016 IEEE 11th Conference on Industrial Electronics and Applications (ICIEA)*, pages 49–54. IEEE. *Cited in page 22*

Sun, J., Yan, C., and Wen, J. (2017). Intelligent bearing fault diagnosis method combining compressed data acquisition and deep learning. *IEEE Transactions on Instrumentation and Measurement*, 67(1):185–195. *Cited in page 24*

Taghizadeh-Alisaraei, A. and Mahdavian, A. (2019). Fault detection of injectors in diesel engines using vibration time-frequency analysis. *Applied Acoustics*, 143:48–58. *Cited in page 21*

Terrazas, G., Martínez-Arellano, G., Benardos, P., and Ratchev, S. (2018). Online tool wear classification during dry machining using real time cutting force measurements and a cnn approach. *Journal of Manufacturing and Materials Processing*, 2(4):72. *Cited in page 42*

Tian, Y., Lu, C., Wang, Z., and Tao, L. (2014). Artificial fish swarm algorithm-based particle filter for li-ion battery life prediction. *Mathematical Problems in Engineering*, 2014. *Cited in page 28*

Tobon-Mejia, D., Medjaher, K., and Zerhouni, N. (2012). Cnc machine tool's wear diagnostic and prognostic by using dynamic bayesian networks. *Mechanical Systems and Signal Processing*, 28:167–182. *Cited in page 42*

Tonks, O. and Wang, Q. (2017). The detection of wind turbine shaft misalignment using temperature monitoring. *CIRP Journal of Manufacturing Science and Technology*, 17:71–79. *Cited in page 19*

Toutountzakis, T., Tan, C. K., and Mba, D. (2005). Application of acoustic emission to seeded gear fault detection. *Ndt & E International*, 38(1):27–36. *Cited in page 19*

Wang, J. (2017). *Safety Theory and Control Technology of High-Speed Train Operation*. Academic Press. *Cited in page 23*

Wang, T. (2010). *Trajectory similarity based prediction for remaining useful life estimation*. PhD thesis, University of Cincinnati. *Cited in page 32*

Wang, T., Yu, J., Siegel, D., and Lee, J. (2008). A similarity-based prognostics approach for remaining useful life estimation of engineered systems. In *2008 international conference on prognostics and health management*, pages 1–6. IEEE. *Cited in page 32*

Wang, X., Feng, H., and Fan, Y. (2015). Fault detection and classification for complex processes using semi-supervised learning algorithm. *Chemometrics and intelligent laboratory systems*, 149:24–32. *Cited in page 26*

Wang, Y., Yang, X., Sun, M., Ma, L., Li, X., and Shi, L. (2016). Estimating carbon emissions from the pulp and paper industry: A case study. *Applied Energy*, 184:779–789. *Cited in page 91*

Welz, Z., Nam, A., Sharp, M., Hines, J. W., and Upadhyaya, B. R. (2014). Prognostics for light water reactor sustainability: empirical methods for heat exchanger prognostic lifetime predictions. In *2nd European Conference of the Prognostics and Health Management Society (PHME'14), Nantes, France, July*, pages 8–10. *Cited in page 91*

Wen, L., Dong, Y., and Gao, L. (2019). A new ensemble residual convolutional neural network for remaining useful life estimation. *Math. Biosci. Eng*, 16(2):862–880. *Cited in page 34*

Widodo, A. and Yang, B.-S. (2011). Machine health prognostics using survival probability and support vector machine. *Expert Systems with Applications*, 38(7):8430–8437. *Cited in page 28*

Wodecki, J., Stefaniak, P., Obuchowski, J., Wylomanska, A., and Zimroz, R. (2016). Combination of principal component analysis and time-frequency representations of multichannel vibration data for gearbox fault detection. *Journal of Vibroengineering*, 18(4):2167–2175. *Cited in page 21*

Wu, D., Jennings, C., Terpenny, J., and Kumara, S. (2016a). Cloud-based machine learning for predictive analytics: Tool wear prediction in milling. In *2016 IEEE International Conference on Big Data (Big Data)*, pages 2062–2069. IEEE. *Cited in page 33*

Wu, J., Hu, K., Cheng, Y., Zhu, H., Shao, X., and Wang, Y. (2020). Data-driven remaining useful life prediction via multiple sensor signals and deep long short-term memory neural network. *ISA transactions*, 97:241–250. *Cited in page 34*

Wu, J., Zhang, C., and Chen, Z. (2016b). An online method for lithium-ion battery remaining useful life estimation using importance sampling and neural networks. *Applied energy*, 173:134–140. *Cited in page 33*

Wu, Q., Ding, K., and Huang, B. (2018a). Approach for fault prognosis using recurrent neural network. *Journal of Intelligent Manufacturing*, pages 1–13. *Cited in page 34*

Wu, T. Y., Chen, J., and Wang, C. (2012). Characterization of gear faults in variable rotating speed using hilbert-huang transform and instantaneous dimensionless frequency normalization. *Mechanical Systems and Signal Processing*, 30:103–122. *Cited in page 20*

Wu, Y., Yuan, M., Dong, S., Lin, L., and Liu, Y. (2018b). Remaining useful life estimation of engineered systems using vanilla lstm neural networks. *Neurocomputing*, 275:167–179. *Cited in page 103*

Xing, Y., Ma, E. W., Tsui, K.-L., and Pecht, M. (2013). An ensemble model for predicting the remaining useful performance of lithium-ion batteries. *Microelectronics Reliability*, 53(6):811–820. *Cited in page 28*

Xu, G., Liu, M., Wang, J., Ma, Y., Wang, J., Li, F., and Shen, W. (2019). Data-driven fault diagnostics and prognostics for predictive maintenance: A brief overview. In *2019 IEEE 15th International Conference on Automation Science and Engineering (CASE)*, pages 103–108. IEEE. *Cited in page 95*

Xu, J., Wang, Y., and Xu, L. (2013). Phm-oriented integrated fusion prognostics for aircraft engines based on sensor data. *IEEE Sensors Journal*, 14(4):1124–1132. *Cited in page 30*

Xu, X. (2017). Machine tool 4.0 for the new era of manufacturing. *The International Journal of Advanced Manufacturing Technology*, 92(5-8):1893–1900. *Cited in page 41*

Yan, H.-C., Pang, C. K., and Zhou, J.-H. (2013). Precognitive maintenance and probabilistic assessment of tool wear using particle filters. In *IECON 2013-39th Annual Conference of the IEEE Industrial Electronics Society*, pages 7382–7387. IEEE. *Cited in page 28*

Yang, C., Liu, J., Zeng, Y., and Xie, G. (2019). Real-time condition monitoring and fault detection of components based on machine-learning reconstruction model. *Renewable Energy*, 133:433–441. *Cited in page 19*

Yeap, Y. M., Geddada, N., Satpathi, K., and Ukil, A. (2018). Time-and frequency-domain fault detection in a vsc-interfaced experimental dc test system. *IEEE Transactions on Industrial Informatics*, 14(10):4353–4364. *Cited in page 21*

Yu, W., Kim, I. Y., and Mechefske, C. (2020a). An improved similarity-based prognostic algorithm for rul estimation using an rnn autoencoder scheme. *Reliability Engineering & System Safety*, page 106926. *Cited in page 32*

Yu, Y., Hu, C., Si, X., Zheng, J., and Zhang, J. (2020b). Averaged bi-lstm networks for rul prognostics with non-life-cycle labeled dataset. *Neurocomputing*. *Cited in page 34*

Yuqing, Z., Xinfang, L., Fengping, L., Bingtao, S., and Wei, X. (2015). An online damage identification approach for numerical control machine tools based on data fusion using vibration signals. *Journal of Vibration and Control*, 21(15):2925–2936. *Cited in page 19*

Zaher, A., McArthur, S., Infield, D., and Patel, Y. (2009). Online wind turbine fault detection through automated scada data analysis. *Wind Energy: An International Journal for Progress and Applications in Wind Power Conversion Technology*, 12(6):574–593. *Cited in page 19*

Zarei, J. (2012). Induction motors bearing fault detection using pattern recognition techniques. *Expert systems with Applications*, 39(1):68–73. *Cited in page 19*

Zarei, J., Tajeddini, M. A., and Karimi, H. R. (2014). Vibration analysis for bearing fault detection and classification using an intelligent filter. *Mechatronics*, 24(2):151–157. *Cited in page 19*

Zhang, C. (2018). *Reliability-based fatigue damage assessment and optimum maintenance strategy of offshore horizontal wind turbine blades*. PhD thesis, University of Greenwich. *Cited in page 2*

Zhang, K., Tang, B., Qin, Y., and Deng, L. (2019). Fault diagnosis of planetary gearbox using a novel semi-supervised method of multiple association layers networks. *Mechanical Systems and Signal Processing*, 131:243–260. *Cited in page 25*

Zheng, C., Liu, W., Chen, B., Gao, D., Cheng, Y., Yang, Y., Zhang, X., Li, S., Huang, Z., and Peng, J. (2018). A data-driven approach for remaining useful life prediction of aircraft engines. In *2018 21st International Conference on Intelligent Transportation Systems (ITSC)*, pages 184–189. IEEE. *Cited in page 34*

Zhou, J.-H., Pang, C. K., Zhong, Z.-W., and Lewis, F. L. (2010). Tool wear monitoring using acoustic emissions by dominant-feature identification. *IEEE Transactions on Instrumentation and Measurement*, 60(2):547–559. *Cited in page 19*

Zhou, W., Habetler, T. G., Harley, R. G., and Lu, B. (2007). Incipient bearing fault detection via stator current noise cancellation using wiener filter. In *2007 IEEE International Symposium on Diagnostics for Electric Machines, Power Electronics and Drives*, pages 11–16. IEEE. *Cited in page 19*

Zhou, Y. and Huang, M. (2016). Lithium-ion batteries remaining useful life prediction based on a mixture of empirical mode decomposition and arima model. *Microelectronics Reliability*, 65:265–273. *Cited in page 28*

Ziani, R., Felkaoui, A., and Zegadi, R. (2017). Bearing fault diagnosis using multiclass support vector machines with binary particle swarm optimization and regularized fisher's criterion. *Journal of Intelligent Manufacturing*, 28(2):405–417. *Cited in page 24*

Résumé —

Cette thèse est réalisée dans le cadre du projet SMART financé par un programme européen, Interreg POCTEFA. Il vise à aider les petites et moyennes entreprises à renforcer leur compétitivité dans le contexte de l'Industrie 4.0 en développant des outils de surveillance intelligente pour la gestion autonome de la santé de leurs systèmes. Pour ce faire, nous proposons des algorithmes orientés données pour le pronostic et la gestion de santé des systèmes industriels. La première contribution concerne la construction d'un nouvel indicateur de santé robuste qui permet de séparer clairement les différents états de santé d'un grand nombre de composants critiques du système. Ce nouvel indicateur est également capable de prendre en compte plusieurs paramètres de surveillance dans diverses conditions de fonctionnement. Ensuite, la deuxième contribution aborde les défis posés par le diagnostic des défauts inconnus dans les systèmes dynamiques, en particulier la détection, la localisation et l'identification de l'origine des dérives des axes de robot lorsque ces dernières n'ont pas été apprises auparavant. À cette fin, une nouvelle méthodologie de diagnostic en ligne basée sur la fusion d'informations provenant des techniques de surveillance directe et indirecte est proposée. Elle utilise la surveillance directe pour mettre à jour, instantanément, le modèle de surveillance indirecte pour diagnostiquer en ligne l'origine des nouvelles dérives. Enfin, notre dernière contribution traite du pronostic de défaillances dans les systèmes industriels contrôlés dont le contrôleur peut avoir un impact négatif sur les prédictions à long terme. Pour remédier à ce problème, nous développons une nouvelle approche de pronostic adaptatif basé sur la combinaison de prédictions issues de plusieurs modèles d'apprentissage sur différents horizons temporels. L'approche proposée permet de capturer la tendance de la dégradation à long terme tout en tenant compte des changements d'état à court terme causés par les activités du contrôleur, ce qui permet d'améliorer la précision du pronostic. Les performances des approches proposées dans cette thèse ont été vérifiées sur différents cas d'études réels représentant les démonstrateurs des partenaires de la thèse.

Mots clés : Pronostic et gestion de santé guidés par les données ; Surveillance intelligente ; Traitement du signal ; Apprentissage machine ; Détection des défauts ; Diagnostic des défauts ; Pronostic de défaillance ; Construction d'indicateurs de santé ; Fusion d'informations ; Estimation de la vie résiduelle restante ; Pronostic des systèmes contrôlés.

Abstract —

This thesis was conducted within the framework of SMART project funded by a European program, Interreg POCTEFA. The project aims to support small and medium-sized companies to increase their competitiveness in the context of Industry 4.0 by developing intelligent monitoring tools for autonomous system health management. To do so, in this work, we propose efficient data-driven algorithms for prognostics and health management of industrial systems. The first contribution consists of the construction of a new robust health indicator that allows clearly separating different fault states of a wide range of systems' critical components. This health indicator is also efficient when considering multiples monitoring parameters under various operating conditions. Next, the second contribution addresses the challenges posed by online diagnostics of unknown fault types in dynamic systems, particularly the detection, localization, and identification of the robot axes drifts origin when these drifts have not been learned before. For this purpose, a new online diagnostics methodology based on information fusion from direct and indirect monitoring techniques is proposed. It uses the direct monitoring way to instantaneously update the indirect monitoring model and diagnose online the origin of new faults. Finally, the last contribution deals with the prognostics issue of systems failure in a controlled industrial process that can lead to negative impacts in long-term predictions. To remedy this problem, we developed a new adaptive prognostics approach based on the combination of multiple machine learning predictions in different time horizons. The proposed approach allows capturing the degradation trend in long-term while considering the state changes in short-term caused by the controller activities, which allows improving the accuracy of prognostics results. The performances of the approaches proposed in this thesis were investigated on different real case studies representing the demonstrators of the thesis partners.

Keywords: Data-driven prognostics and health management ; Intelligent monitoring ; Signal processing ; Machine learning ; Fault detection ; Fault diagnostics ; Failure prognostics ; Health indicators Construction ; Information fusion ; Remaining useful life estimation ; Prognostics of controlled systems.

Tarbes National Engineering School, Toulouse University, 47 Avenue d'Azereix, BP 1629 - 65016, Tarbes, France.